Investigating the influence of electrolyte composition on electrodeposition in copper electrowinning

by

Chalwe Chibwe

Thesis presented in partial fulfilment
of the requirements for the Degree

of

MASTER OF ENGINEERING
(EXTRACTIVE METALLURGICAL ENGINEERING)

in the Faculty of Engineering
at Stellenbosch University

Supervisor
Dr. Margreth Tadie

March 2020

DECLARATION

By submitting this thesis electronically, I declare that the entirety of the work contained therein is my own, original work, that I am the sole author thereof (save to the extent explicitly otherwise stated), that reproduction and publication thereof by Stellenbosch University will not infringe any third party rights and that I have not previously in its entirety or in part submitted it for obtaining any qualification.

Date: March 2020

PLAGIARISM DECLARATION

1. Plagiarism is the use of ideas, material and other intellectual property of another's work and to present is as my own.

2. I agree that plagiarism is a punishable offence because it constitutes theft.

3. I also understand that direct translations are plagiarism.

4. Accordingly all quotations and contributions from any source whatsoever (including the internet) have been cited fully. I understand that the reproduction of text without quotation marks (even when the source is cited) is plagiarism.

5. I declare that the work contained in this assignment, except where otherwise stated, is my original work and that I have not previously (in its entirety or in part) submitted it for grading in this module/assignment or another module/assignment.

Initials and surname: C. Chibwe

Date: 18.02.2020

ABSTRACT

The major concern in copper electrowinning is to deposit smooth, dense, pure copper at high current efficiency and low energy consumption. Electrolyte physicochemical properties namely density, diffusion coefficients and conductivity affect the mass transfer and energy consumption in the cell. These properties are dependent on electrolyte composition. Control of growth and structure of the deposit determines the deposit morphology/smoothness and is strongly dependent on the current distribution over the cathode surface.

The study investigated the influence of electrolyte composition on copper deposition via consideration of electrolyte physicochemical properties and current distribution in the cell. The electrolyte components were copper ions, sulphuric acid, iron ions and polyacrylamide (PAM) additive. The effect of other factors such as cell/electrode alignment on current distribution cannot be ignored, but were beyond the scope of study, therefore were kept constant.

The research approach was divided into two stages: establishing the relationship of electrolyte composition to physicochemical properties and modelling a copper electrodeposition process to predict current distribution at the cathode surface. A 5 factor, 2 and 3 level design of experiment was performed to determine the effect of copper (35 and 45 g/l), sulphuric acid (160 and 180 g/l), iron (1, 3 and 6 g/l), PAM additive (2, 5 and 10 mg/l) and temperature (45 and 55°C) on electrolyte density, conductivity and diffusion coefficient in synthetic copper electrowinning electrolytes. Density and conductivity were measured using a pycnometer and conductivity meter respectively. Diffusion coefficients were determined from the limiting current using linear sweep voltammetry.

COMSOL Multiphysics, a finite element software was used to generate an electrowinning model for predicting current distribution at the cathode surface. Experiments were conducted for model validation. The current density was determined from deposit thickness by applying Faraday's law.

The results showed that increase in copper, acid, and iron concentration increased density but decreased diffusion coefficient. Conductivity improved with addition of acid but reduced with addition of metallic elements (copper, iron). The polyacrylamide additive had no effect on the properties. It was suggested that the addition of high atomic weight (copper, iron) elements increased density whilst impeding the movement of ions in the electrolyte whereas hydrogen ions improved electrolyte conductivity. Mathematical correlations for each property as a function of electrolyte composition were developed and were supported by previous studies.

The copper electrowinning model predicted outputs such as species concentration and current distribution. Model and experimental current distribution compared well with each other. High current densities were

observed near the cathode top and bottom with relatively uniform distribution at the cathode centre. This was attributed to the mass transfer phenomena, which facilitated less resistive path of ions in these regions. The model under-predicted the current density magnitude likely due to model limitations.

The influence of electrolyte composition on current distribution profile was minimal, the effect was primarily on the magnitude of current density. Experimental and modelled current density both slightly increased with increase in copper concentration whereas variation in acid concentration caused a slight increase only in experimental current density, the modelled current density values remained the same.

OPSOMMING

Die groot kommer in koperelektroherwinning is om gladde, digte, suiwer koper by hoë stroom effektiwiteit en lae energiegebruik te deponeer. Elektroliet fisikochemiese eienskappe, genaamd digtheid, diffusie koëffisiënte en geleidingsvermoë, affekteer die massa-oordrag en energie gebruik in die sel. Hierdie eienskappe is afhanklik van elektrolietkomposisie. Beheer oor groei en struktuur van die deposito bepaal die deposito morfologie/gladheid en is grootliks afhanklik van die stroomdistribusie oor die katode-oppervlak.

Die studie het die invloed van elektrolietkomposisie op koperdeponering ondersoek via oorweging van elektroliet fisikochemiese eienskappe en stroomdistribusie in die sel. Die elektrolietkomponente was koperione, swaelsuur, ysterione en poliakrielamied- (PAM) bymiddel. Die effek van ander faktore soos sel-/elektrodebelyning op stroomdistribusie kan nie geïgnoreer word nie, maar is buite die bestek van die studie, en is daarom konstant gehou.

Die navorsingsbenadering is verdeel in twee stadiums: die bepaling van die verhouding tussen elektrolietkomposisie en fisikochemiese eienskappe, en modellering van ’n koperelektrodeponeringsproses om stroomdistribusie by die katode-oppervlak te voorspel. ’n 5-faktor, 2- en 3-vlak ontwerp van eksperiment is uitgevoer om die effek van koper (35 en 45 g/l), swaelsuur (160 en 180 g/l), yster (1, 3 en 6 g/l) PAM-bymiddel (2,5 en 10 mg/l) en temperatuur (45 en 55 °C) op elektrolietdigtheid, geleidingsvermoë en diffusiekoëffisiënt in sintetiese koper elektroherwinning elektroliete te bepaal. Digtheid en geleidingsvermoë is gemeet deur ’n piknometer en geleidingsvermoëmeter onderskeidelik te gebruik. Diffusiekoëffisiënte is bepaal uit die beperkte stroom deur liniêre stryk voltammetrie te gebruik.

COMSOL Multiphysics, ’n eindige element sagteware is gebruik om ’n elektroherwinningmodel te genereer om stroomdistribusie by die katode-oppervlak te voorspel. Eksperimente is uitgevoer vir modelvalidasie. Die stroomdigtheid is bepaal uit depositodigtheid deur Faraday se wet toe te pas.

Die resultate het gewys dat verhoging in koper-, suur- en ysterkonsentrasie digtheid verhoog het, maar die diffusiekoëffisiënt verlaag het. Geleidingsvermoë het verbeter met byvoeging van suur maar verlaag met byvoeging van metaalelemente (koper, yster). Die PAM-bymiddel het geen effek op die eienskappe gehad nie. Dis voorgestel dat die byvoeging van hoë atomiese gewig- (koper, yster) elemente digtheid verhoog het terwyl die beweging van ione in die elektroliet belemmer is, waar waterstofione elektrolietgeleidingsvermoë verbeter het. Wiskundige korrelasies vir elke eienskap as ’n funksie van elektrolietkomposisie is ontwikkel en ondersteun deur vorige studies.

Die koperelektroherwinningmodel het uitsette soos spesiekonsentrasie en stroomdistribusie voorspel. Model en eksperimentele stroomdistribusie het goed vergelyk met mekaar. Hoë stroomdigthede is waargeneem naby die katode se bokant en onderkant met relatiewe uniforme distribusie by die katode se

middel. Dis toegeskryf aan die massa-oordragfenomeen, wat ’n laer weerstandpad van ione in hierdie streke gefasiliteer het. Die model het die stroomdigtheidgrootte ondervoorspel, waarskynlik as gevolg van modelbeperkinge.

Die invloed van elektrolietkomposisie op stroomdistribusieprofiel was minimaal, die effek was primêr op die grootte van stroomdigtheid. Eksperimentele en gemodelleerde stroomdigtheid het beide effens verhoog met verhoging in koperkonsentrasie, waar variasie in suurkonsentrasie ’n effense verhoging slegs in eksperimentele stroomdigtheid veroorsaak het, die gemodelleerde stroomdigtheidwaardes het dieselfde gebly.

ACKNOWLEDGEMENTS

I would like to give my sincere gratitude and thanks to the following:

- My supervisor, Dr Margreth Tadie for affording me the opportunity to study. Her support, guidance, encouragement and advice throughout the study was second to none.
- The academic, technical and administrative staff of the Department of Process Engineering for their support during the course of the study.
- Wilhelm Frank Trust and Department of the Process Engineering for the financial support.
- Friends and family for the unfailing support and encouragement throughout the study. Special thanks go to Lister Miselo for always being there for me in highs and lows. I will always be indebted to you
- Lastly, Jehovah God, for giving the strength and unfailing love. Indeed, without you am nothing.

Table of Contents

List of figures

List of tables

Nomenclature

Symbol	Meaning	Unit
a_c	Cathodic charge transfer coefficient	Unitless
a_{Ox}	Activity for oxidized species	Unitless
a_{Red}	Activity for reduced species	Unitless
C_b	Bulk concentration	mol/m^3
C_i or c_i	Concentration of species i	mol/m^3
de or L	Characteristic length	cm or m
D_i	Diffusion coefficient of species i	m^2/s
E	Electrode potential	V
E°	Standard electrode potential	V
E_{cell}	Applied cell potential	V
E_{eq}	Equilibrium potential	V
F	Faraday's constant	C/mol
Gr	Grashof	Dimensionless
I	Current	A
$\boldsymbol{i}$	Current density	A/m^2
$i_\circ$	Exchange current density	A/m^2
i_l	Diffusion limiting current	A
i_{lim}	Limiting current	A
Kd	Mass transfer coefficient	cm/s
m	Mass	g
M	Molar mass	g/mol
$\boldsymbol{N}_i$	Flux density of species i	mol/cm^2.s
$N_{i,diffusion}$	Diffusion flux of species i	mol/cm^2.s
$N_{i,migration}$	Migration flux of species i	mol/cm^2.s
R	Universal gas constant	J/mol.K
R_i	Production/consumption term of species i	mol/s
Sc	Schmidt	Dimensionless
Sh	Sherwood	Dimensionless
t	time	s
T	Temperature	K/°C
u_i	Mobility of species i in the electrolyte	s.mol/kg
v	Velocity of the bulk fluid	cm/s
z_i	Charge of species i in the electrolyte	Unitless
α_a	Anodic charge transfer coefficient	Unitless

γ_i	Activity coefficient of species i	unitless
Γ	Ionic concentration	mol/cm^3 or g/dm^3
η	Overpotential	V
μ or v	Kinematic viscosity	cm^2
ρ	Density	g/cm^3
σ	Conductivity	mS/cm
Φ	Electric field	V
ω	Angular velocity	rad/s

Acronym	**Meaning**
$C.E$	Current Efficiency
$E.C$	Energy Consumption
EW	Electrowinning
LSV	Linear Sweep Voltametry
PAM	Polyacrylamide
RDE	Rotating Disc Electrode
RMSE	Root Mean Square Error
SX	Solvent Extraction

Chapter 1 : Introduction

1.1 Background

Most metals are electro-processed before the required purity is attained. Two processes are usually employed in electro-processing of metals; electrowinning and electrorefining. In the electrowinning process, the metal is recovered from impure feed solution by electrodepositing it on the cathode whereas in electrorefining process an impure anode undergoes electro-dissolution into an electrolyte from which the metal is electrochemically recovered at the cathode (Isakov, 1970; Schlesinger *et al.,* 2011). The choice on whether to select either electrowinning or electrorefining depends on the initial processing route taken when extracting copper. Most sulphide ores are pyrometallurgically treated which requires electrorefining as the final purification method whereas oxide ores are processed through the hydrometallurgical route, with electrowinning as the final processing method.

Over the past decades, there has been an increase in copper produced via hydrometallurgical route. Literature suggests that the growth is due to the following advantages hydrometallurgy offers over pyrometallurgy: low capital investment, little environmental impacts, low energy consumption per cathode and ability to treat low grade ores (Dresher, 2001; Moats & Free, 2007; ICSG, 2018). Despite the growth, the principles, basic equipment and operations of electrowinning have remained the same for a long period (Beukes & Badenhorst, 2009). The increase in copper produced via hydrometallurgy has necessitated investigations on how to improve the quality of the cathodes while optimizing energy utilization and increasing production rate through study of several factors that improve electrowinning performance.

There are several factors that affect the quality of the deposits and energy utilization in electrowinning, among them being the electrolyte composition (Andersen *et al.*, 1973; O'Keefe, 1984; Gupta, 2003; Beukes & Badenhorst, 2009; Khouraibchia & Moats, 2010; Schlesinger *et al.*, 2011; Anderson, 2017). The effect of electrolyte composition on the purity, quality and energy consumption in electrowinning is manifested through their influence on the electrolyte physicochemical properties. Physicochemical properties such as density, viscosity, diffusivity of ions and conductivity influence the mass transfer and electrolyte resistance; subsequently, affecting the carryover of impurities to the cathode surface and deposit quality as well as energy consumption in the cell (Price & Davenport, 1980, 1981.; Moats *et al*., 2000; Subbaiah & Das, 1989, 1994; Panda & Das, 2001; Kalliomäki *et al*., 2016, 2017, 2019).

Another factor which affects the deposit quality is current distribution at the cathode surface. Current distribution plays a vital role in controlling the growth and structure of the cathode. This is cardinal as proper control of growth and structure ensures high quality deposits during the electrodeposition process. Uniform

current distribution improves the performance of the electrochemical cell by producing evenly distributed deposits whereas poor current distribution usually leads to poor electrodeposits and poor energy utilization. Consequently, ensuring uniformly distributed current improves the quality of cathode produced (Popov *et al.*, 2002).

Current distribution is dependent on cell geometry, cell operating conditions, electrolyte conductivity, electrode kinetics and mass transfer of ions and reactants in the electrolyte (Popov *et al.*, 2001; Popov *et al.*, 2011). Electrolyte conductivity, electrode kinetics and mass transfer of ions and reactants in the electrolyte are influenced by the composition of electrolyte as well as operating conditions (Price & Davenport, 1980, 1981.; Moats *et al*., 2000; Subbaiah & Das, 1989, 1994; Panda & Das, 2001; Kalliomäki *et al.*, 2016, 2017, 2019). Therefore, composition of the electrolyte plays a critical role in the mass transfer of electroactive species and how current is distributed in the electrowinning cell. In so doing, affecting the overall electrodeposition process. Therefore, there is a necessity to investigate the influence of electrolyte composition on the current distribution.

1.2 Problem statement

During copper electrodeposition, quality deposits are produced if there is optimal control of growth and structure of deposit. Current distribution over the cathode is most influential factor in controlling the growth and structure of the deposit. As such, studies have been carried out on the effects of cell geometry, electrode configuration and process parameters on current distribution in the electrolytic cell with a view of ensuring smooth, uniform deposits (Shukla, 2013; Robison, 2014; Choi *et al.*, 2015; Werner *et al.*, 2018; Zhang *et al.*, 2018). In these studies, limited investigations were conducted on the effects of electrolyte composition on current distribution.

On the other hand, there are studies investigating the effect of electrolyte composition which have focused on how electrolyte composition, that is, concentration of copper ions, impurities and acid concentration influence physicochemical properties (conductivity, density, viscosity and diffusivity of ions) and electrowinning performance (Kalliomäki *et al.*, 2016; Moats *et al*., 2000; Price & Davenport, 1980, 1981, Subbaiah & Das, 1989, 1994). Despite work on physicochemical properties of copper electrolytes, the influence of additives on the physicochemical properties was not adequately considered as most of these studies were conducted in the absence of the additives used in the electrolytic recovery of copper. Furthermore, these studies have also not considered the impact of these relationships on prediction of deposit formation (modelling) at the cathode.

In view of the said, there is a need to evaluate the existing knowledge through experimental work in order to gain fresh insight on how electrolyte composition in the presence of additive influences the physicochemical properties and current distribution in the cell. This will enhance the understanding of how

electrolyte composition influences the overall electrodeposition process. A computational model will be used to consolidate the understating of the relative influence of chemical factors within the electrowinning process.

1.3 Research aim and objectives

The overall aim of this project is to investigate the influence of electrolyte composition on the electrodeposition process of copper in the electrowinning process. This aim will be achieved by relating the influence of electrolyte composition to physicochemical properties and current distribution in the electrowinning process and utilising fundamental aspects of electrometallurgy to develop an electrowinning model to predict current distribution using COMSOL Multiphysics 5.3a.

The aim will be achieved by fulfilling the following specific objectives:

- Investigating the influence of electrolyte composition in the presence of additive on the electrolyte physicochemical properties.
- Develop mathematical correlations (models) of the electrolyte physicochemical properties as function of electrolyte composition.
- Develop a copper electrowinning model using a finite element analysis software (COMSOL Multiphysics) to investigate the effect of electrolyte composition on current distribution and validating the electrowinning model using experimental work

To accomplish these objectives, the following questions will be addressed:

- How does electrolyte composition affect physicochemical properties of the electrolyte?
- Does the presence of additive have significant effect on the physicochemical properties?
- How does electrolyte composition affect the current distribution and magnitude of current density in electrowinning cell?
- Do the modelled results represent the physical phenomena in electrowinning process?
- Does the electrolyte composition affect current efficiency in the electrodeposition process?

1.4 Research approach

This project was divided into two parts. The first part studied the effects of electrolyte composition on physicochemical properties. Physicochemical properties: density, conductivity, and diffusivity of copper ions

were measured over varying electrolyte composition using a mixed design of experiments with five variables. Density and conductivity were measured using the pycnometer and conductivity meter respectively. Diffusion coefficients of copper ions were determined from the limiting current density values generated using the rotating disk electrode through the application of linear sweep voltammetry technique. Regression models for each property were developed which were used to define the electrolyte properties in the copper electrowinning model.

The second part involved the development of a copper electrowinning computational model using fundamental electrodeposition principles in COMSOL Multiphysics 5.3a. The electrowinning model was used to study the effects of electrolyte composition on current distribution in the cell. Electrowinning experiments were conducted to validate the model performance.

As mentioned in section 1.1, several factors affect the electrodeposition process of copper. The effect of these factors cannot be ignored but it was beyond the scope of the present study to consider all the factors. Therefore, in this study, all other factors were maintained at constant level, only electrolyte composition, that is, copper concentration, sulphuric acid concentration, impurity (iron) concentration and additive (polyacrylamide) concentration were investigated. The decision of the type of polyacrylamide additive (smoothing agent) to use in this work was based on the study conducted by Coetzee (2018). Furthermore, iron was included as an impurity due to its tendency to undergo cyclic oxidation and reduction as well as its effect on reducing current efficiency.

1.5 Thesis outline

Chapter 2 provides a review of the literature relevant to the current study. Chapter 2 begins by laying down the background information on copper processing and electrowinning, as well as fundamentals of electrodeposition processes. It also provides an overview of composition of the electrolytes used in copper electrowinning and their associated physicochemical properties as well as other key factors that affects electrowinning performance. Chapter 2 ends with a discussion on copper electrowinning modelling and current distribution. Chapter 3 presents the experimental framework for the study of the effect of electrolyte composition on physicochemical properties as well as the experimental work for electrowinning tests conducted for validation of a copper electrowinning model established using COMSOL Multiphysics 5.3a.

Chapter 4 presents and discuss the findings of the experimental work of physicochemical properties. Chapter 5 outlines the model development stages of copper electrowinning model as well as the presentation and discussion of the results on modelling and model validation. The thesis ends with the conclusion and recommendation in Chapter 6. The list of the literature used in the current study and supplementary information are provided under references and appendices.

Chapter 2 : Literature Review

This chapter presents the literature relevant to the current study. This chapter begins with a brief background information on copper processing and electrowinning. This is followed by a discussion of electrodeposition process fundamentals, which includes phenomena such as mass transfer and crystallization process (nucleation and growth), electrodeposition thermodynamics and kinetics as well as current efficiency and energy consumption. Thereafter, a detailed discussion of composition of electrolytes and associated physicochemical properties is presented. Afterward, key operating parameters in electrowinning of copper are discussed. The chapter ends with a review of copper electrowinning modelling and a discussion on current distribution in electrochemical cells.

2.1 Background

Copper is considered to be one of the first metals to be used by humans with its usage dating more than 7000 years ago (Radetzki, 2009). In its early production, it was predominantly used for decorative purposes, coinage and in warfare but with technical breakthroughs like smelting and alloying, its production and usage has expanded (Radetzki, 2009). Traditionally, copper is extracted from copper-bearing ores with a considerable amount produced from copper scrap. Copper ores exist either as sulphide or oxide ores. Sulphide minerals are processed via pyrometallurgical route which involves concentration, smelting, and electrorefining whereas oxide ores are hydrometallurgically treated. Over the years, hydrometallurgy has undergone considerable growth such that at least 20% of world copper is hydrometallurgically produced (Moats & Free, 2007; Robinson *et al.*, 2013; ICSG, 2018).

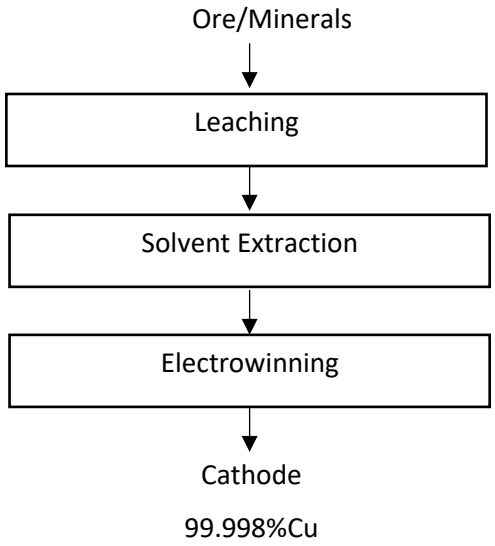

Figure 2.1: Flowchart of the conventional hydrometallurgical route for copper processing (Adapted from Schlesinger et al, 2011)

Figure 2.1 shows the flowsheet for the hydrometallurgical copper processing route. The conventional hydrometallurgical route involves leaching, solvent extraction (SX), and electrowinning (EW), though in certain operations copper can be electrowon directly from the pregnant leach solution. Copper is leached from ores/minerals to produce an impure copper-bearing aqueous solution, which is concentrated and purified to a certain degree via solvent extraction to produce feed solution for electrowinning copper (Schlesinger *et al.*, 2011). Since this work focus on copper electrowinning, the following section provides a description of copper electrowinning.

2.2 Copper Electrowinning

Copper electrowinning is an electrolytic processing method in which copper is recovered from an impure electrolyte (from SX or leaching) by applying an external current and electrodepositing it on the cathode using an inert anode. In simple terms, electrowinning (EW) involves supplying the impure electrolyte to the cell, applying an external electric current to the cell through electrodes submerged in the electrolyte and depositing the pure copper from the electrolyte onto the cathode. The electrowon copper is either melted, cast and stored or processed further for various applications (Schlesinger *et al.*, 2011).

The electrolyte is mainly composed of copper ions, usually in the form of speciated copper sulphate (Cu^{2+} and SO_4^{2-}), sulphuric acid (H_2SO_4), impurities (metallic, entrapped organics and suspended solids) and additives which act as smoothing and levelling agents (Andersen *et al.*, 1973; O'Keefe, 1984; Aromaa, 2007; Schlesinger *et al.*, 2011; Robinson *et al.*, 2013). The anodes are made from inert but conductive material usually cold rolled Pb-Sn-Ca alloy and cathodes are usually 316L stainless steel blanks (Robinson *et al.*, 2013). These electrodes are connected to an external direct current source which causes current to flow through the electrolyte. The anode becomes positive while the cathode becomes negative. As a result, Cu^{2+} ions migrate under the influence of applied current by diffusion and convection to the cathode surface, where they are reduced and electrodeposited as copper metal (Gupta, 2003; Schlesinger *et al.,* 2011). The goal of the electrowinning process is to produce high quality copper at the fastest rate while minimizing energy consumption.

According to Schlesinger *et al.,* (2011), industrial electrowinning cells consist of approximately 60-84 pairs of anodes and cathodes per cell connected in parallel whereas the cells are connected in series. Typical materials for cell construction includes pre-cast polymer concrete or reinforced concrete with a chemically resistant lining (Gupta, 2003; Schlesinger *et al.*, 2011; Robinson *et al.*, 2013). Beukes and Badenhorst (2009) as well as Schlesinger *et al.,* (2011) indicate that the spacing between the electrodes and efficient circulation and flow of electrolyte contribute to the quality of the electrodeposited copper at the cathode (Beukes & Badenhorst, 2009; Schlesinger *et al.*, 2011). Copper is plated onto the cathodes for 6-7 days, after which the cathodes are removed from the cell, stripped from the 316L stainless steel cathode, washed, packed,

strapped and sent to market. The stainless steel blanks are taken back to the cells (Schlesinger *et al.,* 2011). Figure 2.2 below represents a simplified electrowinning cell with a pair of electrodes.

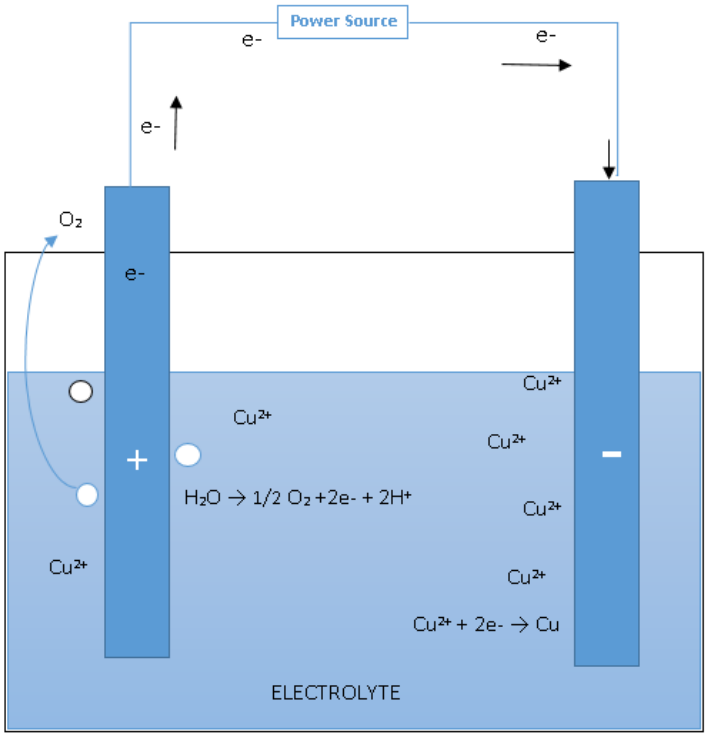

Figure 2.2: Schematic representation of an electrowinning cell for copper deposition

During copper electrowinning, two principal reactions takes place. Copper ions transfer through the electrolyte by migration, diffusion and convection to the cathode surface where they gain the electrons and are reduced as per equation 2.1

$$Cu^{2+}(aq) + 2e^{-} \longrightarrow Cu^{\circ}(s) \qquad E^{\circ} = +0.34V \qquad 2.1$$

At the anode, water decomposes evolving oxygen gas, which is released to the atmosphere as described by equation 2.2

$$H_2O\ (l) \rightarrow H^{+}(aq) + OH^{-}(aq) \rightarrow \frac{1}{2}O_2(g) + 2H^{+}(aq) + 2e^{-} \qquad E^{\circ} = -1.23V \qquad 2.2$$

The overall electrodeposition reaction for copper electrowinning in the presence of sulphate ions is given as:

$$Cu^{2+}(aq) + SO_4^{2-}(aq) + H_2O\ (l) \rightarrow Cu^{\circ}(s) + \frac{1}{2}O_2(g) + 2H^{+}(aq) + SO_4^{2-}(aq) \quad E^{\circ} = -0.89V \qquad 2.3$$

Equation 2.3 shows that apart from oxygen evolution and copper reduction, there is regeneration of acid during electrowinning process. The acid is usually recirculated to the leaching stage.

The reduction of copper is a heterogeneous reaction. It involves the transfer of charge between the electrode and copper ions at the electrode/electrolyte interface, called the double layer. Before the copper ions are reduced at the cathode, they undergo certain steps. The ions move from the bulk of electrolyte through migration, convection and diffusion to the electrode surface where charge transfer occurs. Then, they undergo surface diffusion, nucleation and growth as illustrated in the equation 2.4 and 2.5.

$$Cu^{2+}_{(bulk)} \rightarrow Cu^{2+}_{surf} \qquad 2.4$$

$$Cu^{2+} + 2e^{-} \rightarrow Cu^{0}_{(surf)} \qquad 2.5$$

Electrowinning is based on the principles of electrodeposition. Therefore, it is compelling to review the electrodeposition process.

2.3 Electrodeposition Process

Bard *et al.* (2008) define electrodeposition as "a process of forming a film or a bulk material using an electrochemical process where electrons are supplied by an external power supply" (Bard *et al.,* 2008). In other words, it is a process in which a solid phase is deposited on a material immersed in an ionic conducting electrolyte in contact with an electrical field (Fabian, 2005). The electric current flows between the electrodes in the presence of an external voltage, the electrons move via the electrical components whereas ions move in the electrolyte towards the electrode surface where redox reactions occur (Newman & Thomas-Alyea, 2004). The electrochemical reaction takes place at the electrode/electrolyte interface and charge transfer occurs between the electroactive species and the electrode. Electrodeposition uniformity depends on the distribution of electric current inside the electrolyte towards the surface of the electrode, smoothing agents, mass transfer of species inside the electrolyte and rate of electrochemical reactions (Muhlare & Groot, 2011; Schlesinger *et al.*, 2011).

The metal electrodeposition basically involves mass transfer, charge transfer, and nucleation and growth of the crystal structure in the presence of electric field. Pasa and Munford (2006) proposed the steps involved in electrodeposition process as transfer of electroactive species from the electrolyte (bulk solution) to reaction interface, adsorption of metal species and charge transfer, and crystallization to produce a metal deposit (Pasa & Munford, 2006). The electrodeposition stages were clearly outlined by Budevski *et al.* (1996) and Fabian (2005) as follows:

- Mass transfer of electroactive species through migration, diffusion and convection from the electrolyte to the electrode surface (electrolyte/electrode interface).
- Adsorption and charge transfer on the electrode/electrolyte interface to form metal adatoms.
- Crystallization through nucleation and growth to form a metal phase on the electrode surface via two -dimensional (2D) or three-dimensional (3D) growth.

The stages in electrodeposition process, which are mass transfer of electroactive species to the electrolyte-electrode interface, formation of metal adatoms through adsorption and charge transfer and crystallization (nucleation and growth) are illustrated in Figure 2.3.

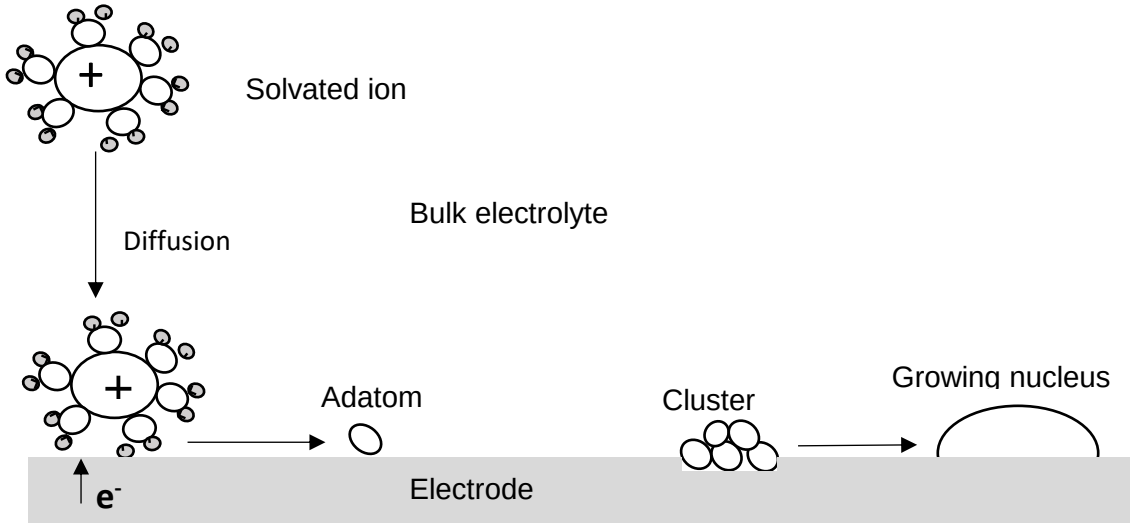

Figure 2.3: Illustration of mechanism of electrodeposition showing nucleation and growth during metal electrodeposition (Adapted from Pasa & Munford, 2006)

2.3.1 Mass transport

Mass transport plays a vital role in the electrodeposition process as it constitutes the first step of the electrodeposition process. As mentioned in the preceding section, ions in the electrolyte need to be transported to the surface of the electrode for the redox reactions to take place. This is accomplished through three mass transfer mechanisms: migration, diffusion, and convection (Newman & Thomas-Alyea, 2004).

Migration is the movement of charged particles in the presence of applied electric field. The electric field creates a driving force for the motion of all ions in solution. When an electric voltage is applied to electrodes in an electrolyte, cations are driven towards the cathode and anions to the anode. The transport of ions by migration mainly occurs in the bulk of the electrolyte. The migration flux density, $N_{i,migration}$ is given as:

$$N_{i,migration} = -z_i u_i F c_i \nabla \Phi \quad 2.6$$

where z_i is the charge of species i in the electrolyte (unitless), u_i is the mobility of species i in the electrolyte (s.mol/kg), F is the Faraday's constant, c_i is the concentration of species i (mol/m^3) and $\nabla \Phi$ is the electric field (V).

Electrochemical reactions at the electrode surface induce changes in concentration across the electrolyte. The variation in electrolyte concentration results in concentration gradients which drives the movement of ions in the electrolyte from a region of high concentration to a region of lower concentration by the process called diffusion (Bard & Faulkner, 2000). Diffusion is predominant near the electrode surface (diffusion layer) in comparison to the bulk electrolyte due to the consumption of ions at the electrode surface. The component of the flux density of a species due to diffusion, $N_{i,diffusion}$ is described by Fick's first law:

$$N_{i,diffusion} = -D_i \nabla c_i \quad 2.7$$

where D_i is the diffusion coefficient (m^2/s) and the other term as defined in equation 2.6.

Convection is the mass transport of species in the electrolyte due to bulk movement of the fluid which can be forced or natural flow (Beukes & Badenhorst, 2009). Natural convection is as a result of density gradients due to concentration or temperature variations in the electrolyte (Pasa & Munford, 2006). The flux density of species by convection, $N_{i,convection}$ is given as:

$$N_{i,convection} = c_i \boldsymbol{v} \quad 2.8$$

where $\boldsymbol{v}$ is the velocity of the bulk fluid (m/s) and the other term as defined in equation 2.6

The net flux density of species i, $\boldsymbol{N}_i$ is given by the combination of migration, diffusion, and convection:

$$\boldsymbol{N}_i = -z_i u_i F c_i \nabla \Phi - \boldsymbol{D}_i \nabla c_i + c_i \boldsymbol{v} \quad 2.9$$

where the terms are defined in equation 2.6

Equation 2.9 is the simplified form of the Nernst-Plank equation. This equation describes the total mass transport in the electrolyte (Newman & Thomas-Alyea, 2004).

The transient material balance is given by:

$$\frac{\partial c_i}{\partial t} = -\nabla . N_i + R_i \qquad 2.10$$

where $\frac{\partial c_i}{\partial t}$ is the accumulation rate, $\nabla . N_i$ is the net input differential volume element and R_i is the production/consumption term.

In most electrochemical processes, a supporting electrolyte such as an acid is added to the system to increase electrolyte conductivity. The presence of supporting electrolyte reduces the effects of migration in the bulk of the electrolyte. At the same time, in the bulk of the electrolyte, electroneutrality condition exists except in the double layer region (nanometres to the electrode surface). The electroneutrality condition and supporting electrolyte makes it possible to neglect the effect of migration on the system. Consequently, mass transfer in the system can be assumed to occur mainly by diffusion and convection and commonly referred to as convective-diffusion mass transfer. Thus, the equation 2.10 can be represented as:

$$\frac{\partial c_i}{\partial t} + \boldsymbol{v} . \nabla . c_i = D_i \nabla^2 c_i \qquad 2.11$$

2.3.2 Nucleation and growth of deposit

Nucleation is the first step in the crystallization process (growth of the deposit). This process begins when electroactive species are transported to the electrode surface where charge transfer takes place to form an adatom and adsorbed on the surface of the electrode (Pasa & Munford, 2006). The adatom then travels to favourable nucleation sites via surface diffusion to form a nucleus and grains that grow into deposits as earlier depicted in Figure 2.3. Nucleation can be divided into two categories: primary and secondary nucleation (Gebbie, 2013).

Primary nucleation occurs on the electrode surface where there was no previously formed crystalline material. Primary nucleation is divided into two categories: homogeneous and heterogeneous nucleation. The difference between these two types of primary nucleation lies on the substrate onto which the nucleation occurs. For homogenous nucleation, small clusters of molecules or atoms are formed spontaneously at the electrode surface without foreign particles or a defect on the electrode surface playing any role in the nucleation process. The nucleation occurs through a spontaneous arrangement of molecules which results in the formation of small clusters. On the other hand, heterogeneous nucleation takes place on the foreign substrate or defects on the electrode surface. Note that not all substrates aid nucleation, some inhibit the nucleation process. Between the two primary nucleation processes, heterogeneous nucleation is likely to occur compared to homogenous nucleation. Gebbie (2013) alluded to the presence of foreign

substrate which decreases the surface free energy, thereby reducing the critical Gibbs free energy required to drive the electrodeposition reaction as the reason heterogeneous nucleation is favoured.

According to Gebbie (2013), secondary nucleation occurs when a seed crystal is introduced in the electrolyte to aid the growth of new crystals. The nucleation process occurs on the introduced seed crystal which is later proceeded by growth of the deposit. Gebbie (2013) also states that the introduction of the seed crystal lowers the surface energy, thereby making secondary nucleation more favourable compared to primary nucleation. This is because the substrate being used is identical to the material that is being crystallised.

The formed nuclei need to undergo growth for the deposit to mature. The growth of the deposits is only possible if the clusters formed reaches a critical size. Crystal growth, the second stage in crystallization begins when the formed nuclei act as secondary sites for further nucleation. This results in the formation of larger crystals as newly formed crystals are incorporated in the crystal surface. Gebbie (2013) outlined the steps involved in crystal growth, which are similar to the nucleation steps given by Pasa and Munford (2006) as: "transport of growth units in solution, adsorption of growth units onto the surface, movement of growth units around the surface and attachment of growth units to surface site."

The structure and morphology of the deposits depend on the nucleation and growth rates. When nucleation is favoured over crystal growth, fine crystallite sizes are obtained. Hence, the kinetics of nucleation and growth are influential in determining deposit morphology and quality as well as the overall electrodeposition process.

2.3.3 Electrodeposition Thermodynamics

As mentioned at the onset of section 2.3, electric potential is applied to the electrodes immersed in an electrolyte for electrodeposition to occur. A potential difference exists between the immersed electrodes which acts as the driving force for the electrochemical reaction similar to Gibbs free energy in thermodynamics reaction. Nernst developed a relationship to determine the potential of an electrode by manipulating Gibbs free energy relationship called the Nernst equation, and its derivation is well documented in the literature (Bard & Faulkner, 2000). The Nernst equation enables the potential of the half-cell reaction at the electrode to be calculated. The Nernst equation is given as:

$$E = E^{\circ} + \frac{RT}{nF} ln \frac{{a_{Ox}}^{m}}{{a_{Red}}^{n}} \qquad 2.12$$

Where E is the electrode potential (V), E° is the standard electrode potential (V), *R* is universal gas constant (J / (mol.K)), *T* is the temperature (K), *n* is the number of electrons (dimensionless), *F* is the Faraday's constant (C/mol), a_{Ox} is the activity for oxidized species (dimensionless), a_{Red} is the activity for reduced

species(dimensionless), m is the stoichiometric coefficient for the oxidized species (dimensionless) and n is the stoichiometric coefficient for the reduced species (dimensionless).

The standard electrode potential is the potential of the electrode reaction at standard conditions and the values for various reactions are available in the literature (usually given as standard reduction potentials)(Bunker & Casey, 2016). The Nernst equation is one of the fundamental equations in electrochemical processes as it enables the determination of the cell potential for the electrodeposition process. The cell potential can be calculated as the difference between the cathodic and anodic half-cell potential:

$$E_{cell} = E_{cathode} - E_{anodic} \tag{2.13}$$

where $E_{cathode}$ is the cathodic half-cell potential and E_{anodic} is the anodic half-cell potential

The cell potential calculated utilizing the Nernst equation is equivalent to the equilibrium potential of a cell at non-standard conditions. In practical situations, however, there is deviation of cell potential from its equilibrium value due to electrode polarization. By definition, polarization is the deviation in electrode potential from the equilibrium half-cell potential. Electrode polarization can be anodic or cathodic and may cause the cell potential to increase, requiring additional potential to be applied to the system for the electrochemical reaction to occur (Aromaa, 2007). The additional applied potential is called overpotential and measures the degree of electrode polarization. The overpotential can be due to kinetic overpotential (charge transfer), concentration overpotential (diffusion), ohmic overpotential (electrical resistance) or adsorption overpotential due to the presence of additives (Bard & Faulkner, 2000; Moats, 2012). The overall overpotential, η is given as:

$$\eta = E_{cell} - E_{eq} \tag{2.14}$$

Where E_{cell} is the applied cell potential (V) and E_{eq} is the equilibrium potential (V)

Equation 2.14 indicates that overpotential is necessary for the electrodeposition to occur. Note that in equation 2.13, the cell potential was given as the difference between the two half-cell reactions. Due to polarization and the potential drop in the system, there is an increase in cell potential. Consequently, the applied potential is given as the sum of all the individual potential as indicated in equation 2.15.

$$E_{cell} = E_{cathode} - E_{anodic} + \eta_{anodic} + \eta_{cathodic} + IR_{electrolyte} + IR_{circuit} \tag{2.15}$$

Where $E_{cathode}$ is the cathodic half-cell potential, E_{anodic} is the anodic half-cell potential, η_{anodic} is the anodic overpotential, $\eta_{cathodic}$ is the cathodic overpotential, $IR_{electrolyte}$ is the ohmic drop due to electrolyte resistance, and $IR_{circuit}$ is the ohmic drop through electrical components.

2.3.4 Electrodeposition Kinetics

The electrochemical thermodynamics provides the information on the possibility of the electrochemical reaction to occur. A kinetic relationship is required to predict the rate of the electrochemical reaction. According to Newman and Thomas-Alyea (2004), the rate of the electrodeposition reaction is measured by the current density and is related to the overpotential, η as follows:

$$\boldsymbol{i} = i_{\circ}\left(exp^{\left(\frac{\alpha_a nF\eta}{RT}\right)} - exp^{\left(\frac{-\alpha_c nF\eta}{RT}\right)}\right) \qquad 2.16$$

where i is the current density (A/m^2), $i_{\circ}$ is the exchange current density (A/m^2), η is the overpotential (V), α_a is the anodic charge transfer coefficient (unitless), α_c is the cathodic charge transfer coefficient (unitless), n is the number of electrons transferred (unitless), F is the Faraday's constant (C/mol), *R* is universal gas constant (J / (mole. K)) and *T* is the temperature (K).

Equation 2.16 is known as the Butler-Volmer equation. The first and second terms are rates for anodic and cathodic direction respectively with the difference being the net rate of reaction (Newman & Thomas-Alyea, 2004). In its indicated form, equation 2.16 does not account for mass transfer limitations in the electrochemical cell. Studies have shown that mass transfer is the rate-determining step as there is a deficit of reactants at the electrode surface as they are consumed during the reaction whereas electrons are readily available necessitating the incorporation of mass transfer limitations in the Butler-Volmer equation as indicated by equation 2.17:

$$i_{loc} = i_0\left(C_R exp\left(\frac{\alpha_a nF\eta}{RT}\right) - C_O\left(\frac{-\alpha_c nF\eta}{RT}\right)\right) \qquad 2.17$$

where C_R and C_O are dimensionless expressions, describing the dependence on the reduced and oxidized species in the reaction.

2.3.5 Quantity of the deposit

The amount of the deposited material can be derived from the quantity of electricity used as expressed by Faraday's law (Schlesinger *et al.,* 2011). Thus, the mass of deposited metal, m is given by:

$$m = \frac{MIt}{nF} \quad 2.18$$

where M is the molar mass (g/mol), I is the current passed (A), t is the time (s), and n is the number of electrons transferred (unitless) and F is the Faraday's constant (C/mol).

Equation 2.18 represents the theoretical mass. This is because in practical situations, not all the current is used to deposit the metal. Current is lost due to side reactions and ohmic drop through electrolyte and electrical components resistance as well as short circuiting in the system. As such, the current efficiency must be factored in when calculating the actual deposited weight.

The Faraday's law can be utilized to determine the average thickness of the deposit using the modified equation:

$$\tau = \frac{m}{a \times \rho} \quad 2.19$$

where τ is the thickness (cm), a is the plated area (cm^2) and ρ is the density of plated metal (g/cm^3).

2.3.6 Current Efficiency

Current efficiency is the ratio of electrical charge used to deposit the required product to the total charge passed during the electrochemical deposition. The current efficiency (C.E.) is usually expressed as the ratio of actual mass of the deposit to the theoretical mass:

$$C.E.(\xi) = \frac{m_{actual}}{m_{theoretical}} \quad 2.20$$

The theoretical mass is calculated using equation 2.18 and the actual mass is measured from the electrodeposit produced.

2.3.7 Energy consumption

Energy consumption in electrolytic deposition is usually expressed as specific energy consumption, that is, the electrical energy consumed per mass of deposit produced, and is given as follows:

$$E.C. = \frac{nFE_{cell}}{\xi m} \quad 2.21$$

where n is the number of electrons involved in the electrochemical reaction, F is the Faraday constant, E_{cell} is the cell voltage (V), and ξ is the current efficiency (%) and m is the mass of deposit.

2.4 Copper electrolytes

The composition and nature of the electrolytes play a significant role in the electrodeposition process. The electrolyte is usually composed of metal ion, a supporting electrolyte (usually an acid), impurities, inorganic additives (Cl^-, Co^{2+}), organic additives (smoothing, and levelling agents) and suspended solids which each having a unique role (O'Keefe, 1984). As Aromaa (2007) puts it, the electrolyte component can have either a positive or negative effect on the quality of the electrodeposit in electrolytic processing of metals. Table 2.1 summarizes the role of each component of the electrolyte in the electrolytic processing.

Table 2.1:Electrolyte components and their role in electrowinning (O'Keefe, 1984)

Component	Role
Metal ion	Source of metal
Supporting electrolyte	Conductivity and pH control
Impurities	Detrimental to efficiency or purity
Inorganic additives	Assist anode life and cathode quality
Organic additives	Cathode morphology and mist suppressor
Suspended solids	Incorporation into cathode deposits

Copper can be electrodeposited from several electrolyte systems such as acidified copper sulphate, cyanide copper, and pyrophosphate electrolytes (Aromaa, 2007). Since acidified copper sulphate electrolyte is commonly found in copper electrowinning, it will be the focus of this discussion. For information on the other copper electrolyte systems, refer to the works Dini and Snyder (2011) and Aromaa (2007).

2.4.1 Composition of copper electrolytes

Copper electrowinning electrolytes are composed of aqueous solutions of copper ions, sulphuric acid, impurities and smoothing agents (Schlesinger *et al.,* 2011). For the SX-EW route, the feed electrowinning electrolyte is made by combining advance electrolyte from the SX process and a bleed of spent electrolyte

from electrowinning process. Additives such as guar gum are added to promote smooth and dense deposits. Common impurities include iron, which is usually present as ferrous (Fe^{2+}) or ferric (Fe^{3+}) iron and manganese. Other inorganic elements such as chloride ions and cobalt ions may be present in the electrolyte either occurring naturally or deliberately added as HCl acid or cobalt sulphate to improve the efficiency of the electrowinning process (Dini & Snyder, 2011; Schlesinger *et al.,* 2011). In addition to metallic impurities, the electrolyte may also contain entrained solvent and solid particulates from the subsequent processes. The presence of impurities and solid matter may affect mass transfer and deposit quality especially if impurity build up occurs (Subbaiah & Das, 1994). Table 2.2 below shows the composition of different industrial electrolytes across the world.

Table 2.2: Electrowinning electrolytes from different parts of the world (Robinson et al., 2013)

	Advanced electrolyte		**Spent Electrolyte**			
Location	Cu(g/l)	H_2SO_4(g/l)	Fe(g/l)	Co(mg/l)	Mn(mg/l)	Cl(mg/l)
N. America with SX	40.6	175	2.7	114	106	23
S. America with SX	41.6	180	1.6	180	53	21
Europe with SX	34.7	175	2.0	80	-	20
Europe direct EW	70.0	90	0.5	3000	10	60
Africa with SX	49.3	171	2.8	1500	670	25
Africa direct EW	56.8	42	3.7	5850	-	35

Components of copper electrolytes has been a subject of investigation for many researchers. These studies have been conducted with a view of improving electrowinning performance, deposit quality and energy utilization in the electrolytic recovery of copper(Andersen *et al.,* 1973; O'Keefe, 1984; Subbaiah & Das, 1994; Owais, 2009; Anderson, 2017). Thus. this section is dedicated to discussing the electrolyte components relation to the electrodeposition of copper, in terms of cathode quality, energy consumption and current efficiency. The relationship of individual electrolyte components to electrodeposition will be discussed separately. Then, section 2.4.2 will focus on copper electrolyte physicochemical properties. It should be mentioned that some of the information between these two sections are intertwined. If such is the case, the information will only be covered in one section.

2.4.1.1 Copper

Copper ions are the source of the metal in electrowinning process. Krishna and Das (1992) studied the effect of copper concentration ranging from 30 to 40 g/l on the current efficiency and copper deposit quality in a copper electrowinning cell so as to enhance operating current density. The work of Krishna and Das (1992) indicates that compact deposits were achieved by raising the copper concentration in the electrolyte (Krishna & Das, 1992). In another study, Das and Krishna (1996) make another observation of the effect of copper concentration on electrowinning. By investigating the effect of copper concentration from 17 to 37 g/l, Das and Krishna (1996) observed that an increase in copper concentration resulted in a slight increase in the current efficiency whereas power consumption increased with decrease in copper concentration. The aforementioned study also noted that the current efficiency fell with decreasing copper. Das and Krishna (1996) alluded this effect to the changes in physicochemical properties (Das & Krishna, 1996).

Although Owais (2009) work focused on copper powder production at lower copper concentration (5 to 15 g/l Cu), the results indicate that better current efficiency and low specific energy demand was achieved at higher copper concentration. The reason given was that the increase in copper ion concentration in the electrolyte, feeds a sufficient and constant amount copper ion to the cathode surface; thereby, improving the deposition rate and consequently the efficiency. It was also noted by Owais (2009) that increase in copper concentration leads to the decrease in concentration polarization as well as decrease in hydrogen overvoltage. An increase in hydrogen overvoltage results in increased cell voltage, thereby affecting energy consumption (Owais 2009). Khouraibchia and Moats (2009) also observed a slight increase in current efficiency and reduction in energy consumption with increase in copper concentration. However, it was suggested by Khouraibchia and Moats (2009) that the energy consumption may increase at higher copper concentration once a certain concentration limit is reached (Khouraibchia & Moats, 2009).

Panda and Das (2001) investigated the effect of copper concentration (10-50 g/l) on cell voltage, anode potential and power consumption during electrowinning of copper in the presence of sulphur dioxide. Their results show that at low concentration, the cell voltage was relatively high whereas on increasing the concentration above 30 g/l, the cell voltage remained constant. However, Panda and Das (2001) observed that power consumption was independent of copper concentration, that is, no significant variation in the power consumption was observed as the copper concentration was being varied (Panda & Das, 2001).

2.4.1.2 Sulphuric acid

Sulphuric acid is added to the electrolyte to improve the conductivity. The work of Das and Krishna (1996) revealed that an increase in sulphuric acid concentration resulted in increase in current efficiency and decrease in power consumption. Their results also show that at 30°C, the current efficiency remained relative the same when the concentration of acid was varied (Das & Krishna, 1996). Similar outcome was observed

by Owais (2009) in which the concentration of H_2SO_4 was varied from 50 to 300 g/l. Owais (2009) reports that the increase in sulphuric acid resulted in increased current efficiency, productivity and yield. At the same time, the decrease in cell voltage and specific energy demand were observed. Owais (2009) attributed this to improved electrolyte conductivity and improved dissolution of Cu ions in the electrolyte. The increase in viscosity and decrease in diffusivity of copper ions due to the increase in sulphuric acid concentration in the electrolyte was also observed (Owais, 2009).

Khouraibchia and Moats (2009) also observed a slight increase in current efficiency as acid concentration was varied from 160 to 220 g/l whereas energy consumption remained the same with variation of sulphuric acid concentration (Khouraibchia & Moats, 2009). The effect of sulphuric acid concentration during copper electrowinning was also studied by Panda and Das (2001) in the range of 30 to 150 g/l. Panda and Das (2001) observed a marginal drop in cell voltage and anode potential as acid concentration was increased. Panda and Das (2001) also indicates that no changes in current efficiency or energy consumption as sulphuric acid concentration was varied (Panda & Das, 2001).

2.4.1.3 Iron

Copper electrowinning electrolytes may contain certain amounts of iron, either as ferric or ferrous ions. This is the case regardless of whether it is direct electrowinning or electrowinning is preceded by solvent extraction (Robinson *et al.*, 2013). Presence of iron in the electrolyte cause loss in current efficiency and often produces poor quality cathode copper as well as increase in power consumption (Das & Krishna, 1996). This is due to the cyclic reduction and oxidation of ferric and ferrous at the cathode and anode respectively, which results in the loss of current. In their work, Das and Krishna (1996) observed that increasing the ratio of ferrous to ferric iron in the electrolyte aided in improving the current efficiency. The reason provided was that addition of ferric ions to the electrolyte helped in counteracting the effect of ferric in electrowinning. Das and Krishna (1996) observed that the addition of ferrous to the electrolyte when ferric was present improved the quality of the deposit (Das & Krishna, 1996).

The results of Khouraibchia and Moats (2009) showed a significant drop in current efficiency as well as an increase in energy consumption when iron concentration was varied from 0 to 6 g/l. The above-mentioned study further notes that the variation in iron concentration did not affect the cell voltage; thus, it was concluded that the increase in energy consumption was as a result of the drop in current efficiency (Khouraibchia & Moats, 2009). Apart from loss of current efficiency, the presence of ferric in the electrolyte can lead to localised corrosion of the deposit especially in places where the diffusion of ferric is higher (Pradhan *et al.*, 1998). Subbaiah and Das (1994) showed that viscosity, density and limiting current increased with increase in ferrous and ferric concentration in the electrolyte, but the conductivity decreased as concentration was increased (Subbaiah & Das, 1994).

2.4.1.4 Cobalt

According to Nikoloski and Nicol (2008), the presence of cobalt ions in the electrolyte promotes oxygen evolution by decreasing its overpotential at the anode. Huang *et al.* (2010) explained that the reduction in oxygen overpotential is due to the reactions which occurs in the presence of cobalt ions. The oxidation of cobalt ions at the anode allows the facile oxidation of water leading to lower oxygen over-potential (Huang *et al.,* 2010). This stabilizes the lead oxide layer on the anode surface. As a result, cobalt minimizes the lead corrosion of the anode, thereby, improving the cathode quality through reduction in lead contamination (Nikoloski & Nicol, 2008; Huang, *et al.,* 2010). Khouraibchia and Moats (2009) did investigate the effect of cobalt on energy consumption. Their results indicate cobalt ions had no effect on energy consumption (100 to 200ppm) in these range (Khouraibchia & Moats, 2009).

2.4.1.5 Chloride ions

Chloride ions may be present in the electrolyte naturally (transferred from the SX stage) or deliberately added as HCl. Chloride ions acts as grain refiners as well as depolarizers (Dini & Snyder, 2011; Moats *et al.,*2016). According to Robinson *et al.*, (2013), the concentration of chloride ions should range between 20 to 30 mg/l. This is because excess chloride concentration can lead localized corrosion of the cathodes (Robinson *et al.*, 2013). Furthermore, increase of chloride ions may lead to enhanced surface roughness and impurity levels on the cathode. As shown by Fabian (2005), chloride ions must be used together with polarizing organic additive in order not to compromise cathode quality.

2.4.1.6 Manganese

Subbaiah and Das (1994) investigated the effect of impurities, including manganese on mass transfer coefficient and deposit quality during copper electrowinning. The effect of manganese was seen in physicochemical properties in which density and viscosity of copper electrolyte increased, and conductivity decreased as the manganous ion concentration was raised. Subbaiah and Das (1994) further reports that the interaction of manganous ion may cause the limiting current density as well as mass transfer coefficient to increase at lower concentration and decrease at higher concentration. In their work, the limiting current density increased until the concentration of manganous reached 5 g/l, after which it dropped with increase in manganous concentration. This was also the case with mass transfer coefficient (Subbaiah and Das, 1994). The effect of manganous concentration on energy was investigated by Khouraibchia and Moats (2009). Their results indicate that manganese concentration (10 to 170ppm) had no effect on energy consumption (Khouraibchia & Moats, 2009).

2.4.1.7 Nickel

The work of Subbaiah and Das (1994) shows that increase in nickel concentrations resulted in decrease in limiting current density. Nickel concentration also affects the electrolyte properties. In the case of Subbaiah and Das (1994), they observed that the viscosity and density increased, whereas the conductivity and mass transfer coefficient decreased with increase in nickel ion concentrations in the electrolyte (Subbaiah & Das, 1994).

2.4.1.8 Additives

Although the concentration of additive in the electrolyte is orders of magnitude less than the other components such as copper, they have profound effect on the electrodeposition through levelling and grain refinement (Andersen *et al.,* 1973). The presence of organic additives in the electrolyte can change the structure and properties such that considerable research has been devoted to additives (Vereecken & Winand, 1976; Rusli *et al.*, 2007). As noted by Robinson *et al.*, (2013), organic additives in the electrolyte ensures that smooth, compact and void free copper cathodes as well as impurity free copper deposits are produced. The production of smooth cathode minimizes the risk of short circuiting as well as reduces energy consumption.

2.4.2 Electrolyte physicochemical properties.

Various studies have been conducted to investigate the interrelation between electrolyte composition and electrolyte physicochemical properties, namely conductivity, density and viscosity as well as the diffusivity of copper ions (Price & Davenport, 1980, 1981; Subbaiah & Das, 1989; Krzyzak *et al.*, 2007; Moats *et al*., 2000; Kalliomaki *et al.*, 2016, 2017, 2019). This is because the physicochemical properties significantly affect the energy consumption and the quality of the cathode product (Subbaiah & Das, 1989). As reported by Price and Davenport (1980, 1981), density and viscosity affect the heat and mass transfer conditions in the cell and thereby determining purity of the deposited metal while conductivity affects the current efficiency and the energy consumption. This section addresses the physicochemical properties of copper electrolytes in relation to composition of electrolyte. The discussion is not limited to copper electrowinning electrolytes but extend to studies on copper electrorefining electrolytes.

2.4.2.1 Density

Density has a considerable effect on the purity of cathode copper and the energy consumption due to its effect on the mass and heat transfer. According to Moats *et al.* (2000), decreasing density increases the mass transfer rate since the diffusivity and mobility of ions increase. Thus, lowering density increases the diffusion coefficient of cupric ion. The work of Price and Davenport (1980, 1981), Subbaiah and Das (1989) and

Kalliomäki *et al.* (2016, 2017) indicate that the density of the electrolyte increases with increase in copper and acid concentration and decreases with increase in temperature.

Different authors have developed mathematical equations relating electrolyte composition to density. For example, Price and Davenport (1981) developed a mathematical model for densities given as:

$$Absolute\ Density = 1.022 + 10^{-3}\begin{pmatrix} 1.04[As] + 2.24[Cu] + 2.37[Fe] \\ +0.55[H_2SO_4] + 2.24[Ni] - 0.58T \end{pmatrix} \quad 2.22$$

Where [X] represents the concentration of species X (g/dm^3) and T is the temperature in °C

Furthermore, Price and Davenport (1981) utilizing the results from their work and results of Classsens (1967) came up with a combined equation:

$$Absolute\ density = 1.02 + 10^{-3}\begin{pmatrix} 2[Cu + Co + Fe + Ni + Na] + 1[As] \\ +3[Mg] + 6[Al] + 0.5[H_2SO_4] - 0.6T \end{pmatrix} \quad 2.23$$

Kalliomäki *et al.* (2016) also developed a mathematical model for density and viscosity for synthetic electrorefining electrolytes by exploring possible interaction effects between the factors. The results of the aforementioned study were in agreement with earlier studies conducted by Price and Davenport (1981) and Subbaiah and Das (1989).

It can be seen that from the equations given by Price and Davenport (1981) as well as Subbaiah and Das (1989), the addition of metallic and sulphate ions in the system led to an increase in density whereas the increase in temperature reduced the density of the electrolyte.

2.4.2.2 Viscosity

Viscosity and density influence the mass transfer of the ions in the electrolyte. Price and Davenport (1980, 1981), Subbaiah and Das (1989) and Kalliomäki *et al.* (2016, 2017) showed that viscosity of copper electrolytes increase with increase in copper, metal impurities and acid concentration and decreases with increase in temperatures.

Subbaiah and Das (1989) measured viscosities of copper electrolytes at different compositions and temperatures. The study observed that the viscosity of copper electrolytes decreased at higher temperatures and increased with the increase of both Cu and H_2SO_4 concentrations. However, Subbaiah and Das (1989) observed that the viscosities of complex solutions containing Fe^{2+} Fe^{3+}, Ni, Co, and Mn increased negligibly with addition of any of the impurities in the range studied (Subbaiah & Das, 1989).

Price and Davenport (1981) suggested that for complex solutions, viscosities can be expressed in terms of ionic concentration, Γ as follows:

$$\Gamma = \sum C_i Z_i^2 \qquad 2.24$$

where C_i is the concentration of ion i (g/dm^3) and Z_i is the valence of ion i (unitless).

For the work of Subbaiah and Das (1989), the values for Γ were obtained from the following equation:

$$\Gamma = 2M_{H_2SO_4} + 8(M_{Cu} + M_{Fe} + M_{Ni} + M_{Co} + M_{Mn}) \qquad 2.25$$

Where M_x represents the concentration of species/metal ions x (mol/dm^3).

A similar correlation was drawn earlier by Price and Davenport (1981):

$$\Gamma = 2M_{H_2SO_4} + M_{As} + 8(M_{Cu} + M_{Fe} + M_{Ni}) \qquad 2.26$$

Expressing viscosities in terms of ionic concentration maybe important to industrial operations which contain various impurities. Thus, Price and Davenport (1980) presented viscosity as a function of ionic concentration as follows:

$$Absolute\ viscosity\ (cP) = 10^{-6}\left(1834 + 2.609\Gamma^{1/2} + 256.9\Gamma - 44.56\Gamma^2\right) \times \exp\left(\frac{1890}{T}\right) \qquad 2.27$$

Where Γ is ionic concentration (mol/dm3) and T is the temperature (K).

Price and Davenport (1981) report that the absolute viscosities in their work can be represented by the equation below;

$$\frac{1}{\underset{(centipose)}{Absolute\ viscosity}} = 0.70 - 10^{-3}(4.6[As] + 8.3[Cu] + 8.8[Fe] + 1.6[H_2SO_4] + 18T) \qquad 2.28$$

Where [X] represents the concentration of species X (g/dm^3) and T is the temperature in °C

However, Hotlos and Jaskula (1988) argued that the proper description of the behaviour of viscosity is more complicated than proposed ionic equations by Price and Davenport (1981) due speciation in the copper sulphate-sulphuric acid-water system.(Hotlos and Jaskula, 1988)

2.4.2.3 Conductivity

The conductivity of the electrolyte has a major contribution toward lowering the power consumption during electrolytic processing of copper (Subbaiah & Das, 1989). Ohmic resistance of the electrolyte is one of the factors which affects the actual voltage of the process. A reduction in the ohmic drop during copper electrowinning could substantially save operational costs. It affects the current efficiency and electrical energy consumption of the electrolytic process. Electrical conductivity depends on a number of variables including the chemical composition and acidity of the electrolyte. The studies conducted by Price and Davenport (1980, 1981), Subbaiah and Das (1989) and Kalliomäki *et al.* (2016, 2017) indicate that the conductivity of the electrolyte is increased with an increase in temperature and acid concentration of the electrolyte. The same studies also showed that an increase in copper concentration resulted in a decrease in conductivity for the range considered. However, Ntengwe *et al.* (2010) observed that cell resistance decreased with the increase in concentration of electrolyte while the current density decreased with the decrease in concentration (Ntengwe *et al.,* 2010). In contrast, Owais (2009) observed that increasing copper concentration in electrolyte resulted into better efficiency and lower specific energy demand with better productivity yield. The reason for the observed trend was mentioned in section 2.4.1.1. Therefore, during electrowinning process performance improvement, it is imperative that conductivity is considered to ensure the effectiveness and efficiency of the process.

Subbaiah and Das (1989) measured conductivities of $CuSO_4/H_2SO_4$ solutions containing impurities such as Co, Mn, Fe^{2+}, Fe^{3+} at different Cu and H_2SO_4 concentrations in the temperature range of 20 to 60°C. The study observed that the presence of these metallic impurities in the complex solution caused reduction in electrolyte conductivity. The conductivity was calculated using the following equation:

$$\frac{1}{\underset{(\Omega^{-1}cm^{-1})}{Conductivity}} = 3.2 + 10^{-3}(1[Co] + 1[Mn] + 9[Ni] + 12[Fe] - 6[H_2SO_4] - 15T) \qquad 2.29$$

Where [X] represents the concentration of species X (g/dm^3) and T is the temperature in °C

An earlier study by Price and Davenport (1980, 1981) investigated conductivities of copper electrolytes and complex solutions containing nickel, arsenic and iron in the range of 0-20 $g.dm^{-3}$, 0-10 $g.dm^{-3}$ and 0-3 $g.dm^{-3}$ respectively. The temperature range was 50-70°C with copper and acid concentration in the range of 30-60 $g.dm^{-3}$ and 165-225 $g.dm^{-3}$ respectively for electrorefining electrolytes. For electrowinning electrolytes, the temperature, copper, acid, Ni, As, and iron concentration ranges were 20-70°C, 5-55 $g.dm^{-3}$, 10-60 $g.dm^{-3}$, 10-165 $g.dm^{-3}$, 0-4 $g.dm^{-3}$, 0-4 $g.dm^{-3}$ and 0-20 $g.dm^{-3}$. Price and Davenport (1980, 1981) report that increasing copper concentration resulted in decreasing the conductivity of the electrolyte whereas increase in acid

concentration resulted in increased conductivity. The results for electrorefining were represented by the following empirical equation;

$$\frac{1}{\substack{Conductivity \\ (\Omega^{-1}cm^{-1})}} = 3.2 + 10^{-3}\,(1.3[As] + 7.3[Cu] + 4.5[Fe] - 5.6[H_2SO_4] + 9.6[Ni] - 14.6T) \quad 2.30$$

Where the terms are defined in equation in 2.29

The effect of copper concentration and impurities on electrowinning electrolytes was no different from that observed by Subbaiah and Das (1989). The model developed by Subbaiah and Das (1989) was similar to the earlier model by Price and Davenport (1981) which is:

$$\frac{1}{\substack{Conductivity \\ (\Omega^{-1}cm^{-1})}} = 3.2 + 10^{-3}\begin{pmatrix}1[Cu] + 2[As + Mg] + 3[Al] + 9[Cu] \\ +12[Fe] - 6[H_2SO_4] + 11[Ni] - 15T\end{pmatrix} \quad 2.31$$

Where the terms as defined in equation in 2.29

Price and Davenport (1981) did not develop a conductivity empirical model for electrowinning. According to Price and Davenport (1981), their conductivity results were not well described by a linear equation. They suggested that better interpretation of their electrowinning conductivity values can be done by analysing the data directly from tabulated data. However, Price and Davenport (1981) does not provide the reasons for not fitting the linear empirical equation for electrowinning conductivity data. The three empirical equations above show similar results for electrorefining electrolytes. Kalliomäki et al. (2016) also developed models for conductivities for synthetic electrorefining electrolytes by exploring interactions effects among the factors.

2.4.2.4 Diffusion Coefficient of Copper

The diffusion coefficient of copper ions in electrolyte is an important property as it affects the mass transfer in the system as well as the current density during electrolysis (Subbaiah & Das, 1989). Most electrowinning plants operate at less than 50% limiting current density, which is the density at which the diffusivity of copper ions are determined if limiting current technique is employed (Moats *et al.,* 2000; Beukes & Badenhorst, 2009). Several studies have been carried out to determine diffusivity of copper in the $CuSO_4$-H_2SO_4 system. Subbaiah and Das (1989) investigated the diffusion coefficient for Cu^{2+} in the $CuSO_4$-H_2SO_4 system at different experimental conditions using a limiting current density technique (Subbaiah & Das, 1989). The empirical equation was developed as shown below:

$$D \times 10^5 = -0.570 - 0.00164[H_2SO_4] - 0.00175[Cu] + 0.0607T \quad 2.32$$

Where $[H_2SO_4]$ and $[Cu]$ is the concentration of sulphuric acid and copper ions respectively (g.dm^{-3}) and T is the temperature (^{o}C)

The results of Subbaiah and Das (1989) indicate that the diffusion values decreased with increase in copper and acid concentration. Subbaiah and Das (1989) attributed the decrease in diffusivity to the forces of interaction among the diffusing species, the hydration phenomena taking place in the electrolyte, and the increase of viscosity of the solution.

Quickenden and Jiang (1984) studied the diffusion coefficient of copper ions.by using chronopotentiometry and rotating disc electrode for copper concentration ranging from 0 to 0.05 mol/dm^3. The results of their study also indicated that the diffusion coefficient decreased with increase in copper concentration. They suggested that the increase in diffusivity of copper ions with decrease in copper concentration possibly be due to aggregation of pairs of copper ions via sulphate bridges at higher concentration, that is, ion complexation (Quickenden and Jiang, 1984).

Moats *et al.*(2000) studied the effect of copper (35-70 g/l), sulphuric acid (160-250 g/), and temperature (40 to 65°C) on the diffusion coefficient in the range of electrorefinning. Moats *et al.*(2000) results show similar trend to that of Quickenden and Jiang (1984). The increase in both the copper and sulphuric acid concentration resulted in a slight decrease in the diffusivity of copper ions in the electrolyte. At the same time, temperature increased the diffusivity of copper ions (Moats *et al.,* 2000).

Gladysz *et al.* (2007) investigated the influence of copper, additive (thiorea and animal glue) and temperature on diffusion coefficient of copper ions for electrorefining electrolytes. The effect of copper concentration and temperature on diffusion coefficient was no different to that observed by Moats *et al.*(2000), Subbaiah and Das (1989) and Quickenden and Jiang (1984). The variation in concentration of animal glue (1 to 5 mg/dm^3) and thiourea concentration (1 to 5 mg/dm^3) had no effect on the diffusion coefficient (Gladysz *et al.,* 2007). Similar observations were made by Araneda-Hernández *et al.* (2014).

Recently, Kalliomäki *et al.* (2019) investigated the diffusion coefficient of copper ions in electrorefinning electrolytes. Though there are variations in impurity between electrowinning and electrorefining, the base metal and supporting electrolyte is the same. Models relating electrolyte composition to diffusion coefficient were provided and the results show good agreement with previous studies (Kalliomäki *et al.*, 2019).

Diffusion coefficient determination

Diffusion coefficient can be determined by various methods such as chronoamperometry and linear sweep voltammetry by application of rotating disk electrode. The rotating disk electrode was used in the current study. In the rotating disk electrode, the electrolyte (fluid) is transferred to the electrode surface through the

rotation of the electrode such that a thin layer of stagnant electrolyte exists at the surface of the electrode. This makes it possible for the mass transfer to be diffusion controlled.

The potential is swept linearly such that limiting current is reached (the current at which the electrochemical reaction becomes mass transfer controlled). Diffusion coefficients can be determined by the application of the Levich equation or Koutecky – Levich equation, given as equation 2.33 and 2.34 respectively.

$$i_l = 0.62nFAD^{2/3}\omega^{1/2}\upsilon^{-1/6}C_b \tag{2.33}$$

$$1/i_{lim} = 1/i_k + 1/i_l = 1/i_k + 1/\left(0.62nFAD^{2/3}\omega^{1/2}\upsilon^{-1/6}C_b\right) \tag{2.34}$$

Where i_l is the diffusion limiting current, i_{lim} is the limiting current, i_k is the activation limiting current n is the number of participating electrons, F is the Faraday's constant, A is the surface area of the working electrode, D is the diffusion coefficient, ω is the angular velocity, υ is the kinematic viscosity, and C_b is the bulk concentration

The Levich equation shows that the diffusion limiting current is the function of the diffusion coefficient of the species. In the case of the Levich equation, the limiting current increases with increase in the rotation speed of the working electrode. As such, a series of voltammograms can be obtained at various rotation speeds from which the diffusion coefficient can be determined. This is achieved by plotting the limiting current against the square root of angular velocity since this is a linear relationship.

When determining the diffusion coefficient using the Koutecky - Levich equation, the reciprocal of the limiting current is plotted against the reciprocal of the square root of the angular velocity. The slope of the plot is used to determine the diffusion coefficient. According to Quickenden and Jiang (1984), Koutecky – Levich equation considers the activation/kinetic current, as such, it was recommended over the Levich equation.

From the foregoing, it is clear that the diffusion limited current provides the basis for mass transfer coefficients determination. At diffusion limited current, species are consumed as they are supplied to the electrode and is given as:

$$i_L = nFK_dC_{0x(bulk)} \tag{2.35}$$

Where n is the number of participating electrons, F is the Faraday's constant, K_d is the mass transfer coefficient and $C_{0x(bulk)}$ is the bulk concentration.

From the equation 2.35, it can be noted that increasing the mass transfer coefficient increases the limiting current. This is a function of the hydrodynamics of the cell and physical properties of the electrolyte such as temperature, viscosity and other competing ions (Beukes & Badenhorst, 2009).

Ettel *et al*. (1975) points out that the values of mass transfer coefficient measured under mass transfer conditions are not the same value as that prevalent under normal operating conditions since mass transfer is depended on the current density itself (Ettel *et al*., 1975). Mass transfer coefficients can be experimentally determined from different empirical correlations based on dimensionless parameters such as Reynolds and Schmidt number. Beukes and Badenhorst (2009) provides a general form for the parallel plate system commonly found in electrowinning. According to Beukes and Badenhorst (2009), the correlation for mass transfer by natural convection is given as:

$$Sh = 0.902\left(\frac{Gr.Sc}{4(0.861+Sc)}\right)^{0.25} \quad 2.36$$

where Sh, Sc, and Gr are Sherwood, Schmidt, and Grashof number respectively given as:

$$Sh = \frac{Kd.de}{D} \quad 2.37$$

$$Sc = \frac{\mu}{\rho D} \quad 2.38$$

$$Gr = \frac{g.\beta(Ts-T)L^3}{V^2} \quad 2.39$$

Where Kd is the mass transfer coefficient, de or L is the characteristic length, D is the diffusion coefficient, μ is the kinematic viscosity and ρ is the density, g is the gravitational acceleration, β is the thermal expansion coefficient, Ts and T is the temperature at the surface and bulk electrolyte respectively

2.5 Factors affecting electrowinning performance of copper

The preceding section covered the influence of electrolyte composition on the cathode quality and energy consumption. Still, there are other key parameters which influence the quality of electrodeposited copper, the rate of production and energy consumption in copper electrolytic processing. This includes but not limited to current density, temperature, additives and cell design. Factors such as copper and acid concentration as well as chloride ions will not be discussed as they have been covered by the previous section.

2.5.1 Current Density

The importance of current density in improving the production rate of the electrowinning process cannot be overemphasized. At the same time, current density influences the morphology of the electrodeposited copper. The amount and the rate of metal deposition is a function of current density. To achieve high deposition rate, higher current density is required which ensures rapid copper plating (Beukes & Badenhorst, 2009). However, increasing current density may result in poor morphology of the electrodeposited copper.

In their work, Das and Krishna (1996) found that increase in current density resulted in nodular growth of deposits which were also powdery. Furthermore, Das and Krishna (1996) also reports that the power consumption increases with increasing current density (Das & Krishna, 1996). Panda and Das (2001) studied the effects of current density (100 to 300 A/m^2) during copper electrowinning on cell voltage, anode potential, power consumption and current efficiency. Their results indicate that the cell voltage and anode potential increase with increase in current density whereas the power consumption was found to increase with increase in current density (Panda & Das, 2001). The norm in the industry is to operate between 30-50% of limiting current density. Robinson *et al.* (2013) reports that industrial current density varies from 200 to 450 A/m^2 in various tank houses across the world (Robinson *et al.*, 2013).

2.5.2 Temperature

The effects of temperature in relation to physicochemical properties were discussed in section 2.4.2. It was discussed that an increase in temperature improves electrolyte conductivity, mass transfer and current distribution as well as current efficiency. This has a positive effect on the morphology of the deposit and energy consumption. However, as observed by Ehsani *et al.* (2016) surface roughness may increase with increase in temperature once certain temperatures are reached (Ehsani *et al.,* 2016). Unnecessary high temperatures may also result in increased energy consumption and unfavourable working environments for the operators.

The work of Andersen *et al.* (1973) suggests that an increase in temperature can contribute significantly to an increase in limiting current (Andersen *et al.,* 1973). The results of Owais (2009) supports this as it showed that increase in electrolyte temperature (35°C to 65°C) increased the current density and consequently reduced the energy consumption. Owais (2009) attributed the effect of temperature on physicochemical properties, that is, decreasing viscosity and density and increasing the conductivity and consequential decreasing in the cell voltage as the reason for the observed trend (Owais, 2009). A Similar outcome was reached by Panda and Das (2001) who also observed the decrease in cell voltage and anode potential as the electrolyte temperature was raised from 30°C to 60°C. Higher temperature was found to improve the quality of the deposit (Panda & Das, 2001).

2.5.3 Flowrate of electrolyte

The flowrate of the electrolyte is another critical parameter to consider when analysing the electrowinning process. Copper ions are transported to the cathode surface via the three mechanisms; diffusion, migration and convection. Convection mode of transportation largely depends on the flowrate of the fluid (Newman & Thomas-Alyea, 2004). Electrolyte flowrate increases the current efficiency and the required energy is decreased. According to Owais (2009), the improved cell performance can be due to the enhancement of Cu ions transfer from the bulk solution to the cathode surface and the decrease of concentration polarization, which subsequently decreases the specific energy requirement. In contrast, decreasing flowrate may slower convection and diffusion of ions to the cathode surface and consequently decrease the rate of deposition. However, high flowrates may cause strong agitation of the deposits which may be separated and cause short circuits between anode and cathode (Owais, 2009).

2.5.4 Electrolyte Additives

The desire to electrowin copper at fast rates always comes with the cost of poor electrodeposits. Additives are added to the electrolyte to promote smooth and strong electrodeposits (Muhlare & Groot, 2011; Muresan, 2000). According to Moats *et al.* (2016), smoothing agents can be classified as brighteners, levellers or inhibitors. Brighteners are responsible for producing a bright and shiny copper cathode surface. This is accomplished through refinement of the grain structure by catalysing the copper reaction and promoting the formation of new grains. On the other hand, levellers assist in producing a smooth surface by inhibiting the growth of protrusions or edges. Inhibitors are known as polarizing agents and are believed to affect both the copper dissolution and deposition process. These additives interact with the surface to produce tighter packed deposits (Moats *et al.,* 2016). Additives make it is possible to apply high current densities during the electrowinning process without which electrodeposited copper would be of poor quality and texture (Schlesinger *et al.*, 2011; Beukes & Badenhorst, 2009). The commonly used additive is guar.

In addition to organic additives, chloride ions may be added as HCl (if not naturally present) to promote the growth of dense, fine grained, low impurity copper deposits (Schlesinger *et al.,* 2011). Most electrowinning operations operate with chloride concentration of approximately 25 mg/L because excess chloride levels may lead to pitting of cathodes. Furthermore, cobalt is added as cobalt sulphate to promote O_2 evolution and avoid Pb oxidation at the anode, thereby reducing Pb contamination of the electrodeposited copper and prolonging anode lifespan.

2.5.5 pH

The value of pH is depending upon the composition of electrolyte (Kumar et al, 2015). The pH of the electrolyte plays a significant role during the electrowinning process especially in terms of current efficiency

and hydrogen evolution. Recall that the anodic reaction is the decomposition of water to form oxygen gas and hydrogen ions which results in a more acidic environment. Additionally, the sulphuric acid in electrolyte contributes to the hydrogen ions in electrolyte.

2.6 Electrowinning modelling

Modelling of electrolytic process offers an opportunity to understand the influence of various factors such as cell geometry, current density, cell hydrodynamics and operating conditions on electrodeposition process. This is important as it can be challenging and costly to use physical experiments to evaluate the effects of these factors on electrowinning. Consequently, various models have been developed to present several electrodeposition processes such as electrorefining, electrowinning, electroplating and electropainting. As such, work pertaining to copper electrowinning modelling is presented with few reference to other electrodeposition processes. The reader should bear in mind that this study focused on electrowinning. Nevertheless, the work dealing with modelling of electrorefining and electroplating as well as electrowinning of other metals were reviewed so as to gain better understanding of the modelling techniques but are not discussed here.

A considerable amount of literature have been published on electrowinning modelling. Ziegler and Evans (1986) developed a mathematical model to provide the means for predicting the bubble distribution within the cell, the electrolyte velocity flow pattern and current distribution. Their work primarily focused on the effect of bubbles on the flow and effective conductivity of the electrolyte in planar electrodes. As such, no consideration was given to the effect of migration and diffusion mechanism. Furthermore, the electrode kinetics for the system are unknown as they were not outlined in the study. The model developed by Ziegler and Evans (1986) predicted mass transfer rates, current non-uniformity and effective resistance of the electrolyte (Ziegler & Evans, 1986).

Tobias (1959) developed a model to predict the current distribution by considering the effects of electrolyte resistance due to bubble generation and polarization of electrodes. Although this work did not focus on electrowinning and used a stagnant electrolyte, it established the theoretical treatment of a cell model by which current distribution can be described (Tobias, 1959). A similar study was conducted by Funk and Thorpe (1969), in which current density distributions was investigated as a function of cell voltage, inlet velocity and slip ratio (Funk & Thorpe, 1969).

Nguyen *et al.* (1986) developed a time dependent model to evaluate the effects of diffusion and migration in parallel plate electrolytic cell using numerical integration technique for a copper chloride system. The model of Nguyen *et al.* (1986) predicted the concentration, potential and local current distribution of the electrowinning of copper from chloride system (Nguyen *et al.*, 1986). Unlike the work of Ziegler and Evans (1986), Nguyen *et al.* (1986) included the electrode kinetic parameters of copper electrowinning. However,

the Nernst Plank equation used was in dimensionless form which can lead to simplification and generalisation of the model.

Free *et al.* (2006) modelled electrowinning process to predict cell performance, particularly current efficiency, energy consumption, electrodeposit morphology and electrodeposit distribution. Electrode thermodynamics, mass transfer and electrochemical kinetics as well as side reactions were considered. A number of species were incorporated in the model (Free *et al.,* 2006). However, it seems similar diffusivity values were used for the species present in the model.

On the other hand, Cifuentes *et al.* (2006) developed a mathematical model for an electrodialysis based copper electrowinning cell. This cell differed from the conventional electrowinning cell in that the anodic reaction was the oxidation of ferrous ion, as opposed to the decomposition of water and the membrane was used to separate the catholyte from the anolyte (Cifuentes *et al.*, 2006). This work was relevant as it provides insight into speciation of copper system in electrowinning. The respective species in the H_2SO_4-$CuSO_4$-H_2O system are provided which are species expected to be incorporated in the electrowinning model.

Leahy and Schwarz (2010) developed a computational fluid dynamics (CFD) model to study the hydrodynamics behaviour of the electrowinning cell with a pair of planar electrodes. A standard two phase gas-liquid CFD model was employed in ANSYS CFX and mass transfer through convection and diffusion as well as the effects of oxygen bubbles were considered. The model provided information on the flow profiles and copper distribution in an electrowinning cell. Based on their previous work (2010), Leahy and Schwarz (2014) carried out further research on the hydrodynamics in electrowinning cell to establish a detailed understanding of instabilities along the electrode surface. They found that natural convection is dominant at the base of the cathode, but becomes disturbed with increase in height by unstable eddies developing along the cathode (Leahy & Schwarz, 2010, 2014).

Kim *et al.* (2013), using the same modelling tool as that of Leahy and Schwarz (2010), developed a CFD model to study hydrodynamics of the electrowinning cell. Navier-Stokes and transport equations were solved to obtain the ionic species concentration and electric field at each position in the cell (Kim *et al.*, 2013). Similar to the work of Nguyen *et al.* (1986), Kim *et al.* (2013) used dimensionless transport equations to describe the transport mechanism in the electrolyte.

Shukla (2013) modelled copper electrowinning using COMSOL Multiphysics to predict short circuiting in electrowinning process. The model incorporated the effect of bubbles and mass transport in the system. The effect of various parameters such copper concentration, electrolyte temperature and current density were considered (Shukla, 2013). Robison (2014) also used COMSOL Multiphysics to model electroplating deposit distributions in copper sulphate solutions. However, Robison (2014) work was based on electrorefining; and Hull and Haring-Blum cells were used, instead of the conventional cells. The work focused on studying the

effects of geometry on deposit distribution (Robison, 2014). The work of Shukla (2013) and Robison (2014) were important to this work as the same modelling software was used.

Najminoori *et al.* (2015) developed a computational model based on Euler-Euler method to predict the performance of copper electrowinning. Najminoori *et al.* (2015) used multiple electrodes as opposed to a pair of electrodes to study the hydrodynamics occurring between the electrodes of copper electrowinning. A two phase system was considered (Najminoori *et al*>, 2015b).

Recently, Werner *et al.* (2018) used COMSOL Multiphysics, a finite element analysis software to simulate electrowinning process for optimization of electrowinning performance. The Nernst--Planck equation was used to describe the mass transfer in the electrolyte and it was coupled with a two-phase computational fluid dynamics (CFD) model to accurately describe mass transport in the system. The effect of different electrode alignment (misalignment of electrodes) on the current distribution at the cathode surface was provided, which allow for accurate deposit morphology prediction (Werner *et al.*, 2018). Expanding on the work of Shukla (2013), Werner (2017) modelled the electrowinning process to study the effects of short circuiting (Werner, 2017).

Based on the modelling approach by Werner (2017), Zhang *et al.*, (2018), developed a model to predict current efficiency and energy consumption in copper electrowinning. The effects of iron on current efficiency was explored (Zhang *et al.*, 2018). One notable observation from the work of Zhang *et al.*, (2018) was the use of multiple species which appears to have improved the predictability of the model.

2.6.1 Modelling Software

There are a number of modelling software which can be used to model electrowinning process. This include but not limited to MATLAB, PHYSICA, Elsyca and COMSOL Multiphysics. Since COMSOL Multiphysics was used, a brief description is provided. A review on COMSOL Multiphysics application in electrochemistry is given by Dickinson *et al.* (2014)

COMSOL Multiphysics is a general-purpose finite element software package for modelling various physical phenomena of scientific and engineering problems (Comsol, 2019). The software is designed to incorporate and couple diverse physical phenomena within one model (Dickinson *et al.*, 2014). The coupling of different physics is important as electrowinning is governed by a number of physical phenomena such as conservation of charge and current at the electrodes and in the electrolyte, conservation of mass and conservation of momentum. At the same time, the changes in electrode thickness must be captured as the electrochemical reaction takes place. Partial differential equations are used to describe these phenomena, and solved on a suitable geometry and timescale (Dickinson *et al.*, 2014). COMSOL Multiphysics has built in sets of physical equations and associated boundary conditions, referred to as physical interface. The physical interfaces are

flexible as they can be modified or the user can define a different set of equations to represent the physical problem to be solved.

The electrodeposition module in COMSOL Multiphysics is of particular interest in this study. This is because it can be used to investigating the effects of various parameters such as cell geometry, electrolyte composition, electrode kinetics and operating condition on electrodeposition. COMSOL Multiphysics can be used to model wide range of electrodeposition process includes electrorefining, electrowinning and electroplating (Comsol, 2017).

2.7 Current distribution

It is well known that the current density varies from point to point on the surface of the electrode and that the rate of the electrochemical reaction is dependent on the current density. The manner in which the current is distributed at the cathode determines the morphology of the deposit (Popov *et al.,* 2001). Thus, the current distribution is one of the important parameters as it influences the morphology of the electrodeposit. Non uniform current density may cause different morphologies of electrodeposited metal at the electrode surface resulting in the growth of dendrites which may cause short circuiting and lower the current efficiency (Bouzek *et al.*, 1995; Choi *et al.*, 2015). According to Popov *et al.* (2011) current distribution in an electrochemical cell is affected by the following factors: cell geometry, conductivity of the electrolyte and electrodes, electrode kinetics, cell operating conditions and mass transport of the reactants and ions in the electrolyte (Popov *et al.*, 2011). As a result, even with proper cell design, good electrode alignment and spacing, poor current distribution can occur. Electrolyte conductivity and mass transfer are influenced by physicochemical properties of the electrolyte, hence, electrolyte composition has a role to play in the manner in which current is distributed in the cell.

The analysis of current distribution can be done on a macro or micro scale depending on the scale used. The macro and micro current distribution are used when analysing deposit thickness of the order of cm and micro/nano scale respectively.

Current distribution may be categorised into three groups; primary, secondary and tertiary current distribution depending on the factors considered to be influencing current distribution in the cell. Primary current distribution takes into consideration the electrolyte conductivity but neglects the influence of activation and concentration overpotential. On the other hand, secondary current distribution incorporates activation overpotential and the rest of the conditions are the same to that of primary current distribution whereas tertiary current distribution incorporates concentration overpotential, electrolyte conductivity, and electrode kinetics. (Popov *et al.*, 2001) Thus, current distribution plays a role in energy consumption during the electrodeposition process.

2.8 Summary

The studies conducted so far have shown that there is link between electrolyte composition and its properties. Viscosity and density have an influence on heat and mass transfer which affects the purity of cathode copper and the energy consumption in electrolytic processing of copper. Mass transfer rate is improved by decreasing the viscosity and density since they will be an increase in the diffusivity and mobility of ions. High electrical conductivity minimizes the power consumption and improves the current efficiency of the process. Additionally, presence of different metallic impurities affects the physicochemical properties and, therefore, influence the energy consumption. Indeed, this information is useful in process optimization and understanding the electrolytic processing.

However, most of the research was conducted on synthetic electrolytes, with few involving complex solutions, mostly being electrorefining electrolytes. At the same time, most of the experiments were performed in the absence of additives. Additionally, a review of the literature showed that there is need to generate more data on metallic impurities as the data available is either inadequate or not available. Recently, Kalliomäki et al. (2016) modelled the effect of composition and temperature on the conductivity, density and viscosity of synthetic copper electrorefining electrolytes to provide accurate models by incorporating impurities and also considering the interaction effect. However, just as it was with the other studies, the presence of additive was neglected and the study focused on electrorefining.

On the other hand, a number of models pertaining to electrowinning have been formulated for performance improvement. Several phenomena such as cell hydrodynamics, mass transfer, short-circuiting and concentration profiles as well as current distribution have been studied through modelling. The effects of various factors such as bubble generation, diffusion and migration, cell misalignment, current density, and temperature on electrowinning process have also been investigated through modelling. Among the literature discussed, the ones dealing with prediction of current distribution are of greater importance to this work as they provide a foundation for the current work. This is because current distribution influences the growth and structure of the deposit.

Chapter 3 : Experimental

The experimental work in this study was divided into two categories: physicochemical property tests and electrowinning experiments for model validation. Physicochemical properties experiments were conducted in order to investigate the influence electrolyte composition on physicochemical properties of copper electrolytes in electrowinning. On the other hand, electrowinning experiments were carried out to validate the electrowinning model developed using COMSOL Multiphysics 5.3a.

3.1 Experimental program for physicochemical property measurements

3.1.1 Materials

The electrolytes used throughout the work were prepared from analytical reagent grade copper (II) sulphate ($CuSO_4.5H_2O$, min. 99%), concentrated sulphuric acid (H_2SO_4, 98%) and Ferrous sulphate ($FeSO_4.7H_2O$, min. 99.5%) supplied by Scienceworld, polyacrylamide (PAM) additive supplied by SENMIN, and distilled water. The solution and additive preparation procedure are outlined in Appendix A which were adapted from Coetzee (2018). All electrolyte preparation was done at room temperature which averaged 25^oC.

3.1.2 Experimental Design

The experimental design approach adopted for the physicochemical measurements was a Mixed 2 and 3 level design. The mixed design was chosen as it allowed for simultaneous study of several factors and interactions effects whilst providing enough data for development mathematical correlations for each property. Five factors were considered: copper concentration, sulphuric acid concentration, iron concentration, PAM additive concentration, and temperature.

Table 3.1: Factors and levels for experimental determination of electrolyte density, conductivity and diffusion coefficient of copper ions.

Factor	**Levels**		
Cu Concentration (g/l)	35	45	
H_2SO_4 Concentration (g/l)	160	180	
Fe Concentration (g/l)	1	3	6
PAM Concentration (mg/l)	2.00	4.99	9.98
Temperature (°C)	45	55	

The levels were chosen based on the literature and industrial values for electrowinning parameters, choosing the upper and lower limits typical of industrial data (Robinson *et al.*, 2013). The selected levels and factors (variables) are shown in Table 3.1. All factors were investigated at low and high levels, except for iron and PAM additive, which were investigated at 3 different levels. This was done to have acceptable number of experiments which would produce valuable information on the possible interactions among the factors. The experiments were conducted twice to ensure the reliability of the experimental data.

The effect of varying PAM additive concentration on the physicochemical properties was further investigated using a one factor at a time approach (OFAT). The chosen conditions were 35 g/l of Cu, 160 g/l H_2SO_4 and 6 g/l Fe concentration at 45°C and 55°C with the concentration of PAM additive ranging from 4.99 to 29.94 mg/l. This was done to fully elucidate PAM additive influence on physicochemical properties as previous studies were conducted in the absence of the additive. PAM additive are made of long chains and have high molecular weight (Vereecken and Winand, 1976), as such, they have a probability of affecting physicochemical properties within the range chosen.

In addition, confirmation runs were carried out to generate experimental values for validating the mathematical correlations which were developed for each investigated property. These experiments were conducted at fixed conditions of iron and PAM additive with copper and acid concentration varied from 35 g/l to 45 g/l and 160 g/l to 180 g/l respectively at 45 and 55°C as shown in Table 3.2

Table 3.2: Experimental conditions for confirmation runs for validation of mathematical correlations of electrolyte density, conductivity and diffusion coefficient of copper ions.

Factor	**Levels**		
Fe Concentration (g/l)	3		
PAM Concentration (mg/l)	9.98		
Temperature (°C)	45	55	
Cu Concentration (g/l)	35	40	45
H_2SO_4 Concentration (g/l)	160	170	180

3.1.3 Density measurements

Several methods are employed in the density determination of the liquid. These include but not limited to the use of electronic density meters, pycnometer, and hydrometer. The choice of the method employed depends on a number of factors, among them being accuracy required, the number of measurements to be carried out, and the nature of the liquid being measured as well as the cost involved.

In this study, the pycnometer (Figure 3.1) was used to determine the density of the electrolyte. It was primarily chosen due to its simplicity and good accuracy, as well as its ability to measure densities of corrosive liquids. Pycnometers provide good and accuracy measurements, primarily due to their ability to precisely determine the volume of liquid from which the density can be extracted through calculations. The work of Price and Davenport (1980, 1981) and Subbaiah and Das (1989) shows that the pycnometer can be an effective tool to measure density as it was the apparatus used in their work.

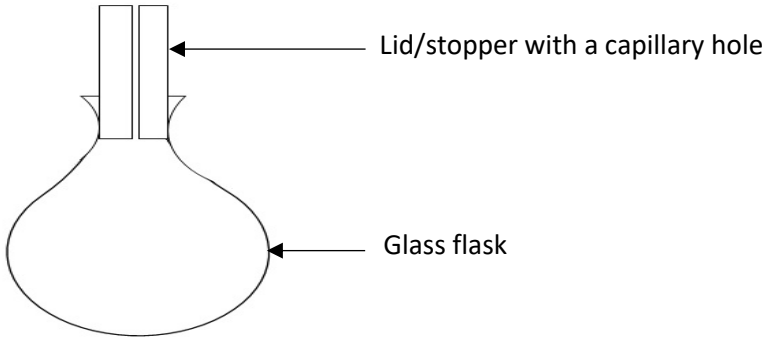

Figure 3.1: Schematic diagram of the pycnometer utilized for density measurements

3.1.3.1 Procedure

Three 50 ml standard pycnometers with lids were marked for easy identification. The pycnometers were calibrated to obtain the volume of the pycnometer (V1). For the calibration procedure, refer to Appendix A. The pycnometers were then dried in natural air for 15 minutes. Thereafter, they were further dried using compressed air to eliminate any trace of moisture. The dried pycnometers with respective lids were weighed and the weight recorded as M1. Then, the pycnometers were arranged, each pycnometer with its lid.

The electrolyte was heated in a separate beaker using the water bath until the required experimental temperature was reached. The beaker had a watertight lid to prevent evaporation so as to minimize water losses. After the electrolyte experimental temperature was reached, the electrolyte was carefully poured into the pycnometer until it was nearly full (only a small volume was left to accommodate the lid). The lid was then carefully placed into the pycnometer until the liquid flashed out of the capillary hole. The excess liquid was then wiped out using a non-sticking disposable wiper until it was completely dry. After which, a visual inspection was done to ensure that no air bubbles were present in the electrolyte inside the pycnometer. If any trace of bubbles were observed, the procedure was terminated and restarted.

The pycnometer (with lid and electrolyte) was weighed and weight recorded as M2. The difference between the weight of the empty pycnometer (M1) and filled pycnometer (M2) was the mass of the electrolyte. The density was determined by dividing the electrolyte weight (M2-M1) by the pycnometer volume (V1) determined in the calibration step as shown:

$$Density = \frac{M2 - M1}{V1} \quad 3.1$$

This procedure was repeated for the other two (2) pycnometers with the average value reported as the final density value.

3.1.4 Conductivity measurements

The conductivity of the solution is the measure of the ability to pass an electric current across an electrolyte through the movement of cations and anions. Conductivity is measured by a conductivity meter which measures current and the potential between two electrodes and converts it to conductance (I/V). The meter then uses the calculated conductance and cell constant to display the conductivity as per following equation:

$$Conductivity = cell\ constant\ \times conductance \quad 3.2$$

In this study, conductivity measurements were carried out using an Orion Star A325 conductivity meter. The meter was used with a 2-electrode sensor 018020MD which had a glass/platinum measuring system and glass casing tube.

Prior to using the conductivity meter, it was calibrated using standard electrolytes provided by Thermo Scientific. Since copper electrolytes have high conductivity, a standard electrolyte with high conductivity (112.5 mS/cm) was used in the calibration process. The standard electrolyte was thermostatted to the temperature of the conductivity measurements to ensure that the meter was calibrated at temperature encompassing the range for conductivity measurements.

3.1.3.1 Procedure

The electrolyte was heated in a beaker, covered with a watertight lid using a water bath until the required temperature was reached. The lid for the beaker was specifically constructed for conductivity measurements, with customized holes for inserting the probe and stirrer. During the heating of the electrolyte, the customized holes on the lid were sealed to minimize evaporation and prevent water losses. It was only during the stirring and measuring process that the holes were opened.

Before each measurement was taken, the electrolyte was thoroughly stirred to ensure uniformity in temperature and that electrolyte was thoroughly mixed. Electrolyte temperature was noted using a glass mercury thermometer as well as by a separate temperature sensor connected to the pH probe of the conductivity meter. In this work, the conductivity cell did not have a temperature sensor. Consequently, the use of a separate temperature sensor. Thereafter, temperature compensation was done on the conductivity

meter. Note that temperature compensation was necessary because of conductivity dependence on temperature and due to the type of the conductivity probe used in these experiments.

The conductivity probe was inserted in the beaker through the customized hole at the centre of the beaker. A visual inspection was done to ensure that all the electrodes of the conductivity cell were completely immersed in the electrolyte and that adequate distance was maintained between the probe and the bottom of the beaker. The conductivity was measured and recorded. The setup for the conductivity measurements is schematically shown in Figure 3.2.

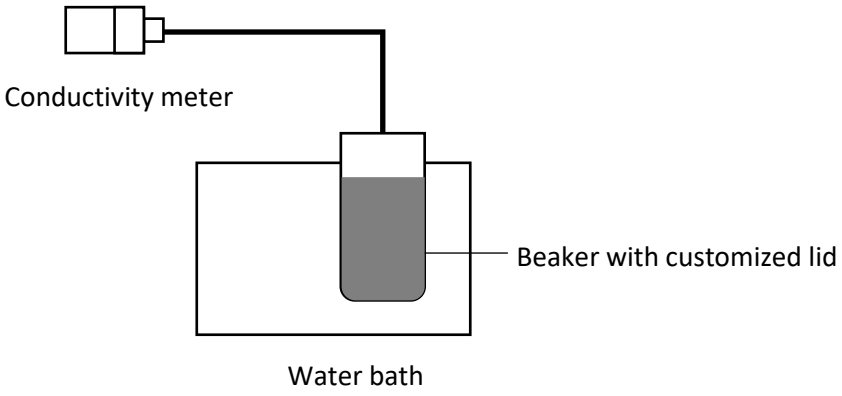

Figure 3.2: Schematic diagram of experimental setup for conductivity measurements

To minimize electrode surface contamination, the probe was thoroughly rinsed after each measurement, gently blotted with a lint-free tissue to remove excess water and dried in natural air before using it for the next measurement. At the same time, it was stored in distilled water between measurements.

3.1.5 Diffusion Coefficient measurements

A number of methods are available for the determination of diffusion coefficients with each having its strengths and weaknesses. These include chronopotentiometry, chronoamperometry, linear sweep voltammetry (LSV) and scanning electrochemical microscopy (Baur, 2007). These methods can be carried out using various types of electrodes such as conventional planar electrodes, rotating electrodes and microdisk electrodes. The rotating disc (RDE) method is one of the common electrochemical techniques employed in diffusion coefficient determination. This is primarily due to its ability to achieve mass transfer by diffusion only through well-defined hydrodynamics and steady state measurements. Thus, in this work, the RDE and LSV were used to determine the diffusion coefficients.

3.1.4.1 Equipment

The experimental equipment (RDE) used in this work is schematically illustrated in Figure 3.3. It consisted of a jacketed electrolytic cell with a total volume of 175 ml. The cell had multiple ports to facilitate the placement of electrodes into the cell. The temperature of the electrolyte was maintained by hot water from the water bath circulating through the cell jacket. The system was equipped with three electrodes: a rotating disk stainless steel working electrode with a surface area of 0.1964 cm^2, Ag/AgCl reference electrode (in 3M KCl, 0.21V vs SHE) and a platinum counter electrode.

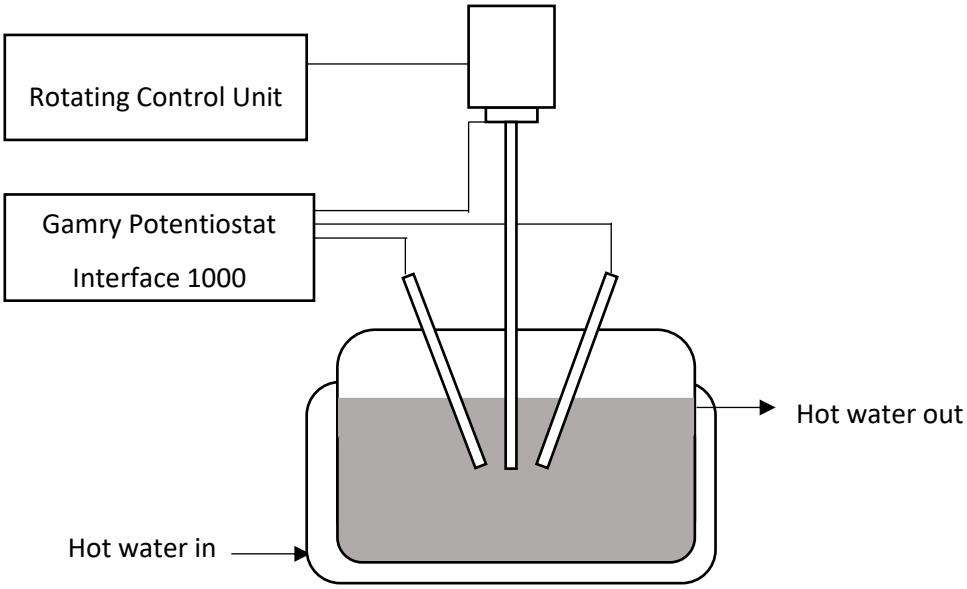

Figure 3.3: Schematic representation of experimental setup (rotating disk electrode) for diffusion coefficient determination of copper ions

The working electrode was attached to the Gamry RDE710 control unit which regulated the rotational rate of the working electrode. The potential of the working electrode against the reference electrode and electrochemical parameters inside the cell were controlled by the Gamry potentiostat, interface 1000: Model 04085. Experimental parameters were inputted and the generated voltammograms recorded by Gamry PHE200TM physical electrochemistry software installed on the computer which was connected to the equipment. The software was also used to monitor the experiments as they were being carried out.

3.1.4.2 Procedure

About 150 ml of the synthetic electrolyte was poured carefully into the electrolytic cell. The electrolyte was then heated by hot water from a water bath circulating through the cell jacket until the experimental temperature was reached (see table 3.1 for the experimental temperatures). Even though the water bath

heater had a temperature sensor, a glass thermometer was used to verify the temperature. After which, the electrodes were carefully placed into the electrolytic cell through the ports on the electrolytic cell. The counter and reference electrode were equidistant and close to the working electrode. This was necessary to reduce the ohmic drop due to solution resistance. The working electrode was cleaned before placing it in the cell by polishing it using 3 µm water-based diamond suspension on the cloth attached on the flat surface, appropriately rinsing and drying it as outlined in Appendix A.

The rotation of the working electrode was initiated by slowly increasing the rotation speed on the Gamry RDE710 rotating knob to the required working speed. The rotation was carried out for at least 5 minutes before commencing the measurement to ensure steady-state hydrodynamic conditions at the electrode surface. Linear sweep voltammetry was performed via Gamry software by sweeping the potential cathodically from 0.03V to -0.75V vs Ag/AgCl reference electrode at the scan rate of 10 mV/s and scan step of 5 mV at rotating speeds of 50, 70, 90, 100 and 200 RPM. The sweep range was chosen so as to encompass the standard copper reduction potential. In addition, the sweeping range was also carefully selected so that the reduction of copper ions (Cu^{2+}) was diffusion-limited and avoid the discharge of hydrogen which can make a significant contribution to the limiting current thereby introducing errors in the diffusion coefficients values(Quickenden & Jiang, 1984). The generated voltammograms of limiting current (Figure 3.4) were used to determine the diffusion coefficient utilizing the Levich and Koutecky - Levich equations.

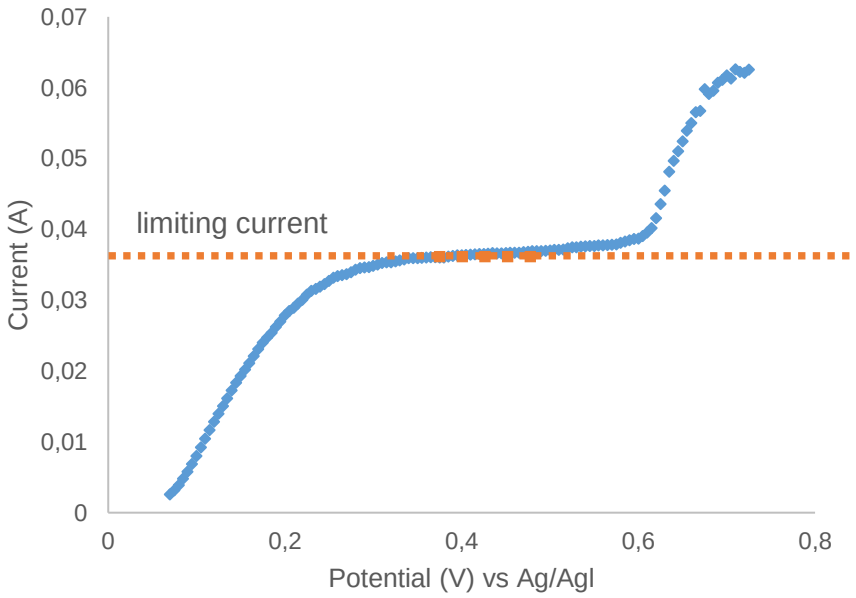

Figure 3.4: Linear sweep voltammogram for the rotating disc electrode showing limiting current density

The rotation speeds of the working electrode were carefully selected. This is because errors can be introduced in diffusion coefficients at either low or high rotation speeds. At low values of rotating speeds,

the diffusion layer becomes large rendering the assumptions in the Levich equation invalid (Baur, 2007). Thus, the lower rotation speed limit was determined according to equation 3.3:

$$\omega > 10\frac{\upsilon}{r^2} \tag{3.3}$$

Where r is the radius of the working electrode and υ is the kinematic viscosity.

At high rotating speed, turbulent flow may occur. As a result, the Levich equation no longer holds. To determine the high rotation speed limit, the Reynolds number, Re was used as given by equation 3.4. Rotation speeds are considered to be too high when the Re becomes greater than 10^5 since the flow can be assumed to be turbulent (Baur, 2007).

$$Re = \frac{\omega r^2}{\upsilon} \tag{3.4}$$

However, for the higher limit, consideration was also given to the nature of the generated voltammograms. At higher rotation speed, the boundary layer thickness may become very thin such that it can be difficult to precisely define the limiting current from the generated voltammograms. Consequently, not only was equation 3.4 used but also the experimental factors were taken into account when choosing the high rotation limit.

Two approaches were adopted in the diffusion coefficient determination: application of Levich equation and Koutecky – Levich equation. This was important because as indicated by Quickenden and Xu (1996), various researchers have used different methods with a wide scattered range of results. Furthermore, the Levich equation has been criticized due to its inability to incorporate activation polarization (assume diffusion controlled reaction), thereby, bringing inaccuracies in diffusion coefficient determination when the limiting current is not properly determined (Quickenden & Jiang, 1984; Quickenden & Xu, 1996). From the aforementioned, it was deduced that it was necessary to compare the outcome of both approaches.

For the rotating disc electrode, the Levich equation is given as:

$$i_l = 0.62nFAD^{2/3}\omega^{1/2}\upsilon^{-1/6}C_b \tag{3.5}$$

Where i_l is the diffusion limiting current, n is the number of participating electrons, F is the Faraday's constant, A is the surface area of the working electrode, D is the diffusion coefficient, ω is the angular velocity, υ is the kinematic viscosity, and C_b is the bulk concentration

The slope of the best fit line of limiting current, i_l against angular velocity, $\omega^{\frac{1}{2}}$ was utilized to extract the diffusion coefficient as per equation 3.6. The kinematic viscosity values were determined from absolute viscosity values of Price and Davenport (1981) and density values from this work.

$$D = \left(\frac{Slope}{0.62nFAv^{-1/6}C_b}\right)^{3/2} \quad 3.6$$

Quickenden and Jiang (1984) noted that linearity of the plot of i_l vs $\omega^{\frac{1}{2}}$ does not justify the use of the Levich equation as their work showed that 10% of activation control can be incorporated in the limiting current before non-linearity can be observed from the plot. It was further stated that this can introduce errors of around 30 % in the diffusion coefficient values (Quickenden & Jiang, 1984). Consequently, the recommendation to use the Koutecky – Levich equation.

The Koutecky – Levich equation is given as:

$$1/i_{lim} = 1/i_k + 1/i_l = 1/i_k + 1/\left(0.62nFAD^{2/3}\omega^{1/2}v^{-1/6}C_b\right) \quad 3.7$$

Where i_{lim} is the limiting current, i_k is the activation limiting current and the other terms as defined in equation 3.5

The plot of $\omega^{-1/2}$ vs $1/i_{lim}$ results in the straight line and the slope was used to determine the diffusion coefficient according to equation 3.8:

$$D = \left(\frac{v^{-1/6}}{Slope \times 0.62nFAC_b}\right)^{3/2} \quad 3.8$$

3.1.6 Analysis method

The objective of this investigation was to understand the relationship between electrolyte composition and physicochemical properties and construct models for physicochemical properties of copper electrolytes as function of electrolyte composition for electrolytes used in electrowinning. Statistica v13.5, a statistical software, was used for both the design of experiment and data analysis.

The descriptive statistics were first obtained to evaluate the raw data. Normality assumption of data was checked by probability plot as well as histogram. Note that only normal probability plots are reported in this work. Based on the evaluation outcome, the data was analysed further or processed for regression models

(herein referred to as mathematical correlations/models) building. In cases were small departures from the normality assumption was observed, the data was assumed to be normally distributed since the model quality was not significantly affected.

Multiple linear regression was used to fit the data in order to build regression models for each property. The models were evaluated for adequacy and refined to attain valid and usable models. Following the recommendation from Montgomery *et al.*, (2012), models adequacy was evaluated by analysing externally studentized residuals (Montgomery *et al.,* 2012). This provided a means of evaluating response values deviation. The constructed and refined models were then validated by comparing to the experimental results from confirmation runs. In cases where property models can be extracted from the literature, the current models were also compared to those in the literature.

Besides that, a further analysis was done to deduce how each component of the electrolyte affect the given property. Note that the validated models from the present study were used to define electrolyte properties in the modelling of copper electrowinning process in COMSOL Multiphysics 3.5a.

3.2 Experimental for model validation

An electrowinning cell was set up to determine deposit thickness across varying electrolyte compositions for model validation. The experiments were carried out to study the influence of electrolyte composition on current distribution.

3.2.1 Materials

The materials used for electrowinning experiments were the same as those described in section 3.1.1. However, no additive was added to the electrowinning experiments since the model did not incorporate the effect of additive.

3.2.2 Experimental design

Electrowinning experiments were conducted using a full factorial design. Three repeats were done to show reproducibility. The levels and factors at which the experiments were conducted are shown in Table 3.3. The tests were carried out at the temperature of 45°C and current density of 300 A/m^2.

Table 3.3: Factors and levels for electrowinning experiments

Factor	**Levels**	
Cu Concentration (g/l)	35	45

Factor	Levels	
H_2SO_4 Concentration (g/l)	160	180
Fe Concentration (g/l)	1	3

3.2.3 Experimental equipment

The electrowinning cell for this work had dimensions of 12 x 8 x 10 cm. The cathode was a 316L stainless steel plate of thickness of 1 mm and dimensions of 3 x10 cm. The anode was made from cold-rolled Pb alloy of thickness 1.5 mm and had the same dimensions as the cathode. Only one side of the cathode was plated since the model simulated only one surface of the cathode. To prevent the electrodeposition of copper, the other side of the electrode was coated with nail polish (nitrocellulose dissolved in ethyl acetate). Furthermore, insulating tape was utilized to cover most of the cathode and anode, leaving a 3 cm by 3.5 cm area exposed to the solution as the deposition area. The depth of the solution above the exposed area was 4.85 cm and the distance between the electrodes was 20 mm. Note that the same dimensions were used both in the model and experiments for easy comparison. The cell used for the electrowinning is shown in Figure 3.5.

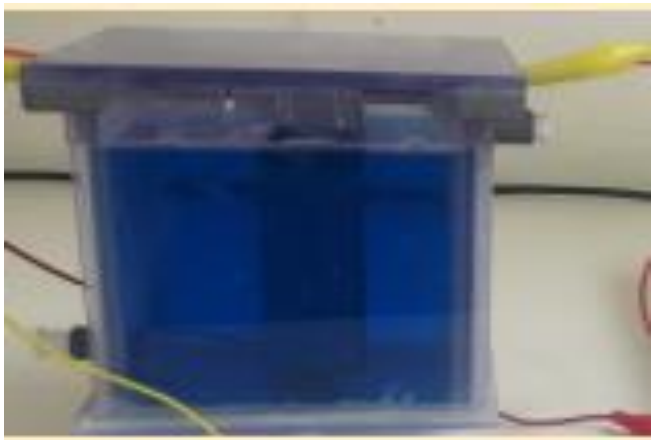

Figure 3.5: Electrowinning cell used for validation experiments

The current was supported by a Velleman programmable DC lab power supply, LABPS3005D. The temperature of the electrolyte was maintained by a temperature controlled water bath at the relevant temperature of 45°C.

3.2.4 Procedure

The electrolyte solution was prepared using the same procedure described in section 3.1.1. The exposed cathode surface area was cleaned by polishing it with sandpaper, washing it with acetone and distilled water.

This was followed by soaking it in the electrolyte for 15 minutes and re-washing with distilled water and electrolyte.

The cell was set up by placing the cathode and anode in the cell. Proper electrode alignment was required for each experiment as any misalignment would introduce errors in the current distribution due to different configurations. Then, the electrolyte was poured into the cell. The net electrolyte volume in the electrowinning cell was 850 ml. Thereafter, the cell was placed in the water bath and heater switched on to keep the electrolyte temperature at the desired temperature. The potentiostat was then connected to the electrodes, and it was only switched on after the electrolyte temperature reached a steady-state temperature (working temperature of 45°C). Electrowinning experiments were carried out for 6 hours for the complete set of parameters.

After depositing the copper, the cathode and anode were removed from the cell and rinsed with distilled water. The tape was removed and cathode together with deposited copper re-rinsed and dried in natural air. The cathode was weighed to determine the mass of the deposited copper.

3.2.5 Analysis method

Before coating the cathode with nail polish, the cathodes were marked and divided into sections by drawing lines along 3 cm dimension of the cathode, that is, 0.5 cm away from the left edge, the centre of the sheet, and 0.5 cm away from the right edge (line A, B and C). Six lines, 0.5 cm apart were then marked across each line. After which, the electrode was coated with nail polish and left to dry. Note that only 3 x 3.5 cm area was exposed to the electrolyte.

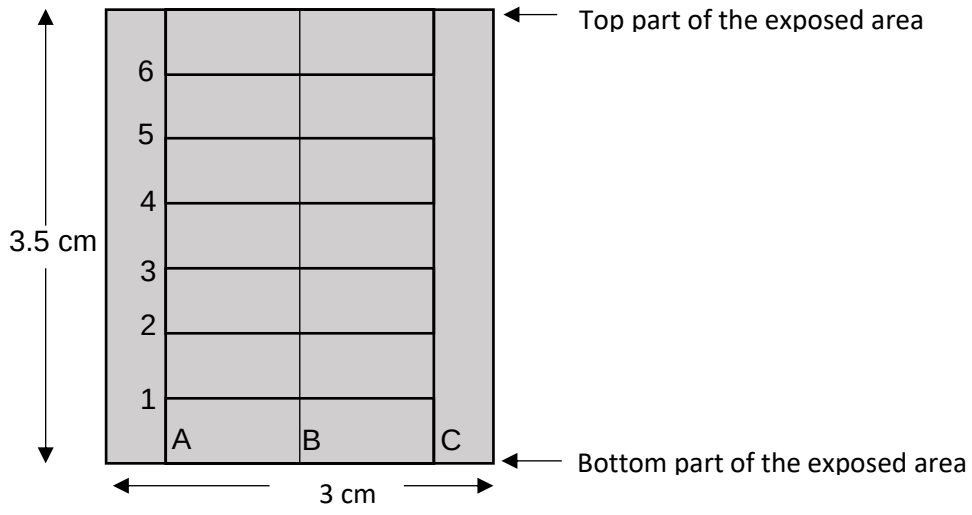

Figure 3.6: Schematic representation of points used for thickness measurements. The thickness was measured on the intersection points

Then, the thickness of the plate (blank cathode) on each intersection point and the three points on the edges (top/bottom) were determined using a digital micrometer screw gauge. This provided the basis for the deposit thickness determination. The reported thickness value was the average of the three measurements lying on the same horizontal line. Figure 3.6 shows the schematic diagram of the marked sections of the cathode.

Note that other methods can be employed to measure deposit thickness. These include, but not limited to optical microscope, scanning electron microscope (SEM) and 3D scanning. The micrometer was chosen as it offers quick, non-destructive and accurate measurements of thickness. A similar approach was adopted by Suggu (2014), though a thickness gauge was used in place of micrometer.

Following the deposition and the drying of the copper deposit on the cathode, the thickness of the intersection points (same points as before the coating process) were measured. The deposit thickness was determined as the difference between the thickness of the plate (together with the deposit) and the thickness of the blank cathode.

The determination of the deposit thickness enabled the local current density to be calculated. Werner *et al.* (2018) proposed a method of converting deposit thickness into depositing current density by utilizing Faradays' law:

$$i_{loc} = \frac{\tau_{loc} n F \rho}{t A_w} \tag{3.9}$$

Where i_{loc} is the local current density, τ_{loc} is the local thickness, n is the number of participating electrons, F is Faraday's constant, ρ is density, t is time, A_w is atomic weight.

Equation 3.9 was very important as it provided the method needed to compare the modelled current density to experimental current density.

Note that the weight of the deposited copper was also measured. This was done by weighing the cathode before placing it in the cell and after the copper had deposited into the cathode. This provided the basis for calculating the current efficiency as given by equation 3.10:

$$Current\ Efficiency\ (C.E.) = \frac{m_{actual}}{m_{theoretical}} \tag{3.10}$$

Where m_{actual} is the actual mass of the mass of the deposit and $m_{theoretical}$ is the theoretical mass of the deposit as given by Faraday's law

Chapter 4 : Results and Discussion of Electrolyte Physicochemical Properties

Section 3.1.2 through to 3.1.5 discussed the experimental approach adopted in the determination of electrolyte physicochemical properties whereas section 3.1.6 outlined the data analysis procedure. A mixed design of experiment was employed to investigate the relationship between physicochemical properties (density, conductivity and diffusivity of copper ions) and electrolyte composition (copper, sulphuric acid, iron, and polyacrylamide additive) at varying temperature. The mixed design was chosen as it made it possible to study several factors at different levels while investigating the interaction between the factors with acceptable number of experiments. The data was fit using multiple linear regression to construct regression models for each property. Regression analysis is the statistical technique for investigating and relationship between variables (Montgomery *et al.,* 2012). The models were evaluated and model adequacy was checked using regression analysis tools. Figure 4.1 summarizes the regression model construction procedure.

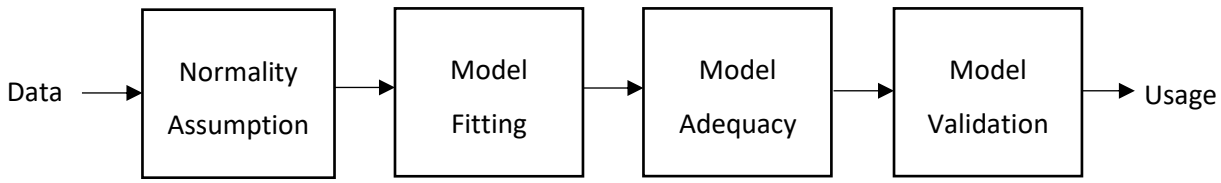

Figure 4.1: Steps taken in model building of physicochemical properties of electrolytes (Adapted from Montgomery et al., 2012)

4.1 Density

The experimental data of density measurements are provided in Appendix B. The reported experimental values are the average of three measurements. The experimental levels and factors are given in Table 3.1. As mentioned in section 3.1.2, the effect of PAM additive on density was investigated further using the one factor at time (OFAT) approach from 5 mg/l to 30mg/l at 35 g/l Cu, 160g/l H_2SO_4, 6 g/l Fe concentration at 45°C and 55°C and the experimental results are provided in Appendix B.

Figure 4.2 shows the normal probability plot of density measurements. The data is assumed to be normally distributed if the points on the graph lie on the straight line. As it can be seen, the density data was normally distributed as no significant skewness was observed. As such, the data was fit to build a correlation relating density to electrolyte composition and temperature.

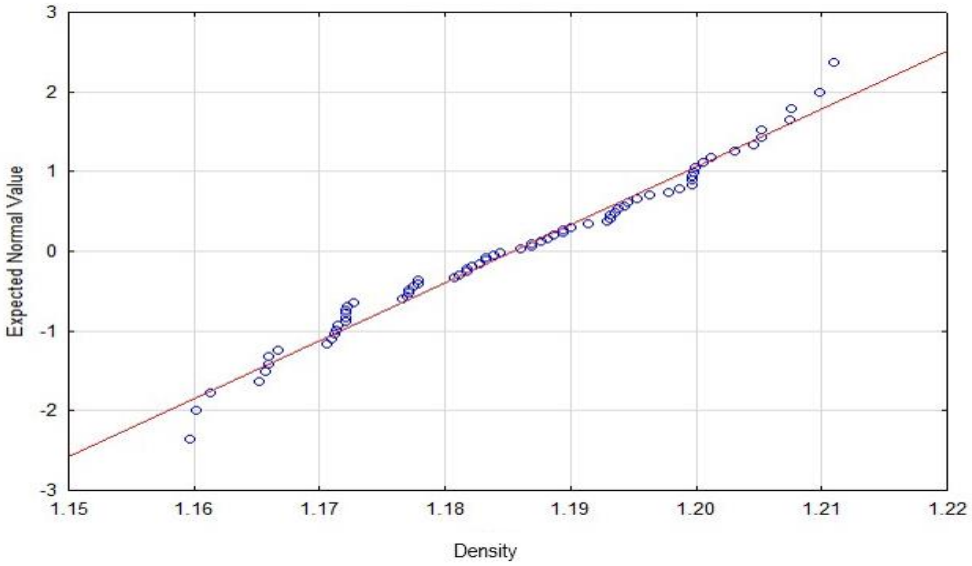

Figure 4.2: Normal probability plot of density measurements

The regression summary statistics for density measurements are shown in Table 4.1. The R^2 and $R^2_{adjusted}$ values are 0.9818 and 0.9798 respectively which indicates that the variability with the specified regressors in the model was well accounted.

Table 4.1: Statistics summary of regression coefficients for density measurements

R^2 = 0.98184; R^2_{adj} =0.97985

Factor	**Coefficient**	**p - value**
Intercept	1.021089	0.000000
Cu	0.002150	0.000000
H_2SO_4	0.000555	0.000000
Fe	0.002540	0.000047
Fe*Fe	-0.000036	0.649805
PAM	-0.000185	0.645133
PAM *PAM	0.000021	0.520163
T	-0.000474	0.000000

From the regression, the unprocessed density model was found to be;

$$\text{Density (g/cm}^3\text{)} = 1.021089 + 0.002150\,[\text{Cu}] + 0.000555\,[H_2SO_4] + 0.002540\,[\text{Fe}] - 0.000185\,[\text{PAM}] - 0.000474T - 0.000036\,[\text{Fe}] \times [\text{Fe}] - 0.000021\,[\text{PAM}]\,X\,[\text{PAM}] \quad (4.1)$$

Where [Cu], [H_2SO_4], [Fe], [PAM], and T represent the concentration of copper (g/l), sulphuric acid (g/l), iron (g/l), PAM (mg/l) and temperature (°C) respectively.

Further analysis of the model showed that the PAM additive did not have a significant effect on density of the electrolyte (higher p-value, greater than alpha = 0.05). This was attributed to the small PAM concentration (in mg/l) present in the electrolyte in comparison to other electrolyte components (in g/l). Also, the interaction terms were found to have no significant effect on the density. Thus, the model was refined by not including the PAM and the interaction terms with $R^2_{adjusted}$ value of 0.9803. The $R^2_{adjusted}$ increased after eliminating non-significant terms which show that the model was improved.

$$\text{Density (g/cm}^3\text{)} = 1.021241 + 0.002150\,[Cu] + 0.000555\,[H_2SO_4] + 0.002279\,[Fe] - 0.000474T \qquad 4.2$$

It can be seen from the model that copper, iron and acid concentration have a positive effect on the density of the electrolyte, that is, increased electrolyte density with increase in concentration. The possible explanation for these results is that the addition of large, high molecular weight metal cations and sulphate anion increased the mass of the electrolyte, thereby increasing the density of the electrolyte. On the other hand, temperature had a negative effect on the electrolyte density. The increase in temperature resulted in a decrease in density. This was due to the increased mobility of ions in the electrolyte as the temperature increased.

A graphical summary of the effect of each factor on the electrolyte density is illustrated by the Pareto chart in Figure 4.3. The Pareto chart shows the standardized effects sorted by their absolute size. The red line indicates the minimum magnitude for a statistically significant effect. Factors that are greater than the minimum magnitude may be significant to the property.

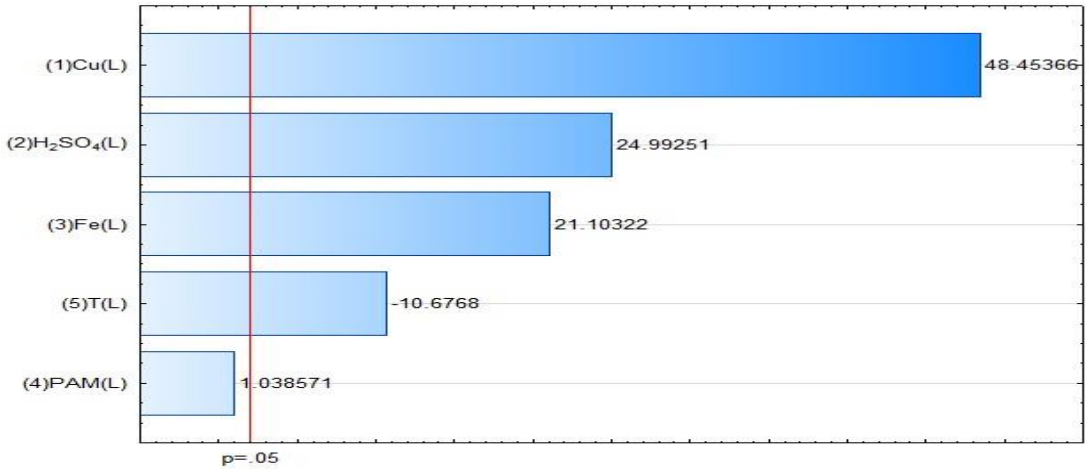

Figure 4.3: Pareto chart illustrating the effect of each factor on density

Based on Figure 4.3, the concentration of copper ions in solution was found to have the strongest influence on the density in the range tested whereas PAM additive had least effect (no significant effect). The probable reasons will be discussed further when considering the effect of each electrolyte component on density.

The model adequacy was then evaluated using the residual plots as shown in Figure 4.4. The model showed good adequacy as plots appear to be random despite having three potential outliers, shown as shaded points in Figure 4.4. The potential outliers appears to be random, possibly due to experimental errors.

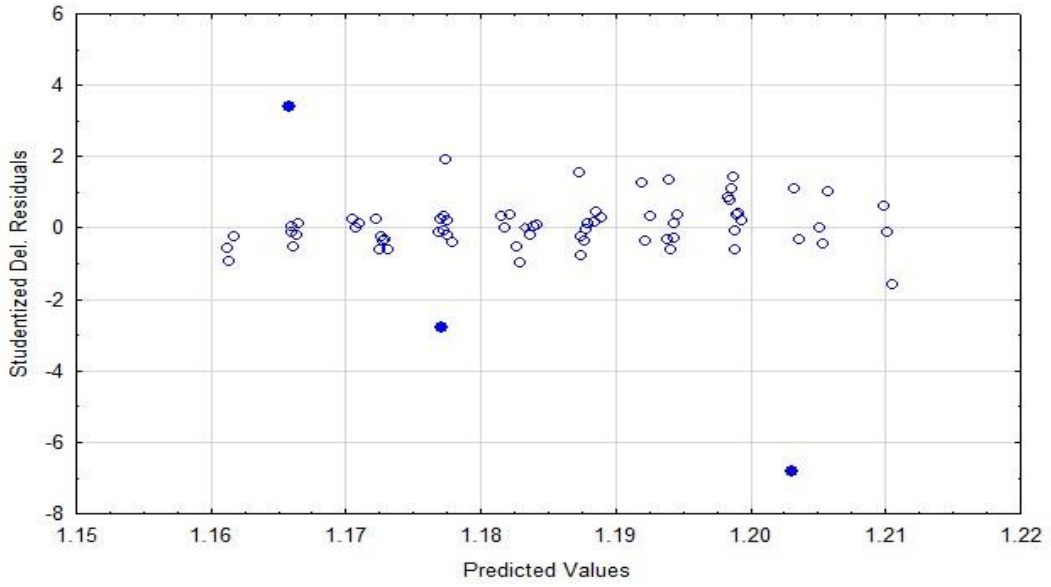

Figure 4.4: Externally studentized residual plots of density model

Figure 4.5 shows the comparison of the model from this study to Price and Davenport (1981) equation as well as experimental density data.

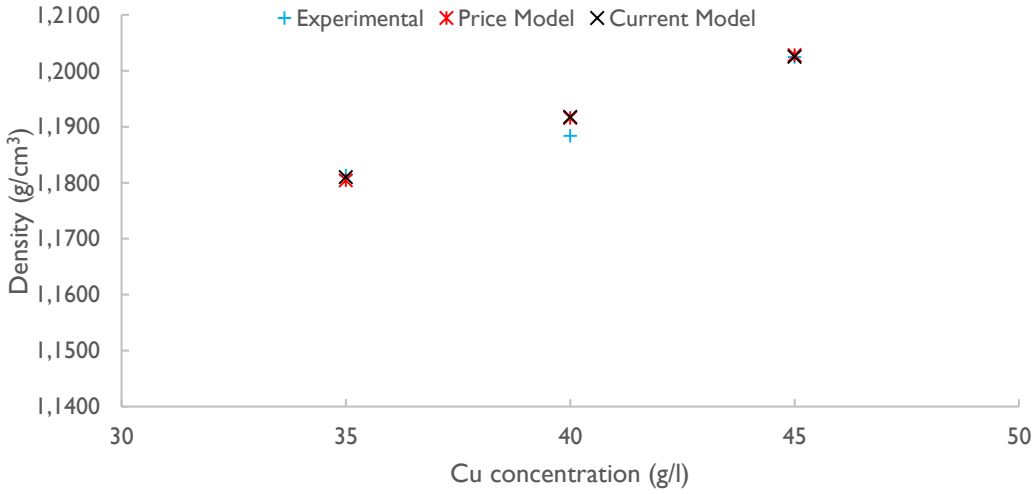

Figure 4.5: Comparison of the current model of density with Price et al (1981) and experimental data at 180 g/l H_2SO_4, 3 g/l Fe and temperature of 45°C.

The density model from this study was in good agreement with Price and Davenport (1981) model as shown by a similar trend when copper concentration was increased. The model also showed a good prediction of data obtained from experiments. This is indicated by the root mean square error (RMSE) of 1.95 x 10^{-3}. The

RMSE is related to the deviation of the prediction errors, that is, how far the observed values are from the predicted values (Willmott, 1981). The RMSE values of the Current model and Price *et al.* (1981) model are 1.94 x10^{-3} and 1.95 x 10^{-3} respectively, which indicates that the models are in good agreement.

4.1.1 Influence of copper concentration

Figure 4.6 shows how copper concentration influences density. It can be clearly observed that increasing copper concentration from 35 g/l to 45 g/l increased the density of the electrolyte. A similar trend was observed by Price and Davenport (1981), and Subbaiah and Das (1989). Though the study of Kalliomaki *et al.* (2017) focused on electrorefining electrolytes, their results had a similar outcome. The increase in density was attributed to the addition of large, high molecular weight which increases the mass of the electrolyte. Also noticeable in Figure 4.6 is the influence of temperature on density. It can be observed that the increase in temperature leads to lower electrolyte density.

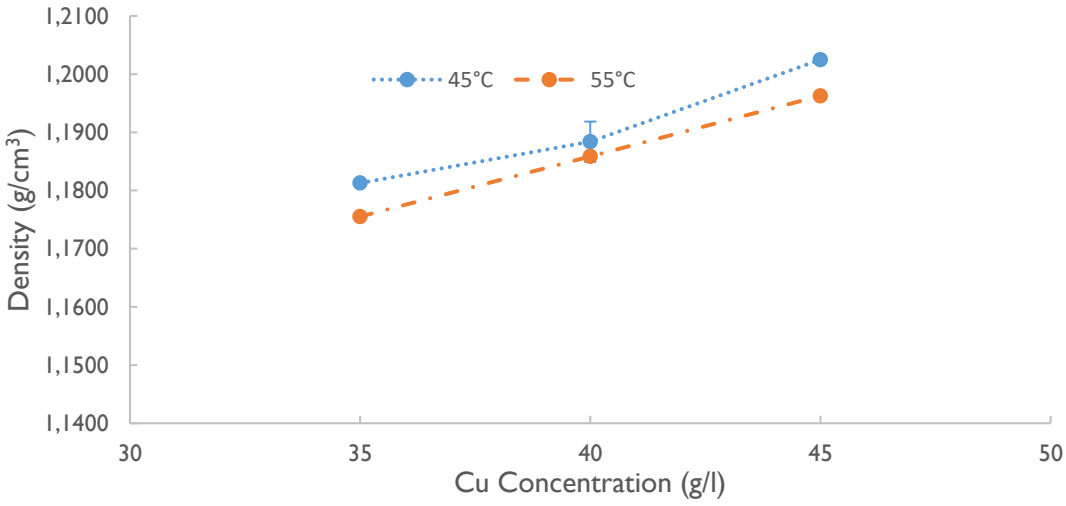

Figure 4.6: Influence of copper concentration on electrolyte density at 180 g/l H_2SO_4, 3 g/l Fe and 9.98 mg/l PAM additive

4.1.2 Influence of Fe concentration

Figure 4.7 illustrates the influence of iron concentration on the density of copper electrolytes. An increase in iron concentration from 1 g/l to 6 g/l resulted in density increase. This is in an agreement with earlier studies conducted by Price and Davenport (1981), and Subbaiah and Das (1989). Price and Davenport (1981) suggested that the increase is due to the increase in mass as more metal cations are added. However, Subbaiah and Das (1989) indicated that though the density increased with an increase in concentration of metallic impurities present in the electrolyte, their contribution to the overall electrolyte density was relatively insignificant. Based on the analysis of Figure 4.3, the concentration of iron had a notable effect on electrolyte density in the present study.

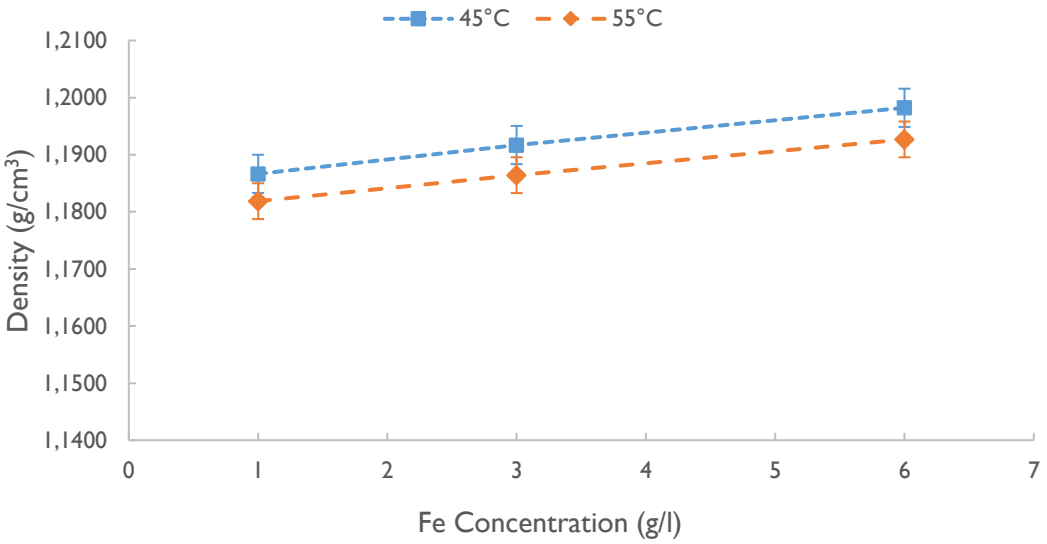

Figure 4.7: Influence of iron concentration on electrolyte density at 160 g/l H_2SO_4, 45 g/l Cu and 9.98 mg/l PAM additive

4.1.3 Influence of acid concentration

Figure 4.8 shows the relationship between acid concentration and electrolyte density. Observe that the increase in acid concentration resulted in the increase of electrolyte density. This is in agreement with the studies conducted by Kalliomaki *et al.* (2017), Price and Davenport (1980, 1981) as well as Subbaiah and Das (1989).

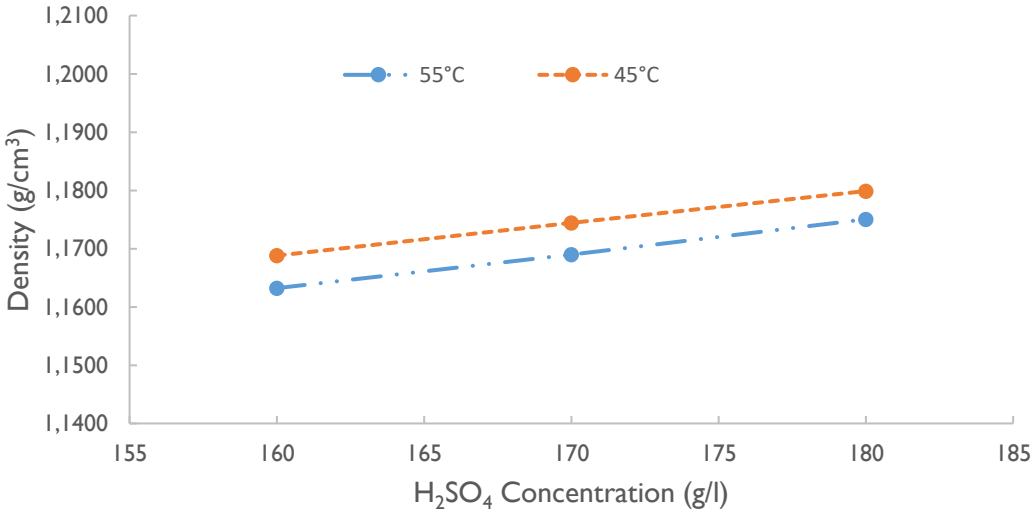

Figure 4.8: Influence of sulphuric acid concentration on electrolyte density at 35 g/l Cu, 3 g/l Fe and 9.98 mg/l PAM additive

In all the studies cited, the results were consistent despite having varying range of sulphuric acid concentration. Price and Davenport (1981) suggested that the increase in density is due to the addition of high molecular weight sulphate ions to the electrolyte. Earlier in Figure 4.3, it was shown that copper had the major effect, followed by acid and iron concentration. This is true considering that the fact that copper has a higher atomic mass and the concentration was high (35 to 45 g/l) compared to iron which has a lower atomic weight and was at lower concentration (1 to 6 g/l).

4.1.4 Influence of PAM concentration

The statistical analysis carried out showed that the additive had no significant effect on the density of the electrolyte. This is supported by Figure 4.9 which shows how electrolyte density is influenced by the concentration of PAM additive from 4.99 mg/l to 29.94 mg/l at 35 g/l Cu, 6 g/l Fe and 160 g/l H_2SO_4.

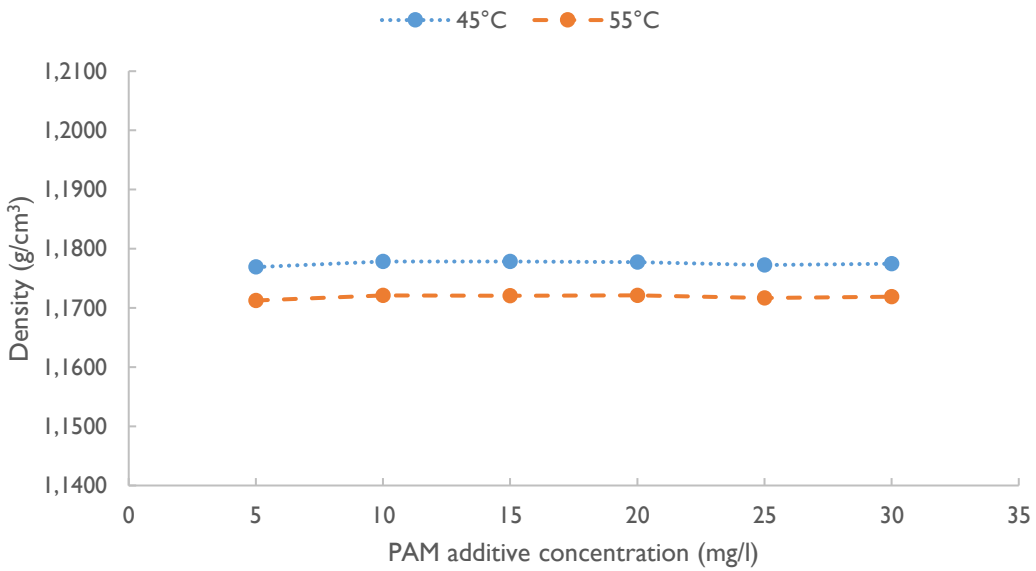

Figure 4.9: Influence of PAM concentration on electrolyte density at 35 g/l Cu, 6 g/l Fe and 160 g/l H_2SO_4

As shown in Figure 4.9, the density was not influenced by the variation in concentration of the PAM additive. It remained constant in the range tested. The low concentration of PAM additive (orders of magnitude lower than other electrolyte components) may be ascribed to the observed trend.

It was necessary to investigate the effect of PAM additive on density because of its higher molecular weight and its nature of being viscous. Studies conducted to investigate electrolyte density were carried out in the absence of the additive. Consequently, it was difficult to compare the current results with results from the literature. Although the studies by Gladysz *et al.* (2007) and Araneda-Hernández *et al.* (2014) focused on investigating the effect of additives on the diffusion coefficient of copper, their work provides an insight on

how additives affect the physicochemical properties. As suggested by Gladysz *et al.* (2007), the influence of the additives on the electrodeposition process is primarily through adsorption at the cathode surface.

4.2 Conductivity

The experimental conductivity results are reported in Appendix B. Figure 4.10 shows the normal probability of conductivity measurements. The figure clearly shows that the conductivity data was normally distributed. As it was mentioned in the preceding section, the normality assumption is considered to be valid, that is, the data is assumed to be normally distributed if the points on the graph lie on the straight line. As it can be observed, the conductivity data was normally distributed as no significant skewness was observed. As a result, regression analysis was applied to fit the data so as to develop the required model for electrolyte conductivity. The model described the relationship between electrolyte composition (copper concentration, sulphuric acid concentration, iron concentration, and PAM additive concentration) as well as temperature to electrolyte conductivity.

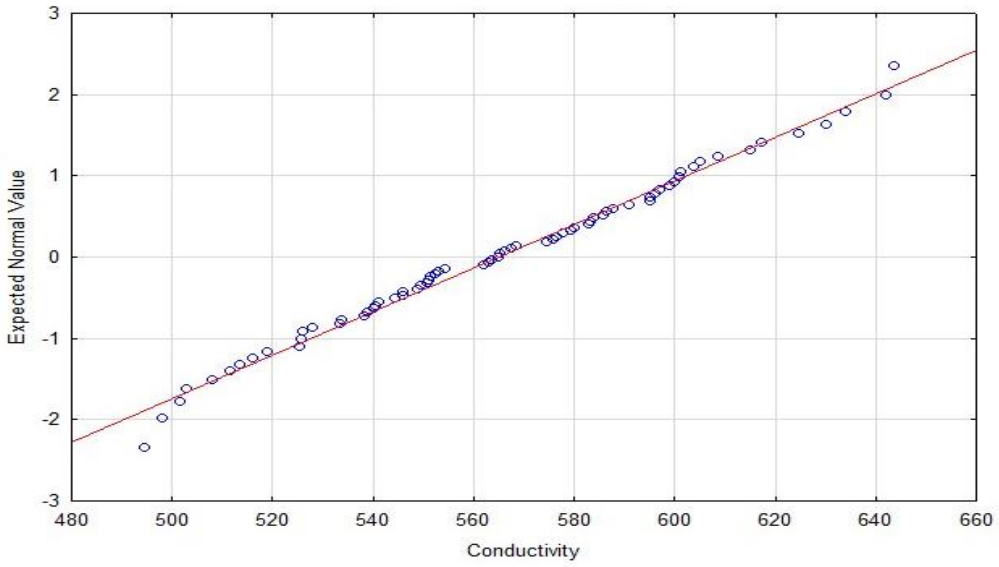

Figure 4.10: Normal probability plot of conductivity values

Table 4.2 shows a summary of the regression coefficients for the conductivity model.

Table 4.2: Statistics summary of regression coefficients of electrolyte conductivity

Factor	R^2 = 0.96423; R^2_{adj} =0.96152	
Factor	**Regression**	**p - value**
Intercept	125.7765	0.000000
Cu	-3.3649	0.000000
H_2SO_4	2.2927	0.000000
Fe	-4.0324	0.000000
PAM	0.4696	0.069912
T	3.8916	0.000000

The unrefined conductivity model is as follows:

$$\text{Conductivity (mS/cm)} = 125.7765 - 3.3649\,[Cu] + 2.2927\,[H_2SO_4] - 4.0324\,[Fe] + 0.4696\,[PAM] + 3.8916T \quad 4.3$$

Where [cu], $[H_2SO_4]$, [Fe], [PAM], and T represents the concentration of copper (g/l), sulphuric acid (g/l), iron (g/l), PAM (g/l) and temperature (°C) respectively.

From Table 4.2, the p-value for PAM was greater than the alpha value (0.05), indicating that it was no statistically significant. Consequently, it was excluded in the refined model and the model had R^2_{ad} value of 0.9624 after exclusion of the insignificant terms. The refined model is given as:

$$\text{Conductivity (mS/cm)} = 128.4375 - 3.3649\,[Cu] + 2.2927\,[H_2SO_4] - 4.0324\,[Fe] + 3.8916T \quad 4.4$$

The regression model shows that an increase in copper and iron concentration had a negative effect on the conductivity, that is, it decreased the conductivity of the electrolyte whereas sulphuric acid concentration had a positive effect on the electrolyte conductivity. The likely explanation is that the addition of large, heavier metallic ions tend to limit movement of ions in the electrolyte compared to the lighter hydrogen ions which have higher mobility (Price & Davenport, 1981). Conductivity in the solution medium is related to the movement of ions within the system. Furthermore, as reported by Subbaiah and Das (1989), the addition of metallic ions in the system increase the viscosity and density, which might affect the conductivity negatively.

The effect of temperature is well documented in the literature. An increase in temperature increases the conductivity due to enhanced ion mobility and reduced viscosity (Bousfield & Lowry, 1903; Barron & Ashton, 2005).

Figure 4.11 shows a summary of the effect of each factor on the electrolyte conductivity. Based on the Pareto chart, the concentration of sulphuric acid in solution was found to have a strong influence on the conductivity. This is supported by the reasoning given earlier, that is, the addition of sulphuric acid in the electrolyte introduces the highly mobile hydrogen ions. As a result, in industrial operations, sulphuric acid is added in the electrolyte to reduce the electrolyte resistance.

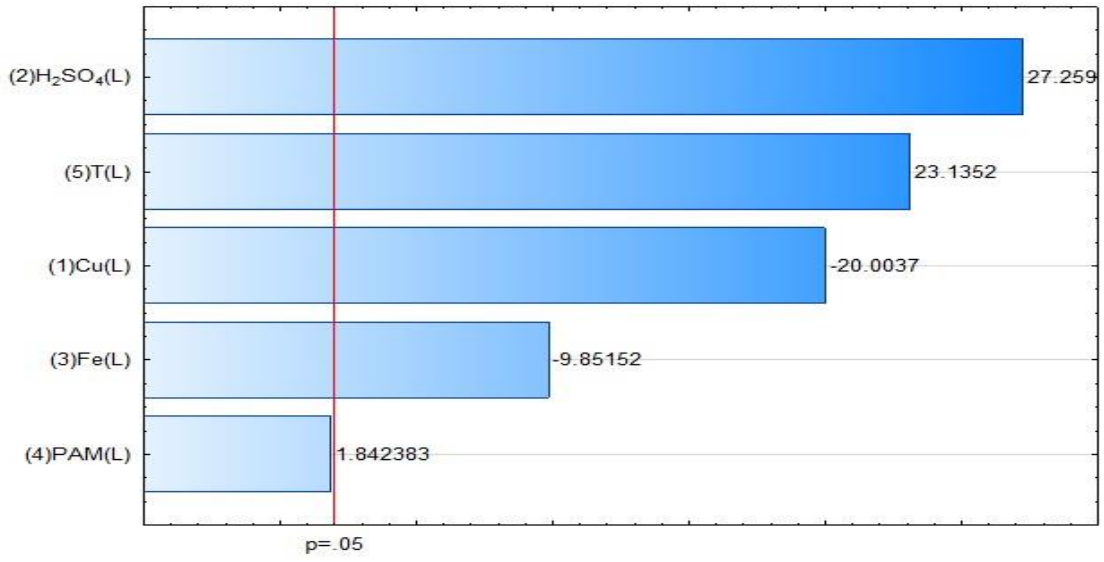

Figure 4.11: Pareto chart of conductivity measurements

The model adequacy was evaluated using the residual plots as shown in Figure 4.12. The analysis of residuals helps in evaluating the model inadequacies. The model is considered to be reasonable if the residual plots are randomized. If signs of pattern in the scatter plots of residuals are observed, it may point to model inadequacy. Figure 4.12 shows that the residual plots were randomized, indicating that there were no substantial inadequacies in the model.

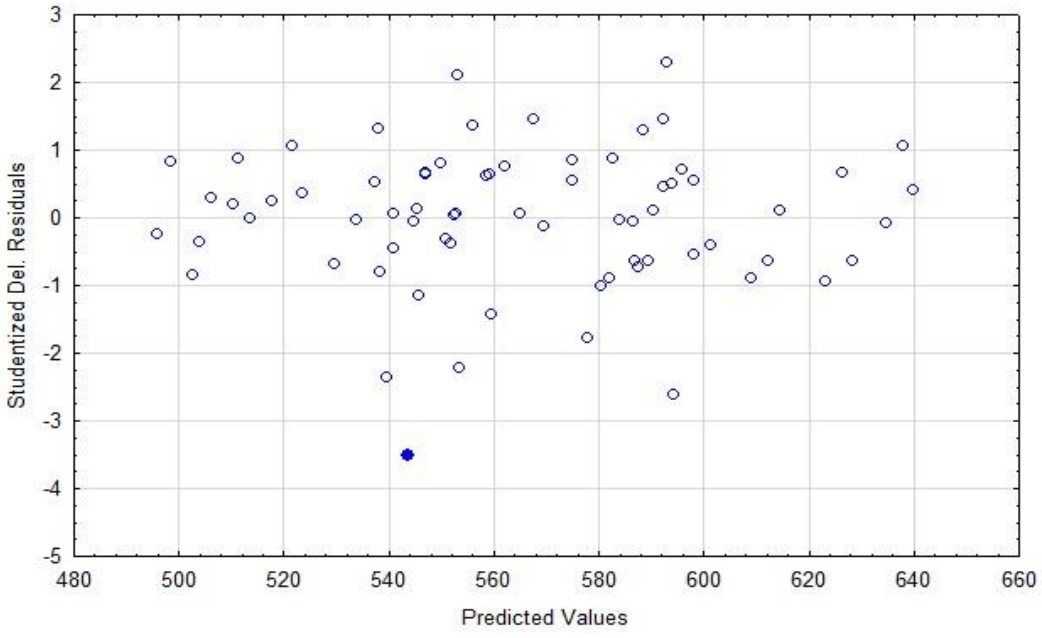

Figure 4.12: Externally studentized residual plots of conductivity model

Figure 4.13 shows the comparison of the model from this study to Price and Davenport (1981) model and experimental conductivity data.

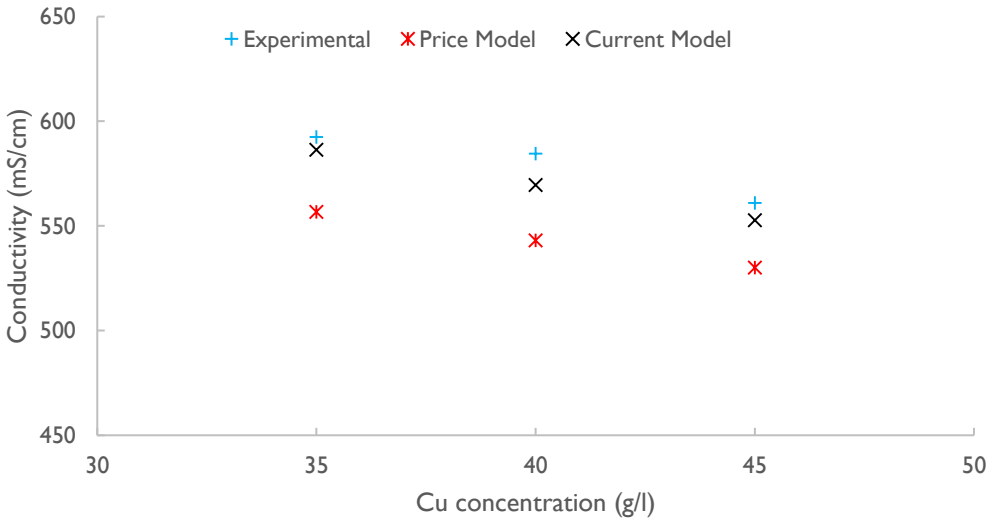

Figure 4.13: Comparison of the current model of conductivity with Price and Davenport (1981) and experimental data at 180 g/l H_2SO_4, 3 g/l Fe and temperature of 45°C

The conductivity model from this study showed a similar trend with a model developed by Price and Davenport (1981) as the copper concentration was being varied. The only noted variation was that the model from this study predicted higher values than the model of Price and Davenport (1981). This is shown by a higher value of RMSE for Price and Davenport (1981) model (36.2289) compared to RMSE value of conductivity model from the present work (10.5255). The difference between the two models may be due to the other metallic impurities present in the Price and Davenport (1981) which were not investigated in the current work. The decrease of conductivity due to the presence of impurities was also observed by Subbaiah and Das (1989). The presence of impurities in the electrolyte leads to the increase in viscosity. At the same time, ion complexation may occur which can hinder the mobility of ions in the electrolyte. The model from this study also showed a good prediction for data obtained from experiments.

4.2.1 Influence of copper concentration

The effect of copper concentration is shown in Figure 4.14. It can be seen that the increase in copper concentration from 35 g/l to 45 g/l resulted in a decrease of electrolyte conductivity. This trend was also observed by Price and Davenport (1980, 1981), Subbaiah and Das (1989) and Kalliomäki *et al.* (2016). Price and Davenport (1981) alluded to the presence of large, high molecular weight copper cations in solution as the cause of a decrease in conductivity. The addition of copper ions in the solution increases the viscosity of the electrolyte; consequently, reducing the mobility of ions. Furthermore, the increase in concentration of copper may have a negatively impacted the dissociation of the electrolyte since the electrolyte was prepared from the sulphate compounds.

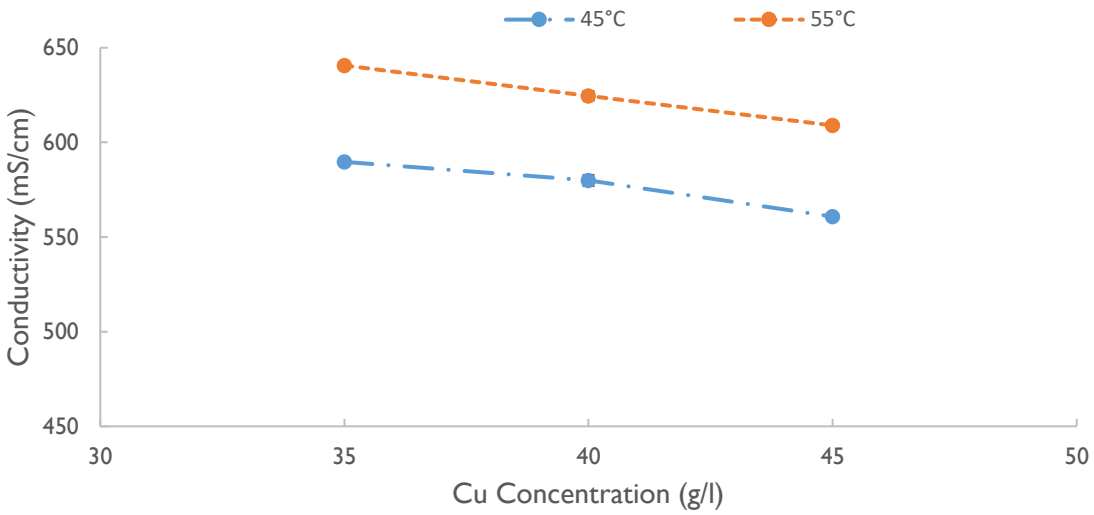

Figure 4.14: Influence of copper concentration on electrolyte conductivity at 180 g/l H_2SO_4, 3 g/l Fe and 9.98 mg/l PAM additive

4.2.2 Influence of Fe concentration

Figure 4.15 shows how iron concentration affects the conductivity of copper electrolyte. Increasing iron concentration from 1 g/l to 6 g/l resulted in a decrease in conductivity. This is in an agreement with earlier studies conducted by Price and Davenport (1981) and Subbaiah and Das (1989). Price and Davenport (1981) suggested that the decrease in electrolyte conductivity is due to the presence of high, large molecular weight iron cations which limits ion mobility in the solution. Also noticeable from Figure 4.15 is the effect of temperature on conductivity, that is, it increases with increase in temperature.

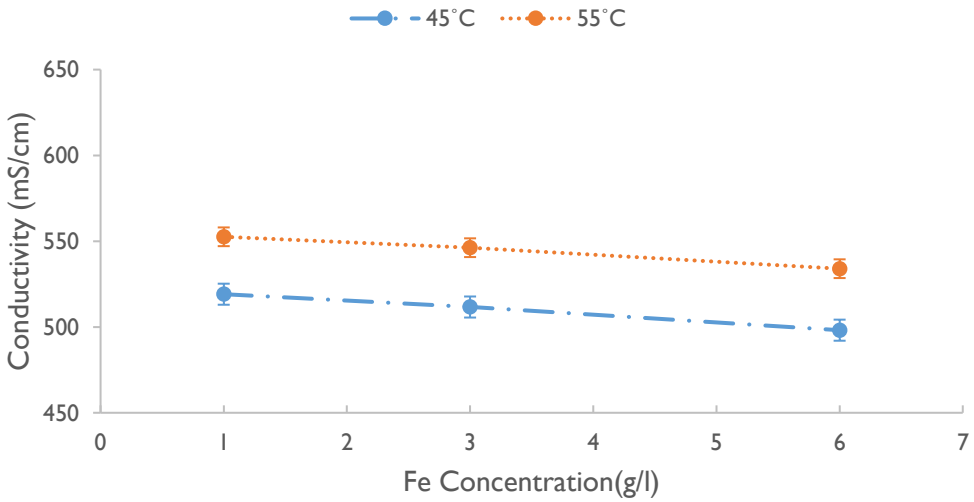

Figure 4.15: Influence of iron concentration on electrolyte conductivity at 160 g/l H_2SO_4, 45 g/l Cu and 9.98 mg/l PAM additive

4.2.3 Influence of acid concentration

As Figure 4.11 showed, sulphuric acid concentration strongly influences electrolyte conductivity. The effect of changing sulphuric acid concentration is illustrated in Figure 4.16.

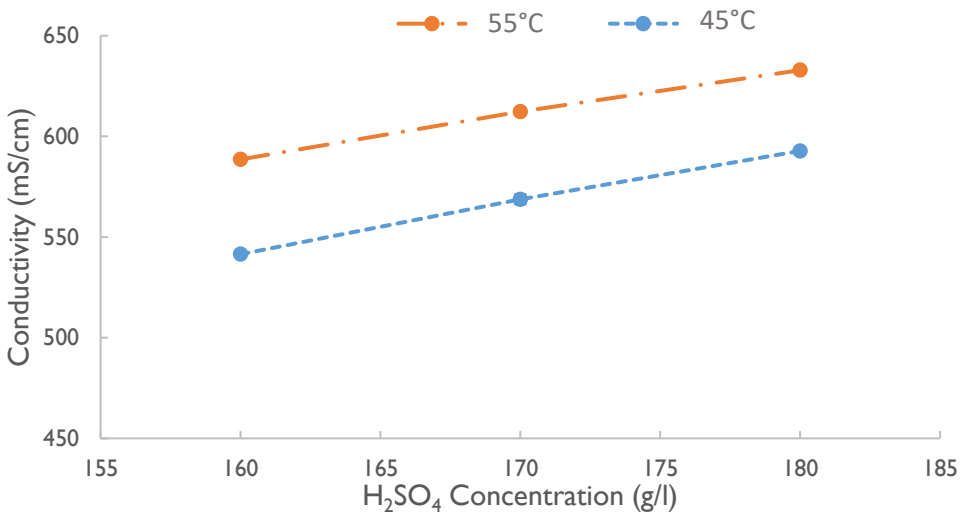

Figure 4.16: Influence of sulphuric acid concentration on electrolyte conductivity at 35 g/l Cu, 3 g/l Fe and 9.98 mg/l PAM additive

Increasing acid concentration from 160 g/l to 180 g/l resulted in an increase in conductivity. This was also reported by Kalliomäki *et al.* (2016), Subbaiah and Das (1989) and Price and Davenport (1980, 1981). The increase in conductivity was attributed to the presence of highly mobile hydrogen ions which carry charge through the solution.

4.2.4 Influence of PAM concentration

The PAM additive did not have any significant effect on the conductivity. This is shown in Figure 4.17 below in which the influence of conductivity was investigated at 35 g/l Cu, 160 g/l acid and 6 g/l iron concentration over 4.99 to 29.94 mg/l of PAM additive concentration. As illustrated in Figure 4.17, there was negligible variation in the electrolyte conductivity over the range tested. PAM consists of very long chains, have low dissociation and form a viscous film near the electrode (Vereecken & Winand, 1976). This implies that they have low ionic conductivity. The observed trend in Figure 4.17 may be attributed to the low concentrations of the additive present in the electrolyte and the manner in which the additive influence the electrodeposition process through adsorption on the electrode surface.

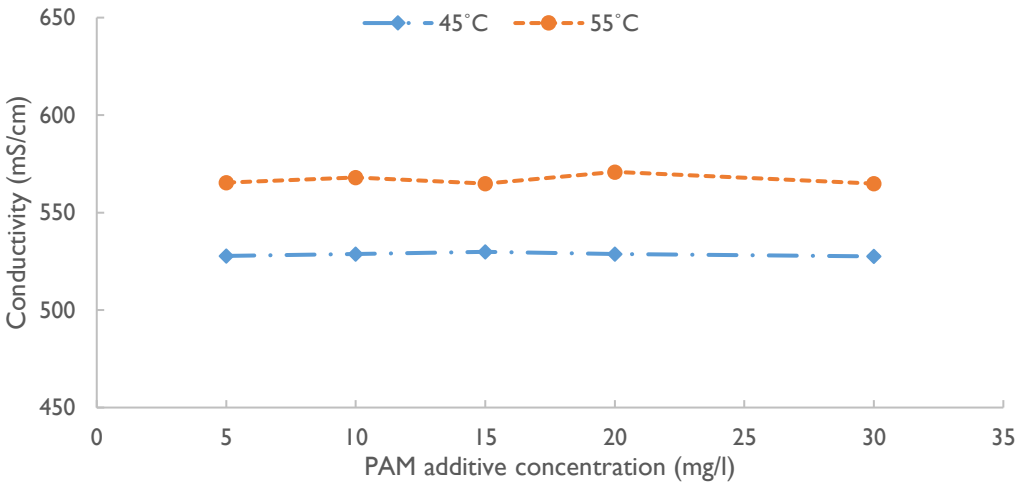

Figure 4.17: Influence of PAM concentration on electrolyte conductivity at 35 g/l Cu, 6 g/l Fe and 160 g/l H_2SO_4

4.3 Diffusion Coefficients

The diffusion coefficients of copper ions were determined from the limiting current using two equation: Levich and Koutecky - Levich equation. The reasons for this approach were outlined in section 3.1.5. As such, the results from both equations will be discussed. The experimental results for the diffusion coefficients of copper ions are given Appendix B.

4.3.1 Diffusion coefficients by Levich equation

Figure 4.18 shows the normal probability plot of the diffusion coefficients measurements. It can be observed from the graph that the diffusion coefficient values are skewed. Consequently, data transformation was tested using logarithm transformation. However, the transformed data appeared to be skewed. As a result, the data was analysed further to troubleshoot the underlying cause of the skewness. Further analysis of the data reviewed that it was split into parts: The left part of Figure 4.18 represents the data of the experiments carried out at 45˚C and the right part represents the data at 55˚C. It appears that the temperature had a contribution towards the skewness. When the data was grouped and treated at separate temperature of 45˚C and 55˚C respectively, the data showed that it was normally distributed at each specific temperature. Therefore, despite the skewness, the data was assumed to be normally distributed. This is because the temperature effect on the regression model needed to be captured.

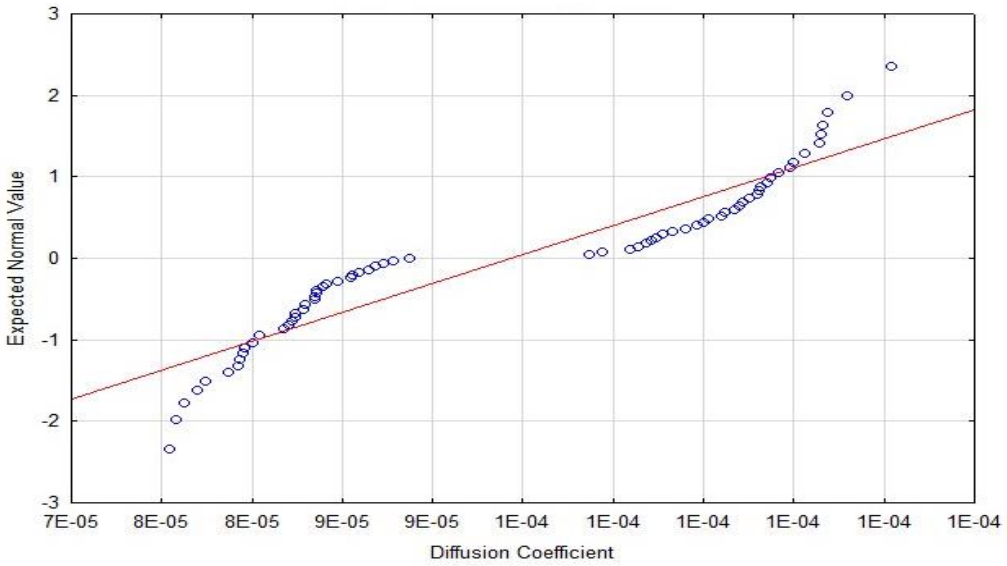

Figure 4.18: Normal probability plot of diffusion coefficients residual values

The regression summary fit for density measurements is shown in Table 4.3. The R^2 and $R^2_{adjusted}$ value are 0.9879 and 0.9870 which indicates that the variability with the specified variables was well accounted for in the model.

Table 4.3: Summary of regression coefficients of diffusion coefficient determined by the Levich equation

	R^2=0.98787; R^2_{adj} =0.98695	
Factor	Coefficient	p - value
Intercept	2.453729	0.000000
Cu	-0.029449	0.000000
H_2SO_4	-0.022538	0.000000
Fe	-0.104641	0.000000
PAM	0.004373	0.411893
T	0.246773	0.000000

The model is given as:

$$\text{Diffusion Coefficient } (cm^2/s) \times 10^{-5} = 2.453729 - 0.029449\,[Cu] - 0.022538\,[H_2SO_4] - 0.104641\,[Fe] + 0.004373\,[PAM] + 0.246773\,T \quad (4.5)$$

The PAM additive term and the interaction terms did not have any significant effect on the diffusivity of the copper ions in the electrolyte as exhibited by their high p-values. Thus, these terms were excluded in the model. After the exclusion of no-significant terms, the value of R^2_{ad} was 0.9782 which indicated that the exclusion of insignificant terms resulted in model improvement. Thus, the final regression model is given as:

$$\text{Diffusion Coefficient } (cm^2/s) \times 10^{-5} = 2.478510 - 0.029449\,[Cu] - 0.022538\,[H_2SO_4] - 0.104641\,[Fe] + 0.246773\,T \quad (4.6)$$

The Pareto chart (Figure 4.19) shows the extent to which these factors influence the diffusion of copper ions. As seen in Figure 4.19, temperature was found to be a major influencer of diffusivity of copper ions.

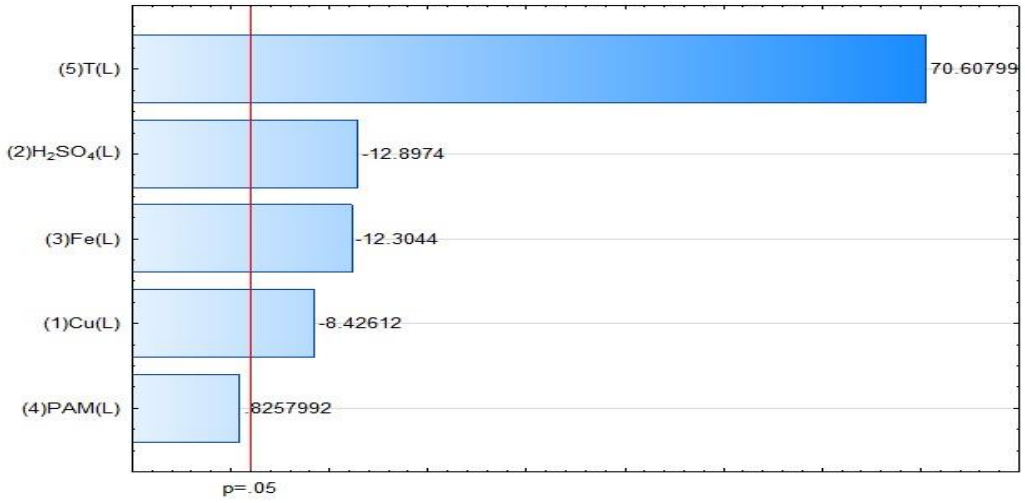

Figure 4.19: Pareto chart of diffusion coefficients using Levich equation

The analysis of model adequacy showed good adequacy despite displaying potential signs of inadequacies as shown in Figure 4.20.

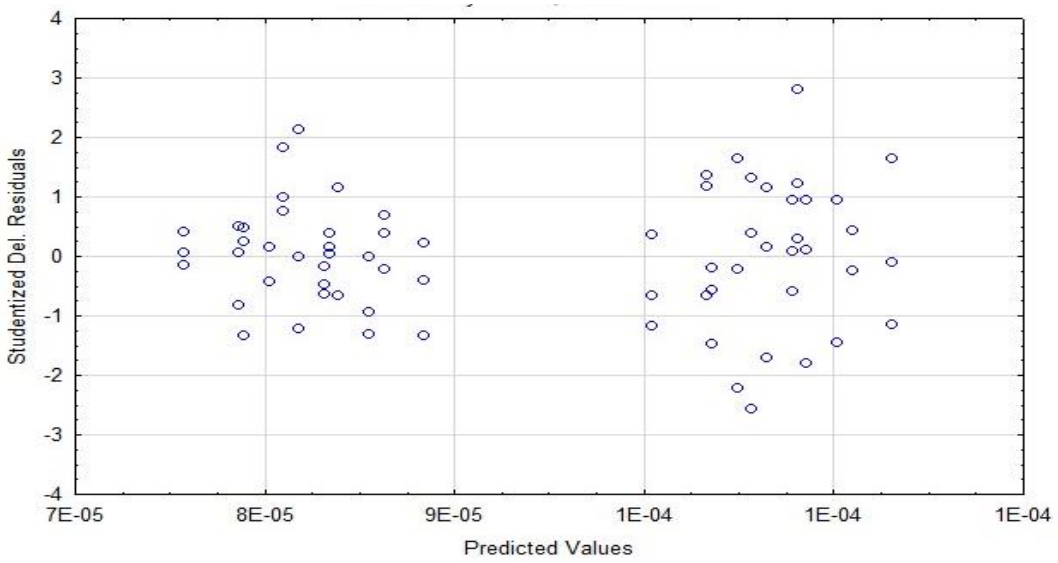

Figure 4.20: Externally studentized residual plots of diffusion coefficient model: Levich equation

The residual plots are randomized, though it seems that the residuals are separated into two categories. This may suggest that two separate models be constructed for each set of data. The split of data was largely due

to the temperature at which the experiments were conducted (45°C and 55°C). As observed from Figure 4.19, temperature had greater influence on the diffusivity of copper ions compared to other factors. Thus, it was necessary to include temperature term in the model rather than having two equations at specific temperature.

4.3.2 Diffusion coefficients by Koutecky - Levich equation

The normal probability plot for the diffusion coefficient values determined by the Koutecky – Levich equation is shown in Figure 4.21. It can be seen from the graph that the diffusion coefficient values were skewed. The reason for the skewness was mentioned earlier in the preceding section, which is the different temperatures at which the measurements were carried out. However, the data was assumed to be normally distributed and the data was fit using multiple regression.

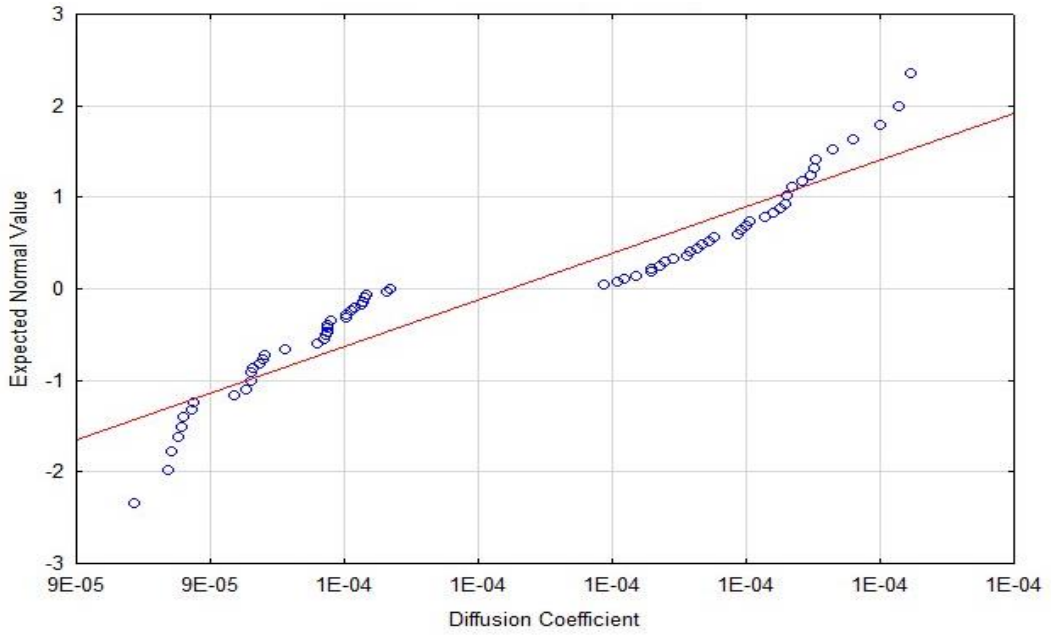

Figure 4.21 Normal probability plot of diffusion coefficients residual values

The regression summary of fit for diffusion coefficients measurements determined by the application of the Koutecky – Levich equation is shown in Table 4.4. The R^2 and $R^2_{adjusted}$ value are 0.9824 and 0.9766 which indicates that the variability with the specified variables was well accounted.

Table 4.4: Regression coefficients of diffusion coefficient calculated using Koutecky – Levich equation

	R^2=0.97979R^2_{adj} = 0.97826	
Factor	**Coefficient**	**p - value**
Mean/Interc.	5.403254	0.000000
Factor	**Coefficient**	**p - value**
Cu	-0.015928	0.000004
H_2SO_4	-0.017949	0.000000

Fe	-0.076145	0.000000
PAM	0.005043	0.299668
T	0.172915	0.000000

The unrefined model is given as

$$\text{Diffusion Coefficient } (cm^2/s) \times 10^{-5} = 5.403254 - 0.015928\,[Cu] - 0.017949\,[H_2SO_4] - 0.076145\,[Fe] + 0.005043\,[PAM] + 0.172915T \quad (4.7)$$

The analysis of the Koutecky – Levich model reviewed a similar outcome to that of the Levich model. The PAM additive term and interaction terms were neglected. This is because the p-values for these terms were greater than alpha value, indicating that there were statistically insignificant. Since non-significant terms were removed, the value of R^2_{ad} became 0.9870 which indicates model improvement.

Thus, the processed model did not include the PAM and the interaction terms as given below.

$$\text{Diffusion Coefficient } (cm^2/s) \times 10^{-5} = 5.431829 - 0.015928\,[Cu] - 0.017949\,[H_2SO_4] - 0.076145\,[Fe] + 0.172915T \quad (4.8)$$

Similarly, the temperature was observed to have a largest effect on the diffusivity of copper ions as shown in Figure 4.22.

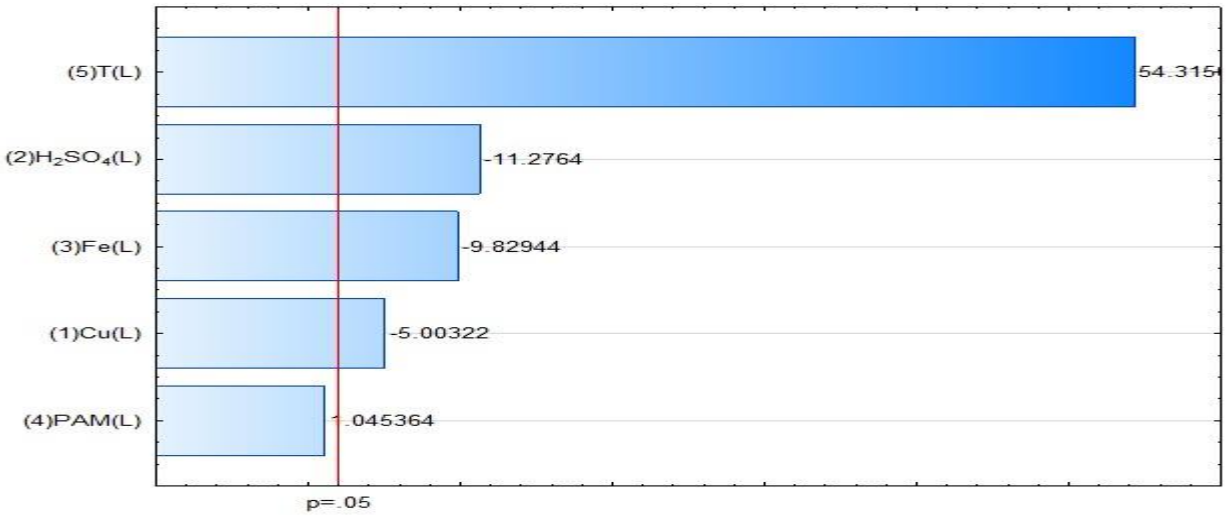

Figure 4.22: Pareto chart showing standardized estimate effect of factors on diffusion coefficient

Figure 4.23 shows externally studentized used to check model adequacy. The model exhibited inadequacies similar to those of diffusion coefficients determined by Levich equation due to the reasons mentioned earlier.

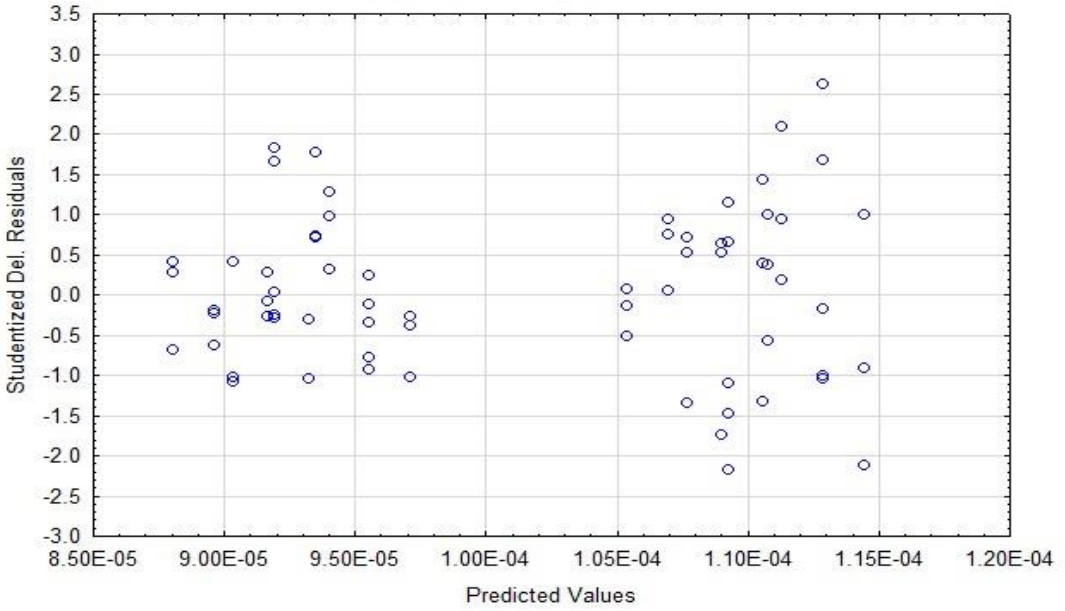

Figure 4.23: Externally studentized residual plots of diffusion coefficient model: Levich equation

The two diffusion coefficients models were compared to each other as shown in Figure 4.24. Though the models exhibited similar trends (lower diffusion coefficient values at higher copper concentration), it was observed that the diffusion coefficients values determined by Koutecky – Levich equation were higher than those by Levich equation with an average difference of 2.42 x 10^{-5} cm^2/s. It is suggested that this is due to the incorporation of the activation current to the mass limited current used in the Levich equation (Quickenden & Xu, 1996). During data fitting, it was observed that minor deviations in the limiting current density had a significant effect on the slope which affected the magnitude of the calculated diffusion coefficient.

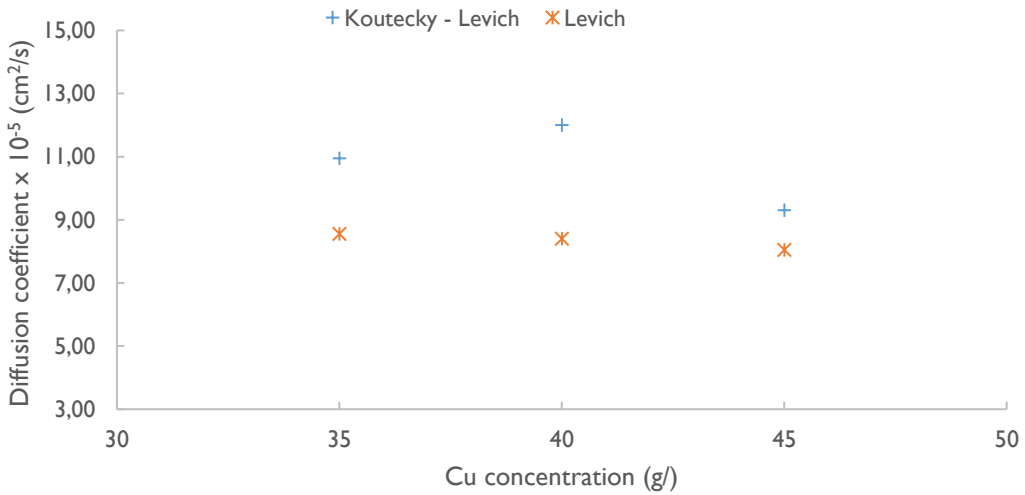

Figure 4.24: Comparison of diffusion coefficients model of Levich and Koutecky - Levich at 180 g/l H_2SO_4, 3 g/l Fe and temperature of 45°C

For industrial applications, the flux of copper ions in solution is better represented by the mass transfer coefficient. This is because mass transfer coefficient is more relevant measure of mass transport than diffusion coefficient. Thus, mass transfer coefficients were determined from the diffusion coefficients of the present study and dimensionless constants (Schmidt number, Sherwood number and Grashof number) utilizing the natural convection correlation by Beukes and Badenhorst (2009) given in section 2.4.2.4 as equation 2.36.

$$Sh = 0.902\left(\frac{Gr.Sc}{4(0.861+Sc)}\right)^{0.25} \qquad 2.36$$

To determine the value of Grashof number, the works of Wilke *et al.* (1953) and Najim (2016).were reviewed. According to Wilke *et al.* (1953), the Grashof number under natural convection can be calculated from equation

$$Gr = \frac{g(\rho_o - \rho_i)\rho^2 x^3}{\rho_i \mu^2} \qquad 4.9$$

Where g is the acceleration of gravity (cm/s^2), ρ_o, ρ_i and ρ is fluid density in the bulk solution, at the surface of the electrode and average density (g/cm^3), x is the vertical height of the electrode (cm) and μ is the average liquid velocity (g/cm^3).

The values of density used were from the present work whereas the viscosity values were extracted from Price and Davenport (1981) model and value of x was assumed to be 1.2m The calculated mass transfer coefficients were compared to mass transfer coefficients values of Beukes and Badenhorst (2009) which were determined from industrial data. These are given in Table 4.5.

Table 4.5: Mass transfer coefficients of the current work and of Beukes and Badenhorst (2009)

	Mass Transfer Coefficient
Levich Equation	1.07 X 10^{-7}
Koutecky – Levich Equation	9.79 X 10^{-7}
Nullabor M	2.18 X 10^{-6}
FQM Bwana Mkubwa	2.13 X 10^{-6}

The mass transfer coefficient calculated using the Levich and Koutecky - Levich equation were compared to Beukes and Badenhorst (2009) and showed differences in magnitude of the determined mass transfer. This may be attributed to the different electrolyte composition between the synthetic and industrial electrolyte, the diffusion coefficient determination method and the temperature range. The industrial electrolyte had

copper concentration ranging from 33 to 55 g/l, 155 to 160 g/l H_2SO_4 and other impurities such Ni, Mn and Co at temperatures 35 to 40°C whereas the present study range was 35 to 45 g/l, 160 to 180 g/l H_2SO_4 at temperatures 45 to 55°C.

It was mentioned earlier that the diffusion coefficients determined by Levich equation tend to be lower than those determined by the Koutecky - Levich equation due to the fact that the former does not take into account the activation polarization. As such, the discussion that follow will based on diffusion coefficients determined using the Koutecky – Levich equation.

4.3.3 Influence of copper concentration

The effect of copper concentration on the diffusion of copper ions is shown in Figure 4.25. There was a slight decrease in the diffusivity of copper ions with an increase in copper concentration. Subbaiah and Das (1989) attributed the decrease to the forces of interaction between electrolyte species, the hydration phenomena occurring in the electrolyte and the increase of the density and viscosity of the electrolyte. Quickenden and Jiang (1984) suggested that aggregation of copper ions via sulphate bridges at higher concentration could be another reason. The decrease in diffusivity of copper ions as the concentration of copper increases was also reported for electrorefining electrolytes by Moats *et al.* (2000), Gladysz *et al.* (2007) and Kalliomäki *et al.*, (2019).

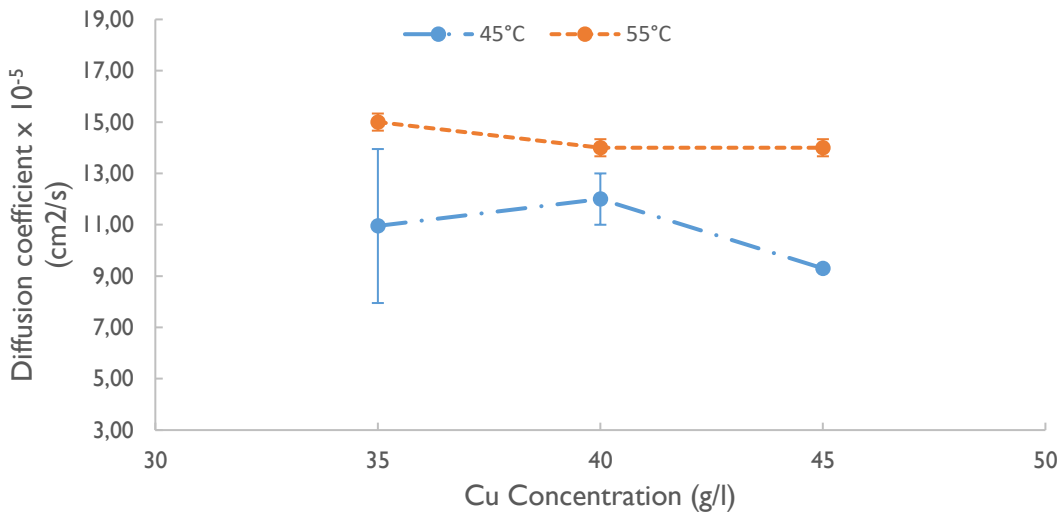

Figure 4.25: Influence of copper concentration on diffusivity of copper ions at 180 g/l H_2SO_4, 3 g/l Fe and 9.98 mg/l PAM additive

4.3.4 Influence of acid concentration

Figure 4.26 illustrates the effect of acid concentration on the diffusivity of copper ions. Increasing acid concentration from 160 g/l to 180 g/l resulted in a slight decrease of the diffusivity of copper ions. A similar

trend was observed in earlier studies by Subbaiah and Das (1989), Moats *et al.* (2000), Gladysz *et al.* (2007) and Kalliomäki *et al.*, (2019).

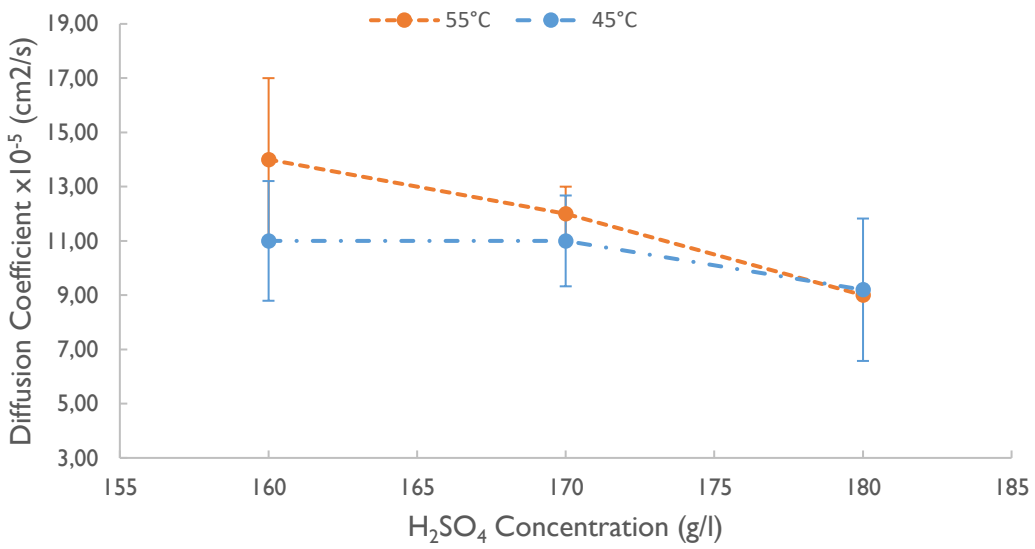

Figure 4.26: Influence of H_2SO_4 concentration on diffusivity of copper ions at 35 g/l Cu, 3 g/l Fe and 9.98 mg/l PAM additive

4.3.5 Influence of Fe concentration

The effect of iron concentration on the diffusivity of copper ions is illustrated in Figure 4.27. Despite the model (equation 4.8) indicating that the increase in iron concentration results in the decrease of diffusivity of the copper ions, Figure 4.27 shows that increasing iron concentration from 1 g/l to 6 g/l resulted in a negligible decrease of the diffusivity of copper ions in the electrolyte.

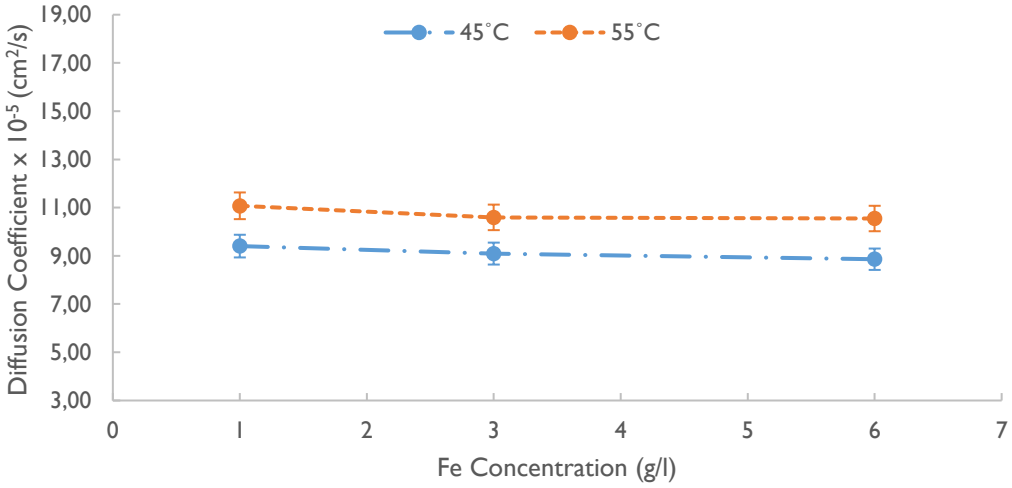

Figure 4.27: Influence of iron concentration on diffusivity of copper ions at 160 g/l H_2SO_4, 45 g/l Cu and 9.98 mg/l PAM additive

4.3.6 Influence of PAM concentration

Within the range investigated, the PAM additive was found to have no significant influence on the diffusivity of copper ions in the electrolyte as shown in Figure 4.28.

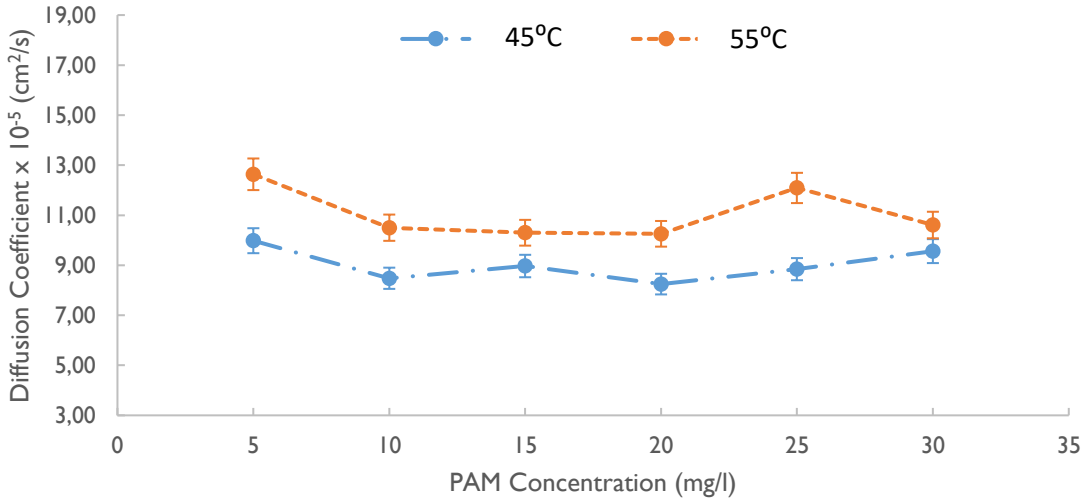

Figure 4.28: Influence of PAM concentration on diffusivity of copper ions at 35 g/l Cu, 6 g/l Fe and 160 g/l H_2SO_4

Even though Gladysz *et al.* (2007) and Araneda-Hernández *et al.* (2014) investigated the effect of different types of additive (thiourea and animal glue) on the diffusion coefficient of copper, their results show similar trend to the current study. These studies showed that the increase in additive concentration from 1 to 5 mg/l (Gladysz *et al.,* 2007) and 1 to 100 mg/l (Araneda-Hernández *et al.,* 2014) did not strongly contribute to the flux of copper ions. Gladysz *et al.* (2007) suggested that this may be due to the manner in which the additives contributes to the deposition process, that is, additives modify the deposition of copper on the cathode surface through adsorption rather than influencing the diffusion of copper ions. Though the additives investigated by Gladysz *et al.* (2007) and Araneda-Hernández *et al.* (2014) are used in electrorefining, they do provide insight on the effect of additive on the diffusivity of copper ions in sulphate electrolytes.

4.3.7 Relationship of physicochemical properties.

The understanding of the relationship between the physicochemical properties of the electrolyte is important for performance improvement of the electrowinning process. Thus, their relationship was investigated to gain valuable insight. This was achieved by analysing two properties trend at varying copper and sulphuric acid concentration, with other conditions held constant.

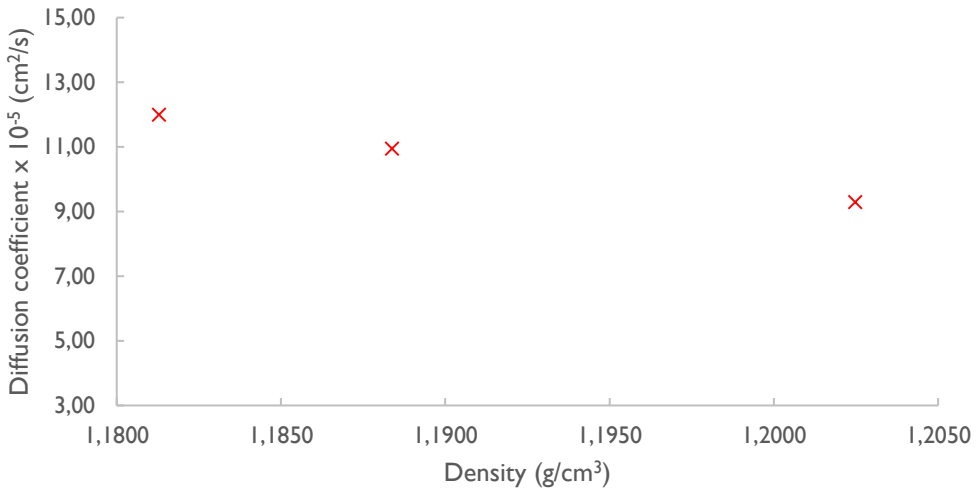

Figure 4.29: Density – Diffusion coefficient relationship at varying copper concentration

Figure 4.29 shows the plot of density against the diffusion coefficient at varying copper concentration. It can be clearly seen that while the density was increasing, the diffusivity of copper ions was decreasing. The probable explanation for the observed trend was suggested in the preceding sections, which is the interaction and agglomeration of metallic ions with the sulphate ions at high concentration. These results imply that the electrodeposition process must be carried out at low density to promote mass transfer of copper ions to the cathode surface.

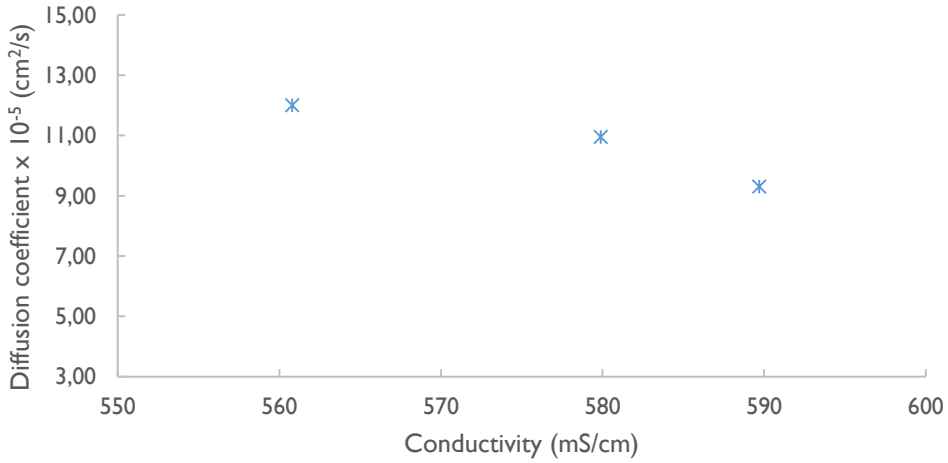

Figure 4.30: Conductivity – diffusion coefficient relationship at varying copper concentration

Figure 4.30 illustrates the relationship between conductivity and diffusivity of copper ions in solution at varying sulphuric acid concentration. As observed in Figure 4.30, an increase in conductivity resulted in a slight decrease of diffusivity of copper ions in the range tested.

These observations are very important since both properties need to be maximized during electrodeposition. Conductivity plays a huge role in energy consumption whereas diffusivity of copper ions play a role in mass transfer of copper ions. Thus, a balance is needed when improving conductivity so as not negatively affect the mass transfer of ions.

Density, conductivity and diffusivity of copper ions have an effect on the performance of electrowinning. This is because conductivity impacts energy consumption whereas density and diffusivity have an influence of mass transfer (Price & Davenport, 1981). To reduce energy consumption, conductivity needs to be maximized and to improve productivity, mass transfer needs to be improved. Therefore, electrowinning must be carried at low densities and high conductivities. As shown in Figure 4.29 and Figure 4.30, these conditions are achieved at low copper concentration. However, low copper concentration has negative effect on other operational parameters such as limiting current density and deposit quality. According to Beukes and Badenhorst (2009), limiting current density can be increased by increasing the concentration of the bulk electrolyte. This is confirmed by considering equation 4.10.

$$I_l = \frac{nFDC_b}{\delta} \qquad 4.10$$

Where n is the number of participating electrons, F is the Faraday's constant, D is the diffusion coefficient, C_b is the bulk concentration and δ is the boundary layer thickness.

The increase in bulk concentration results in the raising of the limiting current density. Low copper concentration can also lead to insufficient supply of copper ions at the cathode and hydrogen evolution (Owais, 2009). Therefore, when choosing conditions for electrowinning, careful consideration of other effects must be carried out.

4.3.8 Summary

The physicochemical properties of copper electrowinning electrolytes were investigated in the presence of polyacrylamide (PAM) additive at varying electrolyte composition. Electrolyte density increased with increase in copper concentration, sulphuric acid concentration, and iron concentration but decreased with an increase in temperature. The PAM additive had no substantial influence on electrolyte density. This was attributed to the additive low concentration in the electrolyte as well as the way the additive interacts in the electrodeposition process. Primarily, the additive affects the electrodeposition through adsorption and inhibition.

For electrolyte conductivity, sulphuric acid concentration was found to have a greater influence. Increase in sulphuric acid concentration and temperature increased conductivity whereas the presence of copper and

iron (metallic) ions decreased the conductivity of the electrolyte. PAM additive did not affect the conductivity.

The diffusion coefficient increased with an increase in temperature but decreased with increase in copper, iron and sulphuric acid concentration. This has been ascribed to the interaction and agglomeration of the ions in the electrolyte. The presence of PAM additive had negligible influence on the diffusivity of copper ions..

Furthermore, mathematical correlations (regression models) for each physicochemical property as a function of electrolyte temperature were constructed. The results from the present study are in agreement with previous studies. These mathematical correlations were utilized in COMSOL Multiphysics 5.3a to describe the electrolyte when investigating the influence of electrolyte composition on the electrodeposition of copper.

It was also shown that the relationship between the physicochemical properties is important. It was observed that the diffusivity of copper ions decreased with increase in conductivity. This implies that conditions must be selected carefully in order to optimize both conductivity and diffusion of copper ions in the system so as to promote mass transfer to the cathode surface and reduce ohmic drop in the electrolyte which may reduce energy consumption.

Chapter 5 : Modelling of copper electrowinning

Modelling and simulations provide an economical approach to examining and understanding the behaviour of the electrochemical process as well as optimizing and controlling the electrodeposition process. Several parameters such as cell geometry, electrolyte composition, electrode kinetics, and operating conditions can be studied through modelling and simulation. Most electrochemical software packages simulate current and potential distribution, solution concentrations and deposit thickness and composition. The ability to simulate current distribution is of greater importance in this work since it is impracticable to determine current or voltage operating on different points on the electrode or within the electrolyte experimentally. The measurable experimental values are the lumped current and voltage acting between the electrodes.

In this study, a finite element analysis software, COMSOL Multiphysics 5.3a was used to simulate the electrodeposition process of copper. The objective was to model the electrodeposition of copper under electrowinning conditions. COMSOL Multiphysics 5.3a was chosen because of its ability to simulate thickness changes of the electrode surface, current distribution and user-friendly interface. The Tertiary Nernst-Plank Interface with electrodeposition module was used. The Electrodeposition, Tertiary Nernst–Planck interface accounts for the transport of species through diffusion, migration, and convection (Comsol, 2017). In accounting for these three modes of transport the modelling adequately covered the effects of variations in composition on the electrodeposition process. Furthermore, the kinetics expressions for the electrochemical reactions accounted for both activation and concentration overpotential.

In this chapter, the approach taken in the development of the copper electrowinning model to study the effect of electrolyte composition on current distribution is presented. In addition, the findings of this work are presented under results and discussion.

5.1 Development of electrowinning model

The Tertiary Nernst-Planck current distribution (TCD) model was utilized to solve for the electrolyte potential, the current density distribution, and the concentrations of various species (Comsol, 2017). Before commencing model development, various works on electrodeposition were reviewed to gain an understanding of the process and establish a modelling procedure. Section 2.6 reviewed the work primarily concerned with copper electrowinning modelling with few reference to other electrodeposition processes. Different works on modelling electrodeposition processes such as electrorefining and electroplating were also reviewed but were not presented in this thesis. The processes might be different, but the underlying fundamental principles are similar. Thus, the review provided a basis for problem formulation and the relevant techniques for model development.

The model development can be categorized into three major steps: Pre-processing, processing and post-processing. The first part (pre-processing) involved problem formulation. During this process, mathematical equations from electrodeposition fundamentals describing the electrowinning process were identified. This included conservation of charge, conservation of current and conservation of mass in the system. Governing equations describing mass transfer within the system were also identified. Factors to be used in the model such as geometric parameters, computational domain, boundary conditions, electrolyte physicochemical properties and process parameters that define the electrowinning process were also identified. In short, the problem formulation involved selection of the geometry, governing equations, electrolyte properties and boundary conditions that defined the electrowinning process. In the processing stage, the formulated problem was simulated in COMSOL Multiphysics to produce the solution to the problem. The post-processing stage, as the name suggests, involved analysing the solution using various tools and visualization as well as model validation. Figure 5.1 summarizes the stages involved in model development.

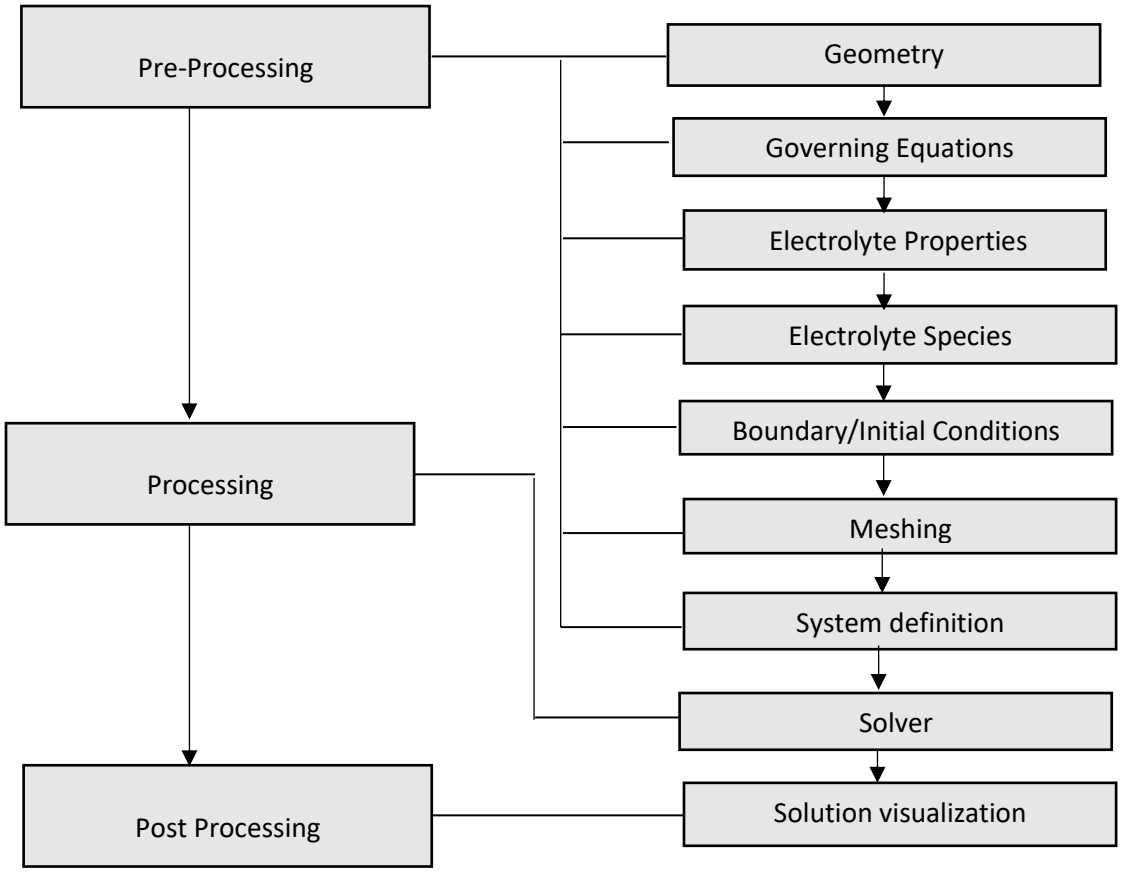

Figure 5.1: Steps involved in model development; the left side of the diagram represents a summary of the steps in model development, which are expanded on the right side of the diagram(Adapted from Datta & Vineet, 2010*).*

5.1.1 Model Assumptions

Before delving into the model development, it is cardinal to highlight key assumptions that were made during model generation. These are:

- There are a number of species present in the copper-sulphuric-sulphate electrolyte solution (Casas, Alvarez and Cifuentes, 2000). In this study, complete dissociation was assumed; therefore, the electrolyte was assumed to be composed of Cu^{2+}, H^{+}, and SO_4^{2}. This was done to simplify the model as the fundamental reactions were captured by the species present. The incorporation of more species may improve the performance of the model as it will be more reflective of industrial electrolytes which contain various species (or impurities) from leaching or solvent extraction stages. For the purposes of this work, it was decided to keep the chemistry relatively simple.
- The additive effects were not modelled as the model did not account for adsorption or inhibition effects at the electrode surface. Additives affect electrodeposition through adsorption and inhibition at the electrode surface. This phenomenon; however, was not captured in the present model.
- A closed electrowinning cell (stagnant electrolyte) was used, that is, in which natural convection occurs. Natural convection is caused by density gradients due to the depletion of copper ions at the cathode as the reduction reaction proceeds as well as oxygen bubbles at the anode. However, it was assumed that natural convection had a negligible effect on the system and a perfectly mixed cell was simulated.
- The decomposition of water at the anode results in bubble generation in the vicinity of the electrode. The bubbles cause changes in the conductivity and diffusivity of ions in the region close to the anode, requiring a two-phase description of the electrolyte domain(Ziegler & Evans, 1986; Leahy & Schwarz, 2014). However, the effect of oxygen bubbles was not considered as separate sets of conditions were required to describe the two-phase system.
- The electrodes were assumed to have high conductivity compared to the electrolyte, that is, with negligible resistance. As a result, it was assumed that the electrodes had constant potential. This implied that cathode and anode were treated as boundaries (electrode surface) in the model.
- The deformation of the cathode was assumed to be time-dependent, that is, the boundary moved as copper was being electrodeposited at the cathode. Therefore, time-dependent study step (system definition) was used.

5.1.2 Geometry Description

A 2D geometry was used to model copper electrowinning and is shown in Figure 5.2. Note that 3D configuration is shown to show the area which was simulated. The choice to use 2D was done to simplify the model complexity. At the same time, the 2D geometry was sufficient to represent the electrowinning process as demonstrated by Werner (2017) and Shukla (2013). The computational domain consisted of an anode and cathode pair (35 mm long) with an electrode spacing of 20 mm as well as an electrolyte domain. The same dimensions were also used in the experimental for copper electrowinning experiments.

The industrial electrowinning cell may consist of up to 40 anode-cathode couples (Aminian *et al.*, 2000). The geometrical symmetry of the electrode configuration in a cell make it possible to model the process with a single anode and cathode pair. For the electrowinning experiments, only one side of the electrode had reactions taking place, the other sides were insulated.

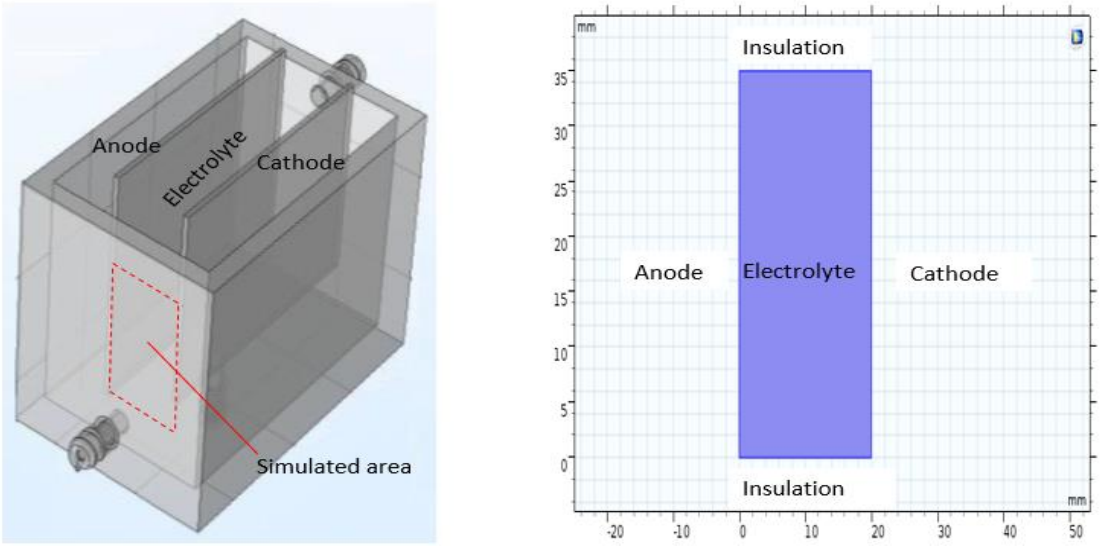

Figure 5.2: 3D and 2D geometry showing boundaries corresponding to cathode and anode (with the other boundaries treated as insulated) for modelling electrowinning in COMSOL Multiphysics 5.3a. The geometry is the side view of the electrowinning cell.

5.1.3 Governing equations

The theory of electrodeposition was discussed in section 2.3 in which various equations pertaining to electrodeposition process were presented. Several governing equations were required to describe the electrodeposition of copper. These sets of equations were used to solve for the major model outputs;

- the electrolyte potential,
- current density distribution
- and concentration of species (Comsol, 2017).

The governing equation will be outlined in the following subsections.

5.1.3.1 Mass transport

The mass transfer of species in the electrolyte was described by the Nernst Plank equation (equation 5.1). This equation ignores ionic interaction and is more suited for dilute solutions. Nevertheless, it has been used to model the electrowinning process effectively.

$$N_i = -D_i \nabla c_i - z_i u_i F c_i \nabla \varphi_l + c_i \boldsymbol{v} \qquad 5.1$$

Where c_i denotes the concentration of species i (mol/m^3), D_i is the diffusion coefficient of species i (m^2/s), z_i is the charge number of the ionic species (unitless), u_i the ionic mobility of species i (s.mol/kg), F denotes Faraday constant (C/mol), φ_l denotes the electric potential (V), and $\boldsymbol{v}$ the velocity vector (m/s)

The ionic mobility, u_i was estimated by relating it to the diffusion coefficient D_i through the Nernst-Einstein equation:

$$u_i = \frac{D_i}{RT} \tag{5.2}$$

5.1.3.2 Conservation of mass

The conservation of mass was maintained for each species in the system and it was assumed that no homogeneous reactions took place in the solution. This is because electrochemical reactions occurs at the electrolyte – electrode interface and involves chemical reactions as well as exchange of electrons between the two phases, inherently making them heterogeneous reaction. Thus, conservation of mass required that:

$$\frac{\partial C_i}{\partial t} + \nabla . \boldsymbol{N}_i = 0 \tag{5.3}$$

5.1.3.3 Electrolyte current density

The electrolyte current density was defined by the sum of all species fluxes as given by equation 5.4

$$\boldsymbol{i}_l = F \sum z_i \boldsymbol{N_i} \tag{5.4}$$

By substituting $\boldsymbol{N_i}$ in equation 5.4, the laws of conservation of mass and charge satisfied the condition of conservation of current:

$$\boldsymbol{i}_l = -F^2 \nabla \varphi_l \sum_i z_i^2 u_i C_i - F \sum_i z_i D_i \nabla C_i + F\nu \sum_i z_i C_i \tag{5.5}$$

Considering electrolyte neutrality condition (equation 5.7) in the electrolyte, the last term in equation 5.5 becomes zero. Consequently, equation 5.5 became:

$$\boldsymbol{i}_l = -F^2 \nabla \varphi_l \sum_i z_i^2 u_i C_i - F \sum_i z_i D_i \nabla C_i \tag{5.6}$$

$$\sum_i z_i C_i = 0 \qquad 5.7$$

Equation 5.2 indicates that the mobility in the model was dependent on the diffusivity of species. This shows that accurate correlations of physicochemical properties are required to describe the system well.

5.1.3.4 Current at electrodes

At the electrodes, the current density, i_s was described by Ohm's law as given by equation 5.8

$$i_s = -\sigma_s \nabla \varphi_s \qquad 5.8$$

Where σ_s is the conductivity of the electrode and $\nabla\varphi_s$ is the potential gradient.

Since the electrode had negligible resistance in comparison to the electrolyte, the potential at the electrode surface was assumed to be constant. The cathode was chosen as the reference electrode (with a potential of 0V) from which all other potentials were measured.

5.1.3.5 Conservation of current

Conservation of current exists between the electrolyte and electrode, and yields the following equation:

$$\nabla . \boldsymbol{i}_k = Q_k \qquad 5.9$$

Where *k* represents an index: *l* for liquid and *s* for the electrode and Q_k is the general current source or sink term. In this model, Q_k = 0, thus equation 5.9 becomes:

$$\nabla . \boldsymbol{i}_k = 0 \qquad 5.10$$

5.1.3.6 Electrode – electrolyte Interface current density

The current density at the electrode – electrolyte interface (local current density), determines the rate of reaction. It was defined by the concentration-dependent Butler-Volmer equation as given by equation 5.11. This enabled charge transfer and concentration effects to be considered.

$$i_{loc} = i_0 \left(\frac{C_{r,s}}{C_{r,b}} exp\left(\frac{\alpha_a z F \eta}{RT}\right) - \frac{C_{o,s}}{C_{o,b}} exp\left(-\frac{\alpha_c z F \eta}{RT}\right) \right) \qquad 5.11$$

Where i_{loc} is the local (charge transfer) current density at the interface, i_0 is the exchange current density, $C_{r,s}$ and $C_{r,b}$ are concentration of the reduced species at electrode surface and in the bulk electrolyte respectively, $C_{o,s}$ and $C_{0,b}$ are concentration of the oxidized species at the surface of the electrode and in the electrolyte solution respectively, α_c and α_a are the cathodic and anodic charge transfer coefficients respectively, z is the number of electrons transferred, F is the Faraday constant, R is the gas constant, T is the absolute temperature, and η is the overpotential as defined in equation 5.12 (Comsol, 2017).

In this model, the works of Mattson and Bockris (1958) as well as Laitinen and Pohl (1988) were consulted for the determination of exchange current density values for the copper reduction and oxygen evolution reactions respectively. The value of $\frac{C_{o,s}}{C_{0,b}}$ was determined from the initial bulk concentration and localized time-dependent concentration at the electrode surface, that is, $C_{o,s}$ was defined by the localized concentration at the electrode-electrolyte interface and $C_{0,b}$ was the initial bulk concentration. For the $\frac{C_{r,s}}{C_{r,b}}$ expression, its value was 1 since the reduced species was copper metal. The cathodic and anodic charge transfer was assumed to be 1.5 and 0.5 respectively. The other parameters are given in Table 5.1

5.1.3.7 Overpotential determination

The local overpotential determined the local current density at the electrode-electrolyte interface and was defined as:

$$\eta = \varphi_s - \varphi_l - E_{eq} \tag{5.12}$$

Where φ_s denotes the electrical potential externally applied to the electrode, φ_l is the potential of the electrolyte adjacent to the electrode, and E_{eq} is the equilibrium potential due to the electrochemical reaction. Since the electrical potential of the electrode was assumed to be constant, variation in overpotential was primarily due to the electrolyte potential. The equilibrium potential was calculated from the Nernst equation:

$$E_{eq} = E^0 - \frac{RT}{nF} ln \frac{a_o}{a_r} \tag{5.13}$$

Where a_o and a_r are the activity for the oxidized and reduced species respectively and the other terms as defined above.

From equation 5.13, it can be seen that accurate values of equilibrium potentials lie in the precise determination of activities of oxidized and reduced species. Thus, the activity of species, a_i were determined using equation 5.14

$$a_i = \gamma_i \frac{c_i}{c_{i,o}} \quad 5.14$$

Where γ_i is the activity coefficient of species i, c_i is the concentration of species i and $c_{i,o}$ is the reference concentration of species i. The values of the activity coefficient were extracted from the literature (Samson *et al.*, 1999).

5.1.3.8 Current density determination

Equation 5.6 and 5.11 describe the current density in the electrolyte and at the electrode-electrolyte interface. Applying conservation of current condition at the electrode-electrolyte interface, it can be deduced that the normal electrolyte current density to the electrode surface equals the local current density as shown in equation 5.15. This relationship was important as it provided the basis for the determination of current density at the electrode surface.

$$\boldsymbol{i}_l . \boldsymbol{n} = i_{loc} \quad 5.15$$

A representation of the solution domain summarizing the equations used to solve for current density, potential and concentration is shown in Figure 5.3.

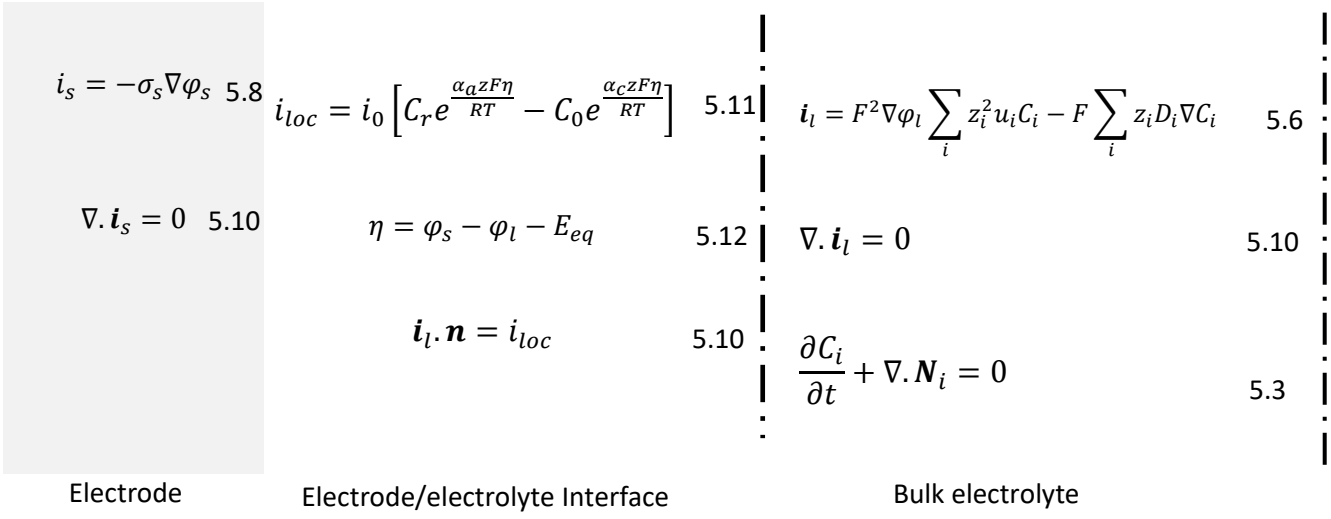

Figure 5.3: Schematic representation of equations describing the system at the electrode, electrolyte – electrode interface, and in the bulk electrolyte used to solve for electrolyte potential, current density and concentration of species.

The figure is an enlarged section of the cell depicting the cathode electrode surface. Note that an electrode has been included for illustrative purposes as electrodes were treated as boundaries in the model. (See section 5.1.1).

Equations 5.6, 5.8, 5.10 and 5.11 were used to provide a link between the electrolyte, electrode-electrolyte interface and electrode surface such that the potential and current distribution were solved. Furthermore, by making use of equation 5.3, species concentration was solved. The equations for the deformation of the electrode will be discussed in section 5.1.8.

To calculate the overpotential (equation 5.12), the electrolyte potential needs to be known. This presents a challenge as the electrolyte potential of the system is unknown. To counter this problem, the conservation of current was employed. The potential at the cathode was fixed to 0 V (as a reference potential) such that the electrolyte potential floated and adapted to fulfill the current balance between the cathode and anode. The evaluated electrolyte potential was utilized to calculate the overpotential, which was then applied in the Butler - Volmer equation to determine the local current density.

5.1.4 Electrode Reactions

At the cathode, copper deposition occurred. It is well known that copper reduction takes place in two steps: the reduction of Cu^{2+} to Cu^{+}, followed by reduction Cu^{+} to Cu metal (Mattson and Bockris, 1958). However, in this model, the cathodic reaction was assumed to be a single step as per equation 5.16:

$$Cu^{2+} + 2e^{-} \longrightarrow Cu \qquad 5.16$$

For the anodic reaction, oxygen was evolved:

$$H_2O \longrightarrow 2H^{+} + \frac{1}{2}O_2 + 2e^{-} \qquad 5.17$$

The equilibrium potentials were calculated from the Nernst equation and Butler- Volmer equation was used to describe rate of reaction as discussed in in section 5.1.3.6 and 5.1.3.7.

5.1.5 Electrolyte Properties

Electrolytes properties were needed to define the electrolyte system for a reliable model. This was important as accurate correlations of properties ensured a true representation of the electrolyte system. Thus, the mathematical correlations constructed in the first part of this work (see Chapter 4) were used to define the electrolyte properties in the model. Since viscosity was not investigated in this work, the correlation of Price and Davenport (1981) was used instead. The models for properties were given in chapter 4 as:

$$\text{Density (g/cm}^3\text{)} = 1.021241 + 0.002150\,[Cu] + 0.000555\,[H_2SO_4] + 0.002279\,[Fe] - 0.000474T \qquad 4.2$$

Conductivity (mS/cm) = 128.4375 - 3.3649 [Cu] + 2.2927 [H_2SO_4] - 4.0324 [Fe] + 3.8916T 4.4

Diffusion Coefficient (cm^2/s) x 10^{-5} = 5.431829 - 0.015928 [Cu] - 0.017949 [H_2SO_4] - 0.076145 [Fe] + 0.172915T 4.8

Where [Cu], [H_2SO_4], [Fe], [PAM], and T represent the concentration of copper (g/l), sulphuric acid (g/l), iron (g/l) and temperature (°C) respectively

These equations were applied across the electrolyte domain and were dependent on the electrolyte composition. However, the conductivity correlation was not utilized in the model as the tertiary current distribution interface did not have provision to define electrolyte conductivity.

5.1.6 Boundary Conditions

Since the reactions only took place at the electrode-electrolyte interface, a no-flux condition for molar flux was imposed on all other boundaries except the electrode surface. The condition was expressed as follows:

$$\boldsymbol{n}.\boldsymbol{N_i} = 0 \quad 5.18$$

It was assumed that current only flowed through the electrodes, with the other boundaries insulated

$$-\boldsymbol{n}.\boldsymbol{i} = 0 \quad 5.19$$

Where $\boldsymbol{n}$ is the unit normal vector to the face of the electrode.

5.1.7 Meshing

Meshing divides (discretize) the model into small elements of geometrically simple shapes were sets of equations are solved. The mesh defined affects the resolution; thereby, affecting the quality and accuracy of the results. Computational accuracy is improved by using finer mesh size. In this model, a physics-controlled mesh with fine element size was employed. COMSOL Multiphysics ranges the element mesh size from extremely coarse to extremely fine. Fine mesh size was chosen as it was able to produce well defined profiles with reasonable computational time.

5.1.8 Electrode surface deformation

The surface concentration variables of the deposited species were used to calculate the thickness of the deposited layer. The depositing rate was used to set the boundary velocity for the deforming geometry. The

deposition was assumed to occur in the normal direction to an electrode boundary, with the velocity being directed into the electrolyte domain (Comsol, 2017).

In this model, copper was deposited at the cathode. Consequently, other boundaries did not undergo geometrical deformation, that is, the anode was inert and other boundaries were considered to be insulating. Thus, the growth velocity, v_{dep} of the cathode was:

$$v_{dep} = \frac{M_{Cu} i_{loc}}{\rho_{Cu} nF} \tag{5.20}$$

where M_{Cu} is the molar mass of copper, ρ_{Cu} is the density of copper and n is the number of electrons involved in the deposition of copper and i_{loc} as defined by equation 5.11

5.1.9 Parameters and conditions

The simulation was performed with parameters and conditions as shown in Table 5.1. The equilibrium potentials for the reduction and oxidation reaction and electrolyte properties are not included in the table as they were covered in section 5.1.3.7 and 5.1.5. The range for copper and acid concentration as well as temperature were based on the experimental conditions for model validation experiments. For the exchange current density values for the copper reduction and oxygen evolution, the works of Mattson and Bockris (1958) and Laitinen and Pohl (1988) were reviewed. The exchange current density for the oxidation reaction was adjusted which resulted in improved performance of the model. As discussed in section 5.1.3.8, the potential at the cathode was fixed to 0 V and the anode potential was equivalent to the cell potential.

Table 5.1: Parameters and conditions of variables of the simulation of copper electrowinning model

Description	Values
Copper concentration (g/l)	35/45
Sulphuric acid concentration (g/l)	160/180
Temperature (°C)	45/55
Exchange current density, Cu reduction (A/m^2)	70
Exchange current density, O_2 evolution (A/m^2)	0.89
Cathodic transfer coefficient, Cu reduction (α_{c_Cu}) (unitless)	1.5
Anodic transfer coefficient, Cu reduction (α_{c_Cu}) (unitless)	0.5
Cathodic transfer coefficient, O_2 evolution ($\alpha_{c\_O_2}$) (unitless)	0.8

Description	Values
Anodic transfer coefficient, O_2 evolution ($\alpha_{a\_O_2}$) (unitless)	1.2
Diffusion coefficient, sulphate ions (m^2/s)	1.13×10^{-9}
Electric potential, anode (V)	2.3
Electric potential, cathode (V)	0

5.1.10 Simulation of the model

COMSOL Multiphysics software uses the conservation principles (governing equations) to solve for electrolyte potential, current density distribution and concentration of species. These equations are defined in the physics interface, coupling them with electrode thermodynamics and reaction kinetics. Then, the parameters and variable conditions, as well as initial and boundary conditions, are set in the physics interface. The appropriate meshing and system definition were done, and the problem was computed with electrolyte potential, current density distribution, electrode thickness and concentration as the output. A schematic representation of problem simulation is shown in Figure 5.4.

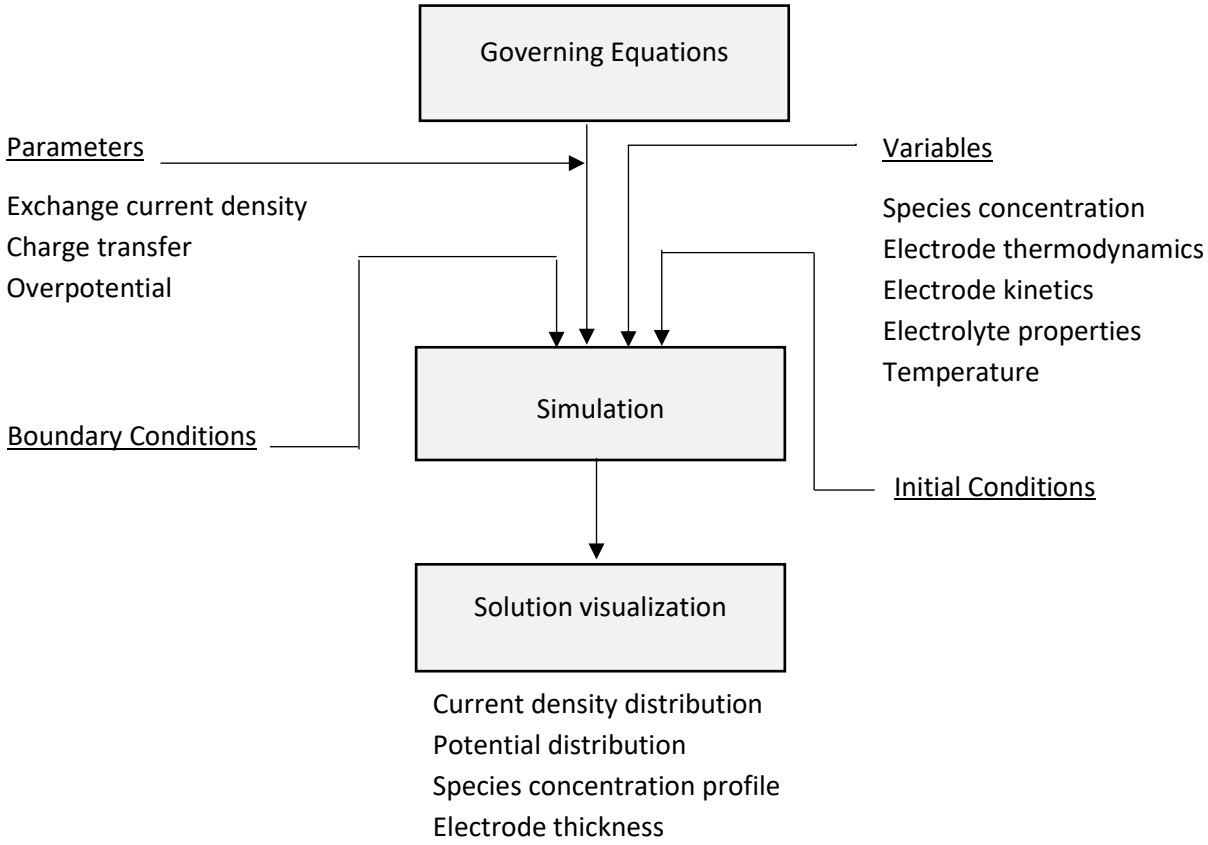

Figure 5.4: Schematic representation of the problem simulation showing parameters and system outputs.

5.2 Results and discussion of copper electrowinning model

Section 5.1 presented the procedure for mathematical model development using COMSOL Multiphysics to predict electrolyte potential, current density distribution and concentration of species whereas the preceding section outlined the experimental for the model validation. This section discusses the results of the electrowinning model as well as the results of the experiments which were conducted to validate the model. The general model outputs are discussed to show the predicting capabilities of the model. This is followed by the effects of various parameters on model output; that is, cell voltage, copper concentration and sulphuric acid concentration on current distribution. Thereafter, experimental model validation is presented.

5.2.1 Electrolyte potential

Figure 5.5 shows the electrolyte potential distribution between the two electrodes after 3 minutes. It can be seen that the electrolyte potential exhibited a normal trend, that is, the electrolyte potential spread out from the anode to the cathode across the electrolyte. As pointed out in section 5.1.3.8, the potential was applied at the anode and that the cathode was considered as the reference electrode. The electrolyte potential had to float and adjust so that the conservation of the current condition is fulfilled.

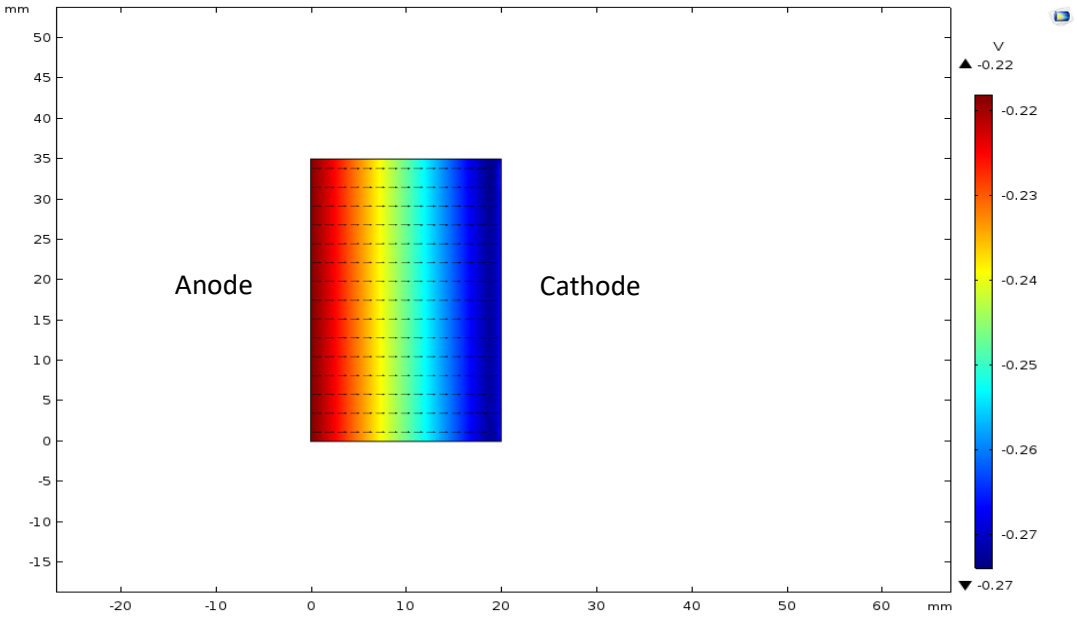

Figure 5.5: Example of electrolyte potential distribution between the anode and cathode at 35 Cu g/l and 160 g/l H_2SO_4 at 45°C temperature

Figure 5.6 shows the plot of electrolyte potential between inter-electrode spacing at different time steps in the simulation. It can be noted that as time progressed, the electrolyte potential became more negative. The increase in overpotential with time may be ascribed to the concentration polarization phenomena in the cell. The results of the physical electrowinning experiments also indicated an increase in cell potential with time before reaching a steady-state condition. Figure 5.6 also shows the same potential at the cathode –

electrolyte interface at different time step. The tentative explanation for the observed trend may be the effect of fixing the potential at the cathode.

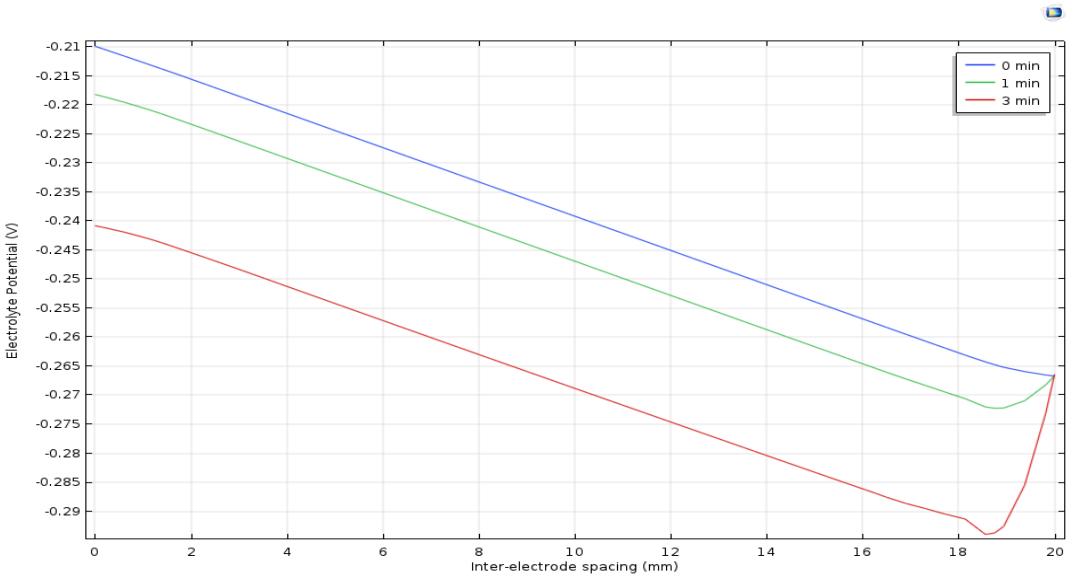

Figure 5.6: Electrolyte potential distribution between the anode and cathode at 35 Cu g/l, 160 g/l H_2SO_4 at 45°C temperature at different times.

5.2.2 Concentration profiles

The concentration profile of the copper ions as predicted by the model is shown in Figure 5.7. In the bulk electrolyte, a uniform concentration was maintained. Towards the cathode, it can be observed that there is a depletion of copper ions. This is due to the electrochemical reduction of copper ions.

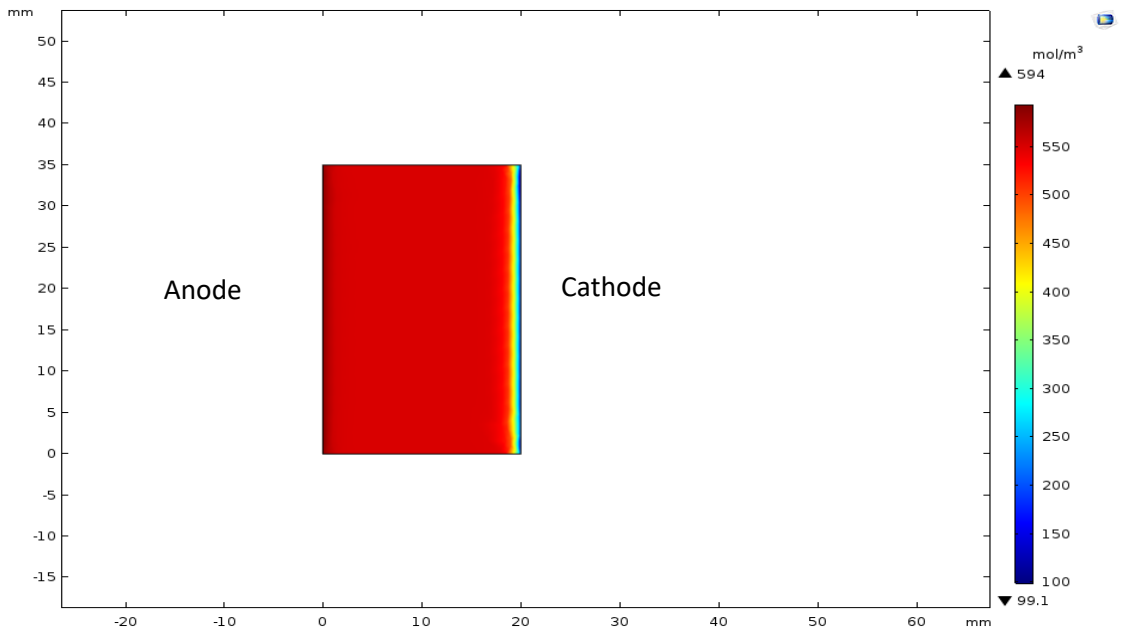

Figure 5.7: Cu concentration profile between the anode and cathode at 35 g/l Cu and 160 g/l H_2SO_4 at 45°C temperature

Figure 5.8 is an extract from the concentration profile of Figure 5.7 which shows concentration profile of copper ions between the inter-electrode spacing at different times.

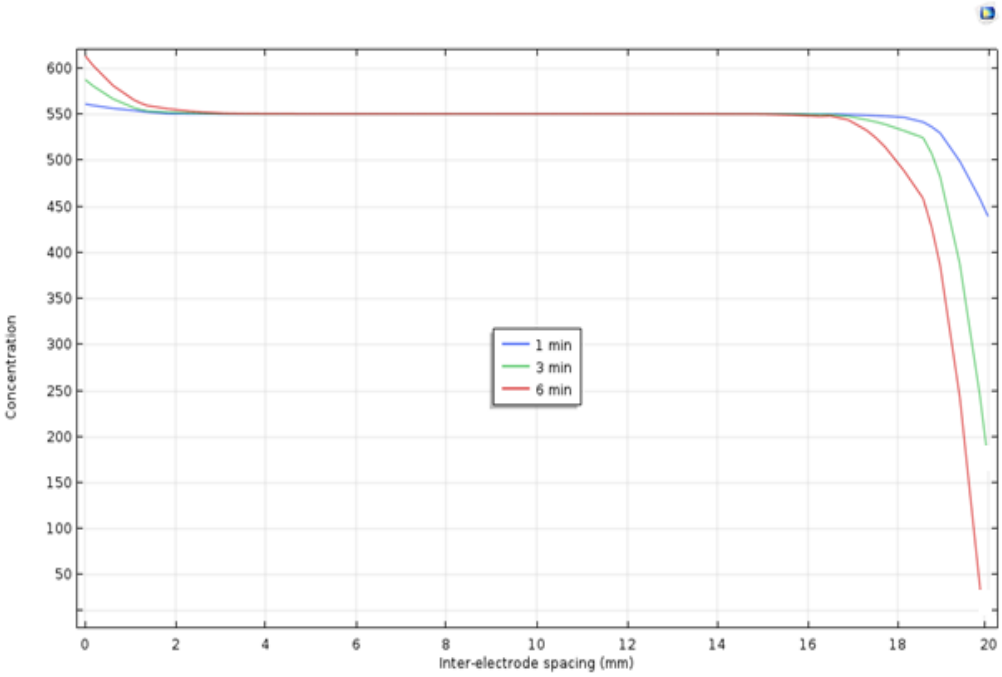

Figure 5.8: Cu concentration profile between the anode and cathode at 35 g/l Cu and 160 g/l H_2SO_4 at 45°C temperature showing the depletion of Cu at the cathode with time

It can be seen from Figure 5.8 that the concentration of copper ions follows the expected profile in the cell, that is, lower concentration towards the cathode with a constant concentration in the bulk electrolyte. Furthermore, there was a reduction in concentration at the cathode as time progressed. This is expected as the copper ions were being reduced in the cell as per equation 5.16.

Figure 5.8 also shows that the electrodeposition process may be diffusion limited. At 6 minutes, the concentration of copper ions was almost depleted at the cathode surface. According to Beukes and Badenhorst, (2009), the diffusion limiting current is reached when the surface concentration of species is zero. This implies that the surface species are consumed immediately they are supplied at the cathode. It seems possible that the observed trend was due to the nature of the hydrodynamics in the cell as well as the kinetics. The model was based on a stagnant electrolyte (no fresh electrolyte was added to the system). The reduction of copper ions at the cathode may have led to the completely consumption of species. Furthermore, since there was no convection in the system, the only possible transfer mechanisms were migration and diffusion. Note that electrowinning of copper is carried out below the limiting current.

5.2.3 Current Distribution

The flux of the copper ions were used to calculate the electrolyte current density. Figure 5.9 shows the electrolyte current density distribution between the anode and the cathode predicted by the model.

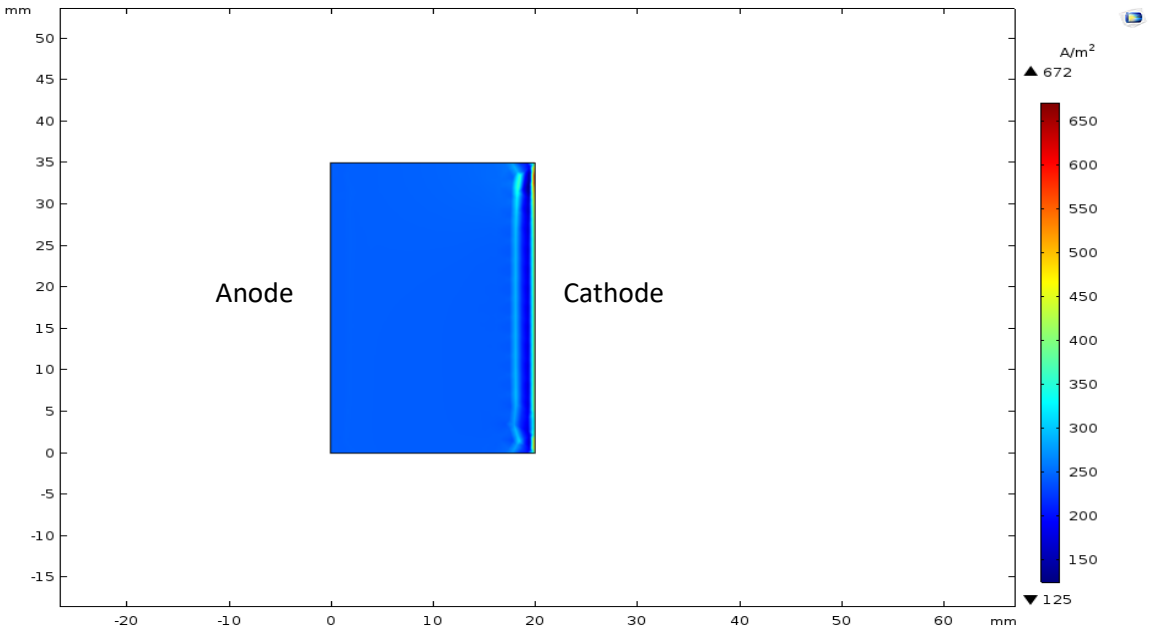

Figure 5.9: Electrolyte current density distribution between the inter-electrode gap at 35 g/l Cu and 160 g/l H_2SO_4 at 45°C temperature

It can be observed that the current distribution in the electrolyte was almost uniform with high current density occurring towards the top of the cathode. The variation of current density at the cathode surface (top) can be attributed to the reaction kinetics as well as the mass transfer phenomena taking place in the cell. The reacting species and electrons follow a path of least resistance (at the top); thus, leading to higher current density (Obaid et al., 2013)

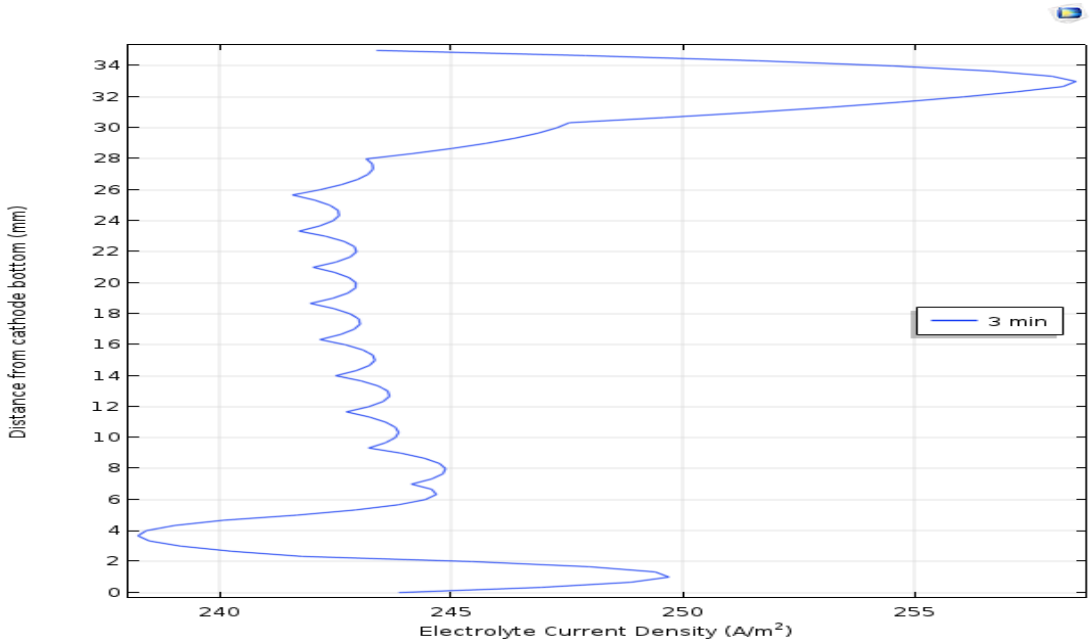

Figure 5.10: Current density distribution at the cathode surface at 35 Cu g/l and 160 g/l H_2SO_4 at 45°C temperature

Figure 5.10 is an example of a current distribution profile at the cathode surface, that is, the current density variation along the cathode surface. The magnitude of current density is higher at the top and bottom of the

cathode with relative consistency in the middle part of the cathode. Although the study of Werner *et al.* (2018) investigated the effect of electrode configuration on current density distribution in copper electrowinning, their results show higher current densities at the top and bottom of the electrode. The reason for this observable trend was brought out earlier: phenomena of mass transfer and electrochemical reaction at the cathode. Another observable trend is the roughness exhibited by current density in the middle of the cathode which was independent of the mesh size. The only difference was that at coarse mesh, the graph did smooth out compared to the fine mesh which became rougher (See Appendix B.6). Similar roughness was also observed by Werner *et al.* (2018) who ascribed this to numerical aberrations of the mesh size being utilized in the simulation whereas Robison (2014) pointed out that the roughness may be due to crosscurrents, i.e. current running in counter direction due to the movement of solution occurring in the system. According to Robison (2014), crosscurrents can cause asymmetry and irregular profiles (Robison,2014).

As discussed in section 2.7, current distribution over the cathode surface plays a critical role in controlling the growth and structure of the deposit. Poor current distribution leads to poor morphology of the deposit and loss of current efficiency. As such, the following subsections will focus on current distribution at the cathode surface. Modelled results on how different factors affect the current distribution will be discussed.

5.3.3.1 Effect of cell potential

The cell potential is an important aspect of electrowinning as it is the driving force. Typical cell potential requirement for electrowinning process is approximately 2.0 V (Schlesinger *et al.*, 2011). Thus, the effect of cell potential at 1.8 V, 2.0 V and 2.3 V on current density was simulated and is shown in Figure 5.11.

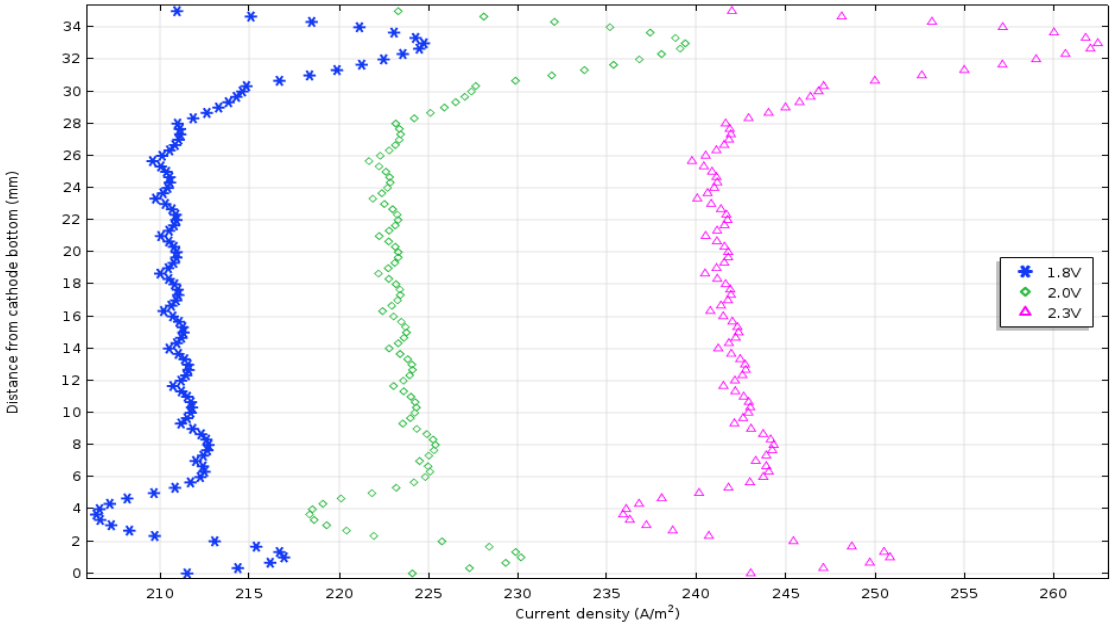

Figure 5.11: Current density distribution at the cathode surface with varying cell potential at 35 g/l Cu and 160 g/l H_2SO_4 at 45°C temperature

The current density profile was not influenced by the changes in cell potential. The observed variation was in the magnitude of the current density values which is expected as per Ohm's law. The model showed that the current density increased with increase in cell voltage, likely due to the fact that the cell resistance remained constant in the electrolyte. Even in cases where the Ohms law condition is not strictly obeyed, current density usually increase with increase in potential.

5.3.3.2 Effect of copper concentration

Figure 5.12 shows the current distribution at a different copper concentration of 35 g/l, 40 g/l, and 45 g/l.

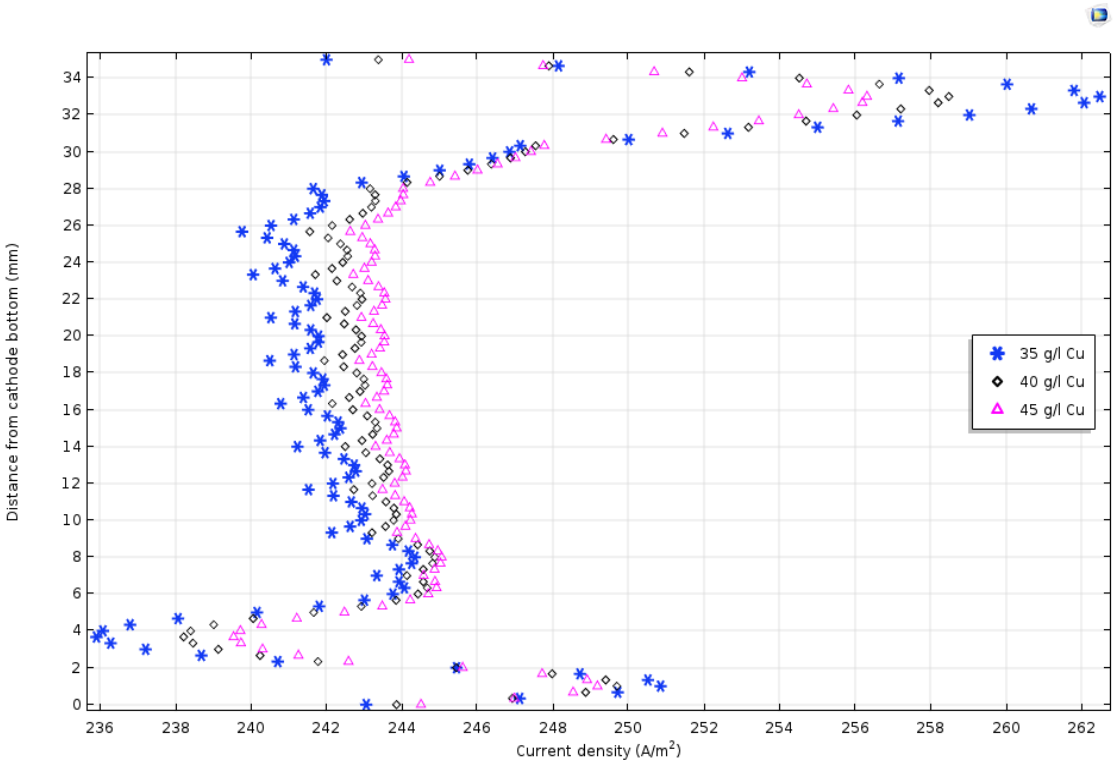

Figure 5.12: Current density distribution at the cathode surface with varying copper concentration at 160 g/l H_2SO_4 at 45°C temperature

As seen in Figure 5.12, the increase in copper concentration resulted in an increase in current density. Literature indicates that increasing the concentration of the bulk reactant increases the diffusion-limited current (Beukes & Badenhorst, 2009). This is despite the negative effect of copper concentration on the diffusivity of ions in the system. As brought out in section 4.3, the copper concentration contribution to the diffusion coefficient was minimal compared to the other factors such as temperature. As such, the impact of copper concentration due to changes in diffusion coefficient was not pronounced.

5.3.3.3 Effect of sulphuric acid concentration

The effect of acid concentration on current distribution was investigated from 120 g/l to 180 g/l. Figure 5.13 shows the model current density distribution at varying sulphuric acid concentration.

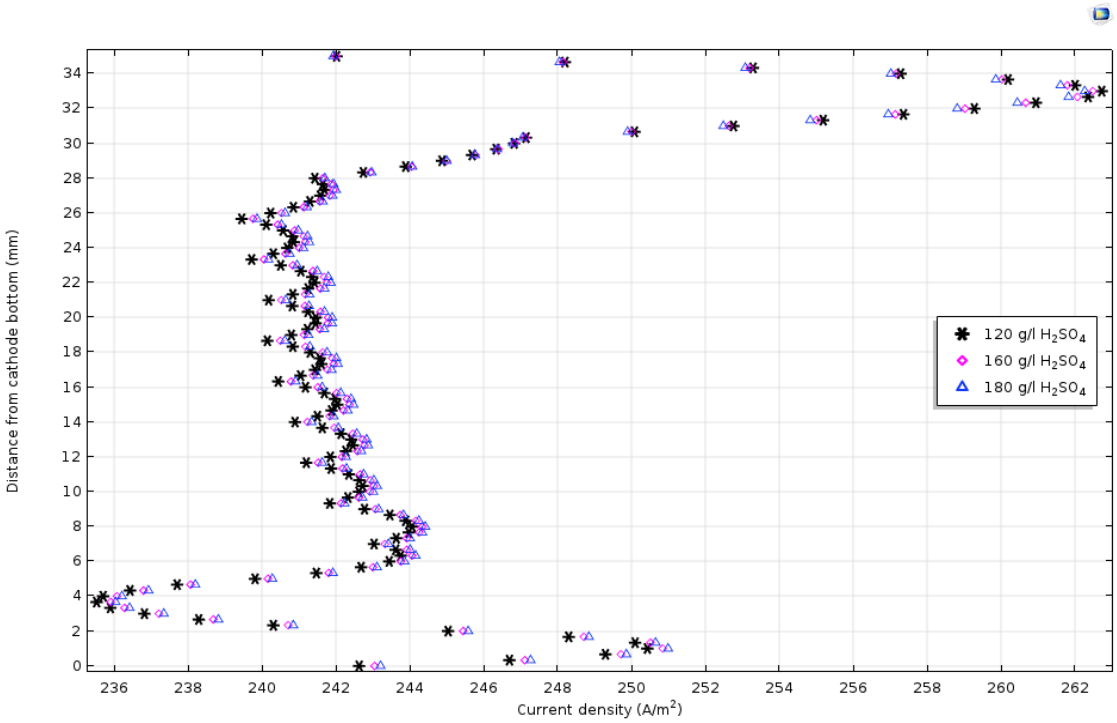

Figure 5.13: Current density distribution at the cathode surface at 35 Cu g/l at 45°C temperature at varying H_2SO_4 concentration

The modelled current distribution showed minimal change with increase in acid concentration. A possible explanation for the observed trend maybe the way COMSOL Multiphysics evaluate electrolyte density. Section 5.1.3.3 showed that that electrolyte current density is described by the sum of flux of species present in the electrolyte. In other words, the electrolyte current density is dependent on the diffusion coefficient as well as the concentration of species in the electrolyte. The results from section 4.2 and 4.3 indicates that the increase in sulphuric acid concentration leads to reduction in the diffusivity of ions in the electrolyte but an increase in electrolyte conductivity. At the same time, the mobility of ions in COMSOL Multiphysics is calculated from the diffusion coefficient values (equation 5.2). This implies that COMSOL Multiphysics will compute the electrolyte current density based on the negative effect (decrease) of diffusivity, whereas in practical situations there is improved conductivity due to the addition of highly mobile hydrogen ions. This was also pointed out by Robinson (2014) who used the same finite element analysis software to model electrorefining process for thickness distribution prediction.

5.2.4 Model Validation

The key to the validation of this model was to compare the experimental current density distribution to the modelled current density distribution. The local depositing current density was determined from the deposit thickness utilizing Faraday's law as outlined in section 3.2.5. The measured thickness values are given in Appendix B. The reported experimental current density value at each specific height of the cathode is the average of the current density values measured from the intersection points of three values lying on the

same horizontal line (See Figure 3.6 for a schematic representation). The model and experimental current densities were plotted against the distance from the cathode bottom so as to validate the model. During the preliminary analysis, it was noted that the model under-predicted the current density. This was attributed to the way the model was developed compared to the electrowinning experiments. The model was simulated under conditions of constant applied potential whereas electrowinning experiments were carried out at constant current.

Figure 5.14 shows the current distribution from the electrowinning experiments and their corresponding model results at different copper concentration.

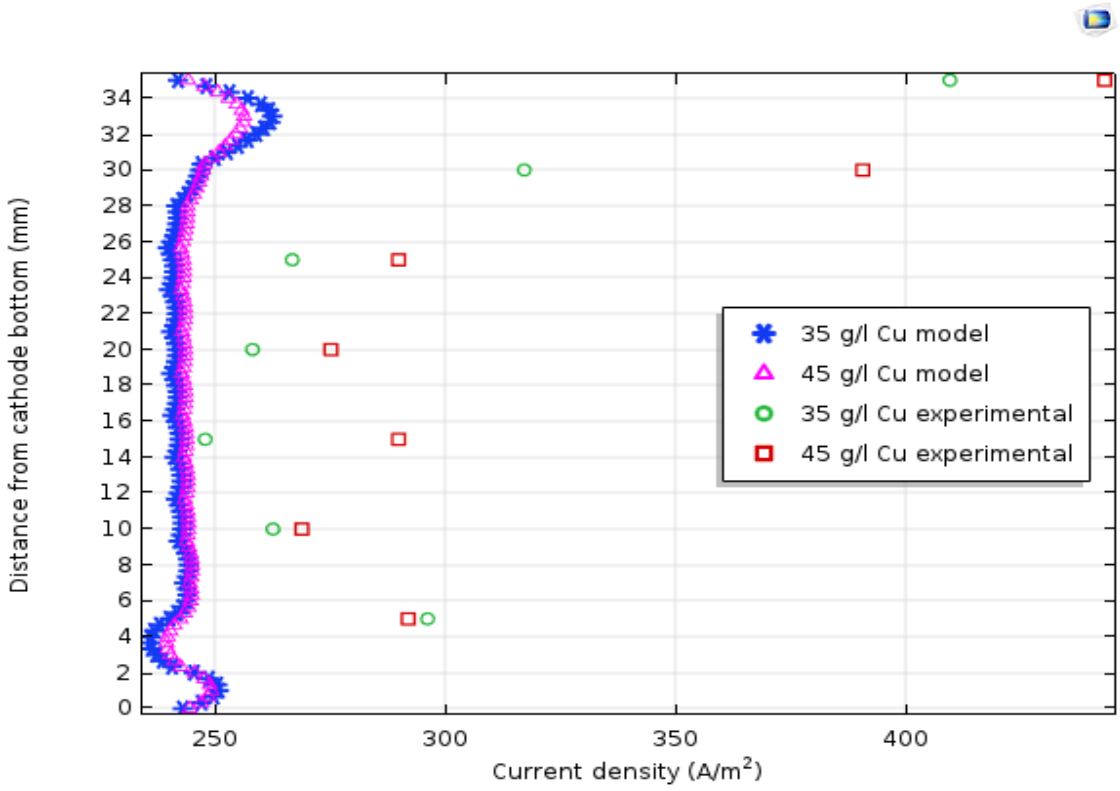

Figure 5.14: Current density distribution at the cathode surface at 160 g/l H_2SO_4 at 45°C temperature at varying copper concentrations.

The model predicted a fairly uniform current density with higher current densities towards the bottom and the top of the cathode (about 3 mm from the bottom and top of the cathode). The experimental current distribution profile did correlate well with the model in the middle of the cathode although at different magnitudes. However, higher current densities were observed at the top of the cathodes for the experimental values. The probable cause for the variation in current density profile could be the effect of mass transfer and oxygen evolution which enhanced mass transfer at the top of the electrode (Leahy and Schwarz, 2010; 2014); thereby, facilitating the easy passage of ions and accumulation of current (Obaid *et al.*, 2013). Furthermore, according to Popov *et al.* (2011), higher current densities are experienced at the edges than at the centre of the electrode. This causes thick deposits at the electrode edge. In addition, the

insulation tape used to insulate the cathode could have acted as the nucleation site, thereby, resulting in thicker deposit at the top of the cathode for the experimental results (Deconinck, 1994). Note that the effect of bubble generation was not included in the model due to the requirement of the two-phase system.

The effect of acid concentration on current distribution was investigated from 160 g/l to 180 g/l. Figure 5.15 shows the model and experimental current density distribution at varying sulphuric acid concentration.

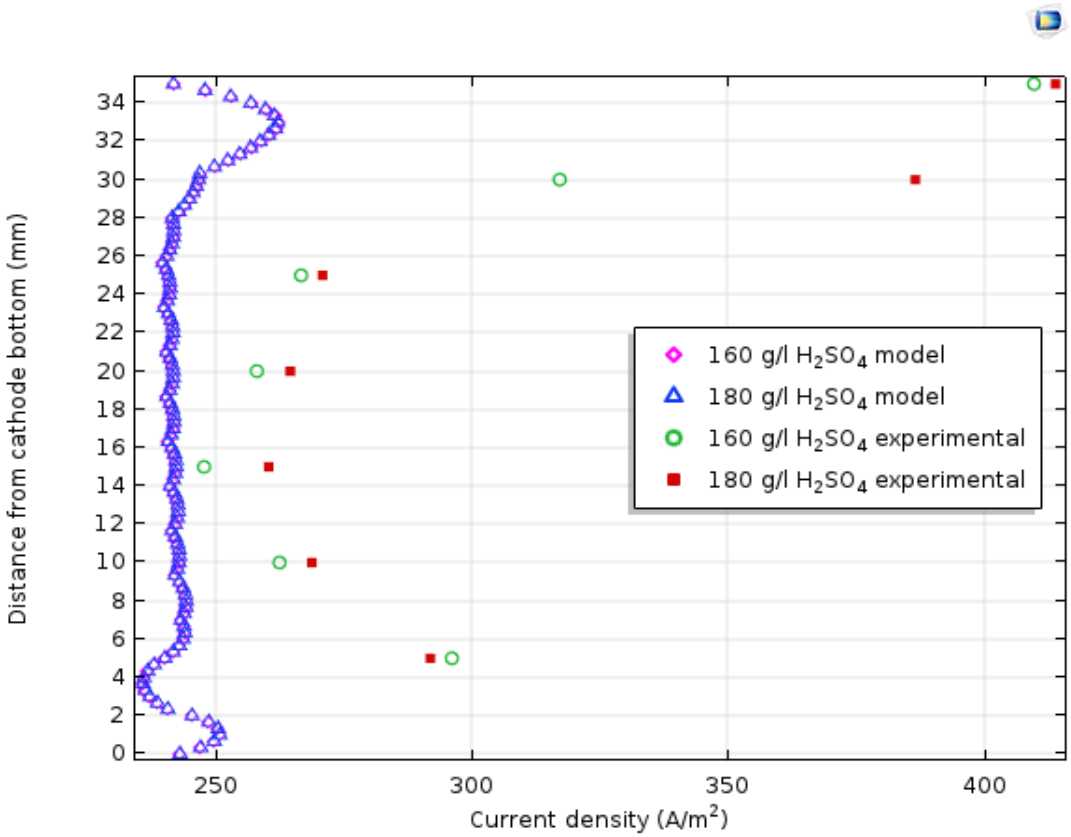

Figure 5.15: Current density distribution at the cathode surface at 35 Cu g/l at 45°C temperature at varying H_2SO_4 concentration

For the model current distribution, the profile was the same despite the increase in acid concentration. The reason for this trend was given in section 5.3.3.3. The experimental current densities showed an increase in current density with increase in acid concentration. This is expected as the addition of sulphuric acid reduces the electrolyte resistance, thereby, facilitating easy flow of ions in the system. A closer look at the current distribution profile show a similar trend as exhibited when copper concentration was varied.

5.2.5 Electrowinning performance

Several key performance indicators can be monitored in electrowinning of copper. The performance indicators include current efficiency, energy consumption and cathode quality (Abbey, 2019). As Khouraibchia and Moats (2009) stated, the energy consumption is affected by the composition of the electrolyte as well as the physicochemical properties such as density, diffusivity of ions and conductivity. As

such, the effect of electrolyte composition on current efficiency and energy consumption was evaluated using the experimental results from the copper electrowinning cell. The experimental deposit weight as well as respective current efficiency and energy consumption are given in Appendix B

The current efficiency for the model was compared to the experimental current efficiency. The model gave 100% current efficiency since there were no side reactions included in the model as well as the effects of short-circuiting were not incorporated. The current efficiency for the physical electrowinning experiments ranging 98.34 ± 0.5% was achieved (see Appendix B). The current losses may be due to electrical components of the cell, the electrolyte resistance as well as the presence of iron. The effect of iron was not pronounced as it was present in form of ferrous ions. At the same time, the current efficiencies obtained from the experiments were greater than those achieved in industrial operations. For industrial operations, current efficiency range from 85 to 95% (Robinson *et al.,* 2013). This is expected as the conditions are controlled in the experiment compared to the industrial operations.

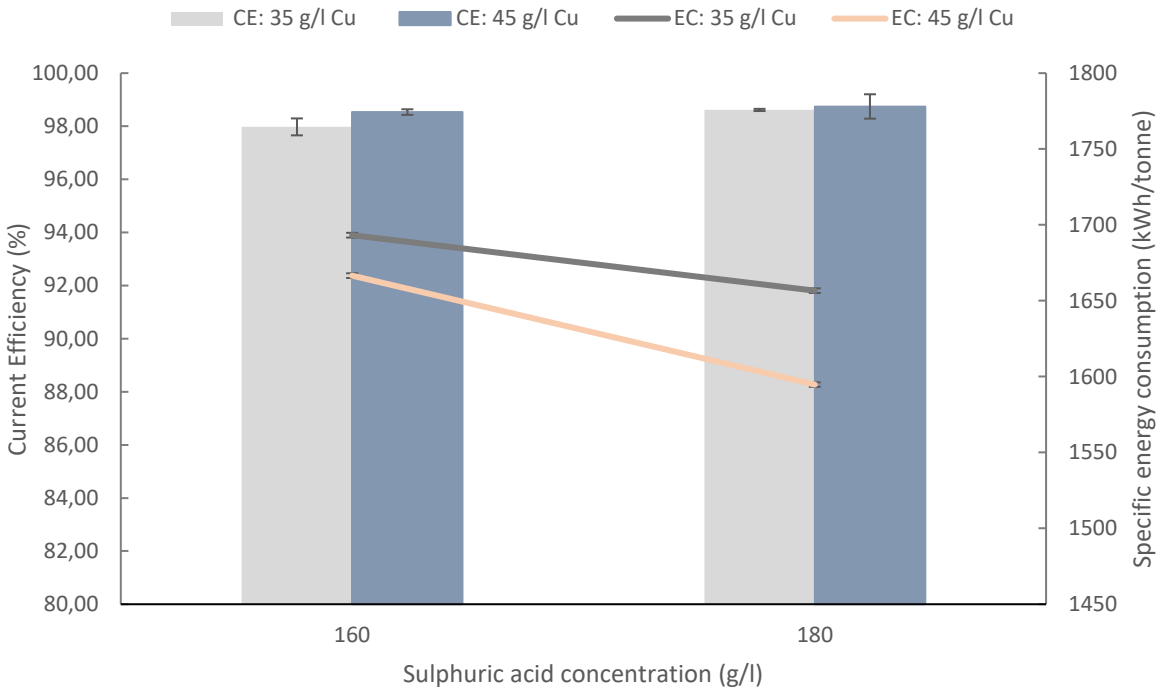

Figure 5.16: The effect of copper and acid concentration on current efficiency and energy consumption. CE and EC denotes current efficiency and energy consumption respectively.

Figure 5.16 shows the effect of copper concentration and sulphuric acid concentration on current efficiency and energy consumption. In the range of the present study, the increase in both the concentration of copper and sulphuric acid not only increased the current efficiency but also reduced the energy consumption. As observed in section 4.2, an increase in sulphuric acid concentration increases the conductivity of the electrolyte, thereby, reducing the potential requirement for the cell. At the same time, the increase in copper concentration ensures constant supply of copper ions to the cathode surface as well as increases the diffusion

limited current. The overall effect is the increase in current efficiency and reduction in energy consumption. This is despite the fact that density and viscosity is increased with increase in both copper and sulphuric acid concentration.

The increase in current efficiency and reduction in energy consumption in the present study was minimal. For example, a current efficiency increased by 0.64% when the sulphuric acid concentration was increased from 160 g/l to 180 g/l at 35 g/l copper concentration. A similar observation was made by Moats and Khouraibchia (2009), in which a slight increase in current efficiency was reported when the acid concentration was varied from 160 g/l to 220 g/l whereas no notable changes were experienced on energy consumption. Studies by Krishna and Das (1992; 1996) as well as Panda and Das (2001) also supports the observed trend. In case of copper concentration, the present study agrees with the earlier findings of Panda and Das (2001) who observed a slight increase in current efficiency and slight drop in energy consumption. The slight increase in current efficiency as the copper concentration may be due to the reasons brought out in the preceding paragraph as well as the decrease in concentration polarization and decrease in hydrogen overvoltage (Owais, 2009).

From the foregoing, it can be mentioned that electrolyte composition contributes to the variation in current efficiency as well as energy consumption, though, in the range of the present study, the effect was minimal. The effect of physicochemical properties such as conductivity was seen as the current efficiency slightly increased as the conductivity increased due to the addition of highly mobile hydrogen ions. Furthermore, although the increase in copper concentration results in the increase of density, and consequential increase in viscosity, the decrease in concentration polarization and constant supply of copper ions to cathode surface compensated this effect. Thus, a balance must be maintained when carrying out electrowinning operations to improve conductivity while maintaining favourable density and viscosity.

On the other hand, the model achieved a current efficiency of 100% and the reasons were stated earlier. The Tertiary Current Distribution Interface computes current density based on the summation of flux of ions in the system (Comsol, 2017). As such, it's difficult to explicitly single out the effect of conductivity on the system unless side reactions and other potential drop are incorporated in the model. As a result, variation in electrolyte composition will not have any effect on the modelled current efficiency. This is because the current for copper reduction reaction and the total cathodic current were the same. It is recommended that this area be explored further (inclusion of conductivity and ohmic drop) so that the model will be able to predict current efficiency and energy consumption.

5.2.6 Summary

The copper electrowinning model was developed and an attempt was made to validate the model using experimental data. Though the experimental and model current density values were different, the current

density profiles showed similarities as both exhibited high values at the top and bottom of the electrode. The effect of copper and acid concentration on current distribution were evaluated. The findings show that copper concentration had an effect on the modelled and experimental current density magnitude, that is, increased with an increase in copper concentration but the current distribution profile remained the same. This is in line with what is in the literature; the increase in copper concentration results in the increase in the limiting current density. Furthermore, it is reported that the current maldistribution occurring in the electrolytic cell may be due to cell configuration and electrode misalignment (Werner *et al.,* 2018). For sulphuric acid, the modelled current density was insensitive to the variation in acid concentration. However, the effect of acid concentration was observed for the experimentally determined current density. Similarly, the changes in acid concentration did not have any effect on the current density profile.

The effect of electrolyte composition on current distribution in the present study was investigated on the macro level. The study has shown that in terms of current density magnitude, the electrolyte composition has an effect. Yet, the effect in the current density distribution profile was not observed especially for the model. The model might be improved by incorporating phenomena taking place at double layer region, which is on micro level. Furthermore, the nucleation and growth phenomena were not considered from micro level. It will be interesting to find out how incorporating these phenomena can affect the current performance of the model, with regard to the effect of electrolyte composition on current distribution.

Chapter 6 : Conclusion and Recommendations

6.1 Conclusion

The purpose of the current study was to investigate the influence of electrolyte composition in copper electrowinning processes. This was achieved by studying how electrolyte composition, in the presence of additive, influences its physicochemical properties. In addition, a copper electrowinning model was developed to predict current distribution, which is the influential factor in controlling the growth and structure of the deposit using COMSOL Multiphysics software. Current density distribution is dependent on several factors, among them being mass transfer of ions and electrolyte conductivity. Electrowinning experiments were conducted at different copper and acid concentrations to deposit copper for model validation. The purpose of the study was accomplished by addressing three objectives.

The first objective of this study was to investigate the influence of electrolyte composition in the presence of the additive (polyacrylamide additive) on the electrolyte physicochemical properties. It was found that an increase in copper concentration, sulphuric acid concentration, and iron concentration had a positive effect on density (increased the density) whereas temperature had a negative effect. The PAM additive had no effect on electrolyte density. The lack of effect of PAM additive on density may be attributed to the low concentration in the electrolyte which was orders of magnitude lower (in mg/l) than other components. Furthermore, the manner in which the additive interacts in the electrodeposition is more pronounced at the electrode surface through adsorption and inhibition than in the bulk electrolyte, which is where the measurements were made.

Electrolyte conductivity was found to be affected positively when sulphuric acid concentration and temperature were increased, that is, increased with increase in the aforementioned factors whereas the increase in copper and iron concentration had a negative effect. It was also observed that sulphuric acid was the most influential factor in improving the conductivity of the electrolyte, likely due to the addition of highly mobile hydrogen ions. Just as was the case with density, the PAM additive did not affect the conductivity.

It was also shown that the diffusivity of copper ions decreased with an increase in copper, iron and acid concentration but increased with temperature. The interaction and complexation of ions (aggregation of pairs of ions via bridges at high concentration) in the electrolyte was suggested as the reason for decrease in diffusion coefficients. The effect of temperature was ascribed to the increase in thermal energy which enhanced the mobility of ions. Similarly, to other results, the presence of PAM additive had no influence on the diffusivity of copper ions in the present study.

The second objective was to develop equations relating electrolyte physicochemical properties as function of electrolyte composition for implementation in modelling. Regression models relating electrolyte composition to physicochemical properties (density, conductivity and diffusion coefficient) were constructed and compared to equations found in the literature as well as experimental data. The findings of the current study are consistent with the work of previous studies.

The third objective was to develop a copper electrowinning model using finite element analysis to predict current distribution in the cell and to conduct electrowinning experiments to deposit copper for model validation. The copper electrowinning model was developed using COMSOL Multiphysics 5.3a and deposit thickness (from electrowinning experiments) as well as Faraday's law were used to extract current density distribution for model validation.

The modelled and experimental current distribution showed good agreement in current density distribution, that is, uniform current densities were observed at the center of the electrode with higher current densities just before the top of the cathode. However, the model under-predicted the current density magnitude. Furthermore, it was observed that the current distribution profile remained relatively the same with variation in electrolyte composition, that is, changes in copper and acid concentration had minimal effect on the current density profile at the cathode surface. Marginal increase in the value of current density was observed for the modelled and experimental current density distribution when the copper concentration was increased. For sulphuric acid, modelled current density was insensitive to the variation in concentration due to model limitations. Yet, experimental current density showed an increase with an increase in acid concentration due to the increase in conductivity. It is concluded therefore that conductivity is not captured sufficiently in the model and further work can be recommended to address this matter. Similarly, the current density distribution profile was not affected by the changes in acid concentration.

From the copper electrowinning experiments, it was observed that an increase in copper and acid concentration resulted in a slight increase in current efficiency (approximately 0.5 to 1%) and a slight decrease in energy consumption. The aforementioned trend was attributed to constant supply of copper ions to the cathode surface, improved conductivity and increase in limiting current density due to the addition of copper ions and sulphuric acid. However, the model predicted 100% current efficiency as side reactions and ohmic drop were not incorporated in the model development.

6.2 Recommendation

Based on the current work, the following recommendations are made:

- The effect of electrolyte composition on electrodeposition was investigated on the macro level, that is, in the bulk electrolyte. Yet, there are phenomena taking place in the double-layer region (or at the

electrode surface), which is on micro-level such as nucleation and growth, adsorption of the additive. It will be worthwhile to consider how the electrolyte composition affects these phenomena as it may enhance the ability to improve the electrowinning performance.

- Since the industrial electrowinning electrolytes contain several impurities, further research is required to include a number of impurities when investigating the properties of the electrolyte as it will be a more accurate representation of the industrial process.
- The current copper electrowinning model considered few species. The incorporation of mores species in the model development may improve the performance of the model. It will be interesting to compare the model performance after the inclusion of more species in the system as the presence of species (impurities) affect electrowinning performance.
- Additives are added in the electrolyte to control the deposition process of copper in order to deposit smooth, dense and bright cathodes. The effect of additive through adsorption and inhibition was not explored in the current copper electrowinning model. Future modelling should integrate the phenomena of additive when modelling the electrodeposition process.
- It will be also interesting to assess the effects of forced and natural convection, as well as bubble generation on the electrowinning process, which were not included in the current model due to associated model complexity that is, a fully coupled multiphase computational fluid dynamics copper electrowinning model.

References

Abbey, C. E. (2019) Improving base metal electrowinning. *PhD Thesis,* Missouri University of Science and Technology.

Aminian, H. *et al.* (2000) 'Simulation of a SX-EW pilot plant', *Hydrometallurgy*, 56(1), pp. 13–31.

Andersen, T. N., Wright, C. N. & Richards, K. J., 1973. Important Electrochemical Aspects Of Electrowinning Copper From Acid Leach Solutions. *The American Institute of Mining, Metallurgical, and Petroleum Engineers*.

Anderson, G. C., 2017. Optimization of Industrial Copper Electro Winning Solutions, *Journal of Advanced Chemical Engineering*, 7(1), pp. 1–3.

Araneda-Hernández, E., Vergara-Gutierrez, F. & Pagliero-Neira, A., 2014. Effect of additives on diffusion coefficient for cupric ions and kinematics viscosity in CuSO4-H2SO4 solution at 60° C., *Dyna*. 2006, *Revista DYNA*, 81(188), pp. 209–215.

Aromaa, J. (2007) Aqueous Processing of Metals. In D. D. Macdonald, & P. Schmuki (Eds.), *Encyclopedia of Electrochemistry vol 5.Electrochemical Engineering* (pp. 159-223). Weinheim

Bard, A. J. & Faulkner, L. R., 2000. Electrochemical Methods: Fundamentals and Applications.

Bard, A. J., Inzelt, G. & Scholz, F., 2008. Electrochemical dictionary. *Springer Science & Business Media*.

Barron, J. J. & Ashton, C., 2005. The effect of temperature on conductivity measurement'.

Baur, J. E., 2007. Diffusion coefficients. *Handbook of Electrochemistry*, pp. 829–848.

Beukes, N. T. & Badenhorst, J., 2009. Copper electrowinning: Theoretical and practical design. *Journal of the Southern African Institute of Mining and Metallurgy*, 109(6), pp. 343–356.

Bousfield, W. R. & Lowry, T. M., 1903. Influence of temperature on the conductivity of electrolytic solutions. *Proceedings of the Royal Society of London*. The Royal Society London, 71(467–476), pp. 42–54.

Bouzek, K., Borve, K., Lorentsen, O. A., Osmundsen, K., Rousar, I. & Thonstad, J., 1995. Current Distribution at the Electrodes in Zinc Electrowinning Cells. *Journal of the Electrochemical Society*, 142(1), pp. 64–69.

Budevski, E., Staikov, G. & Lorenz, W. J., 1996. Electrochemical Phase Fomation and Growth*:* an introductionto the initial stages of metal deposition*. John and Wiley and Sons*

Bunker, B. C. & Casey, W. H., 2016. Aqueous Chemistry of Oxides. in Oxford University Press.

Casas, J. M., Alvarez, F. & Cifuentes, L., 2000. Aqueous speciation of sulfuric acid-cupric sulfate solutions. *Chemical Engineering Science*, 55(24), pp. 6223–6234.

Choi, N. S., Kim, D. W., Cho, J. & Kim, D. H., 2015. A fully optimized electrowinning cell for achieving a uniform current distribution at electrodes utilizing sampling-based sensitivity approach. *Journal of Electrical Engineering and Technology*, 10(2), pp. 641–646.

Cifuentes, L., Castro, J. M., Crisóstomo, G., Casas, J. M. and Simpson, J., 2006. Modelling a copper electrowinning cell based on reactive electrodialysis. *Applied Mathematical Modelling*, 31(7), pp. 1308–1320.

Coetzee, C., 2018. Characterizing the Role of Organic Additives in Copper Electrowinning. *Masters Thesis*. Stellenbosch University.

Comsol, 2017. Electrodeposition Module. *COMSOL Multiphysics 5.3a User Guide*.

Comsol, 2019. COMSOL Multiphysics User manual. Available at: https://www.comsol.com/ (Accessed: 23 October 2019) .

Das, S. C. and Krishna, P. G., 1996. Effect of Fe(III) during copper electrowinning at higher current density. *International Journal of Mineral Processing*, 46(1–2), pp. 91–105.

Datta, A. & Vineet, R., 2010. An introduction to modelling mass transport processes: Application to biomedical systems.

Deconinck, J., 1994. Mathematical modelling of electrode growth. *Journal of Applied Electrochemistry*, *24*(3), 212–218.

Dickinson, E. J. F. (2014) *No Title*, *Theory of Current Distribution*.

Dickinson, E. J. F., Ekström, H. & Fontes, E., 2014. COMSOL Multiphysics®: Finite element software for electrochemical analysis. A mini-review. *Electrochemistry Communications*. Elsevier B.V., 40, pp. 71–74.

Dini, J. W. & Snyder, D. D., 2011. Electrodeposition of copper. *Modern Electroplating, Fifth Edition*. Wiley Online Library, pp. 33–78.

Dresher, W. H., 2001. How hydrometallurgy and the SX/EW process made copper the" green" metal. *Copper Applications in Mining and Metallurgy*.

Ettel, V. A., Gendron, A. S. & Tilak, B. V., 1975. Electrowinning copper at high current densities. *Metallurgical and Materials Transactions B*, 6(1), pp. 31–36.

Fabian, C. P., 2005. Copper electrodeposition in the presence of guar or activated polyacrylamide. *PhD Thesis.* James Cook University.

Free, M., Bhide, R., Rodchanarowan, A., & Phadke, N., 2006. Electrochemical modeling of electrowinning performance. *2006 TMS Fall Extraction and Processing Division: Sohn International Symposium*.

Funk, J. E. & Thorpe, J. F., 1969. Void Fraction and Current Density Distributions in Water Electrolysis Cell. *Electrochem Soc-J*, 116(1), pp. 48–54.

Gebbie, J., 2013. A theoretical study of crystal growth in nanoporous materials using the monte carlo method.

Gladysz, O., Los, P. & Krzyzak, E., 2007. Influence of concentrations of copper, levelling agents and temperature on the diffusion coefficient of cupric ions in industrial electro-refining electrolytes. *Journal of Applied Electrochemistry*, *37*(10), 1093-1097.

Gupta, C. K., 2003. Chemical Metallurgy principles and pratice. *John Wiley & Sons.*

Hoffman, D. O. & Zakhary, R., 1951. The Effect of Temperature on the Molluscacidal Activity of Copper Sulfate', *Science*, 114(2968), pp. 521–523.

Hotlos, J. & Jaskuła, M., 1988. Densities and viscosities of $CuSO_4$-H_2SO_4-H_2O solutions. *Hydrometallurgy*, *21*(1), pp.1-7.

Huang, H., Zhou, J. Y. & Guo, Z. C., 2010. Effect of added cobalt ion on copper electrowinning from sulfate

bath using doped polyaniline and Pb-Ag anodes. *Transactions of Nonferrous Metals Society of China,20*, pp. s55–s59.

ICSG, 2018. The World Copper Factbook 2018. *International Copper Study Group*.

Isakov, V. T., 1970. The Electrolytic Refining of Copper. *Metallurgiya*.

Kalliomaki, T., Aji, A.T., Rintala, L., Aromaa, J. & Lundstrom, M., 2017. Models for viscosity and density of copper electrorefining electrolytes. *Physicochemical Problems of Mineral Processing*, *53*.

Kalliomäki, T., Aji, A.T., Aromaa, J. & Lundström, M., 2016. Viscosity and density models for copper electrorefining electrolytes. In *E3S Web of Conferences* (Vol. 8, p. 01050). EDP Sciences .

Kalliomäki, T., Wilson, B.P., Aromaa, J. & Lundström, M., 2019. Diffusion coefficient of cupric ion in a copper electrorefining electrolyte containing nickel and arsenic. *Minerals Engineering*, *134*, pp.381-389.

Kalliomäki, T., Aromaa, J. & Lundström, M., 2016. Modeling the Effect of Composition and Temperature on the Conductivity of Synthetic Copper Electrorefining Electrolyte. *Minerals*, 6(3), p. 59.

Khouraibchia, Y. & Moats, M., 2009. Effective Diffusivity of Ferric Ions and Current Efficiency in Stagnant Synthetic Copper Electrowinning Solutions. *Mineral and Metallurgical Processing*, 26, pp. 176–190.

Khouraibchia, Y. & Moats, M. S., 2010. Evaluation of the effect of copper electrowinning parameters on current efficiency and energy consumption using surface response methodology. *ECS Transactions*. The Electrochemical Society, 28(6), pp. 295–306.

Kim, K.R., Choi, S.Y., Paek, S., Park, J.Y., Hwang, I.S. & Jung, Y., 2013. Electrochemical hydrodynamics modeling approach for a copper electrowinning cell. *International Journal of Electrochemical Science*, *8*(11), pp.12333-12347.

Krishna, G. P. & Das, S. C., 1992. Enhancement of operating current density in a copper electrowinning cell', *Hydrometallurgy*, 31(3), pp. 243–255.

Kumar, S., Pande, S. & Verma, P., 2015. Factor Effecting Electro-Deposition Process. *International Journal of Current Engineering and Technology*, 5(2), pp. 700–703.

Laitinen, T. & Pohl, J., 1988. The Kinetics of Oxide Growth and Oxygen Evolution During Polarization of Lead in H_2SO_4 electrolytes—investigations on the temperature dependence. *Electrochimica acta*, *34*(3), pp.377-385.

Leahy, M. J. & Schwarz, M. P., 2014. Flow and mass transfer modelling for copper electrowinning: Development of instabilities along electrodes. *Hydrometallurgy*. Elsevier B.V., 147–148, pp. 41–53.

Leahy, M. J. & Schwarz, P. M., 2010. Experimental validation of a computational fluid dynamics model of copper electrowinning. *Metallurgical and Materials Transactions B: Process Metallurgy and Materials Processing Science*, 41(6), pp. 1247–1260.

Mattson, E. & Bockris, J. M., 1958. Galvanostatic studies of the kinetics of deposition and dissolution in the copper+ copper sulphate system. *Transactions of the Faraday Society*, *55*, pp.1586-1601.

Moats, M., 2012. How to evaluate current efficiency in copper electrowinning. *in Separation Technologies for Minerals, Coal, and Earth Resources*, pp.333-339.

Moats, M. & Free, M., 2007. A bright future for copper electrowinning. *Jom*, 59(10), pp. 34–36.

Moats, M. and Khouraibchia, Y., 2009. Effective diffusivity of ferric ions and current efficiency in stagnant

synthetic copper electrowinning solutions. *Minerals and Metallurgical Processing*, 26(4), pp. 179–186.

Moats, Michael S., Hiskey, J. B. & Collins, D. W., 2000. Effect of copper, acid, and temperature on the diffusion coefficient of cupric ions in simulated electrorefining electrolytes. *Hydrometallurgy*, 56(3), pp. 255–268.

Moats, M. S., Luyima, A. & Cui, W., 2016. Examination of copper electrowinning smoothing agents. Part I: A review. *Minerals & Metallurgical Processing*, 33(1), pp. 7–13.

Montgomery, D. C., Peck, E. A. & Vining, G. G., 2012. Introduction to Linear Regression Analysis. *John Wiley and Sons, Inc*.

Muhlare, T. A. & Groot, D. R., 2011. The effect of electrolyte additives on cathode surface quality during copper electrorefining. *Journal of the Southern African Institute of Mining and Metallurgy*, 111(5), pp. 371–378.

Muresan, L., Varvara, S., Maurin, G. & Dorneanu, S., 2000. The effect of some organic additives upon copper electrowinning from sulphate electrolytes. *Hydrometallurgy*, *54*(2-3), pp.161-169.

Najim, S. T., 2016. Estimation of Mass Transfer Coefficient for Copper Electrowinning Process. *Journal of Engineering*, *22*(4), 158–168

Najminoori, M., Mohebbi, A., Arabi, B.G. and Daneshpajouh, S., 2015. CFD simulation of an industrial copper electrowinning cell. *Hydrometallurgy*, *153*, pp.88-97.

Newman, J. S. & Thomas-Alyea, K. E., 2004. Electrochemical systems. *John Wiley & Sons*.

Nguyen, T. V., Walton, C. W., White, R. E. and Van Zee, J., 1986. Parallel-Plate Electrochemical Reactor Model A Method for Determining the Time-Dependent Behavior and the Effects of Axial Diffusion and Axial Migration. *Journal of the Electrochemical Society*, *133*(1), pp.81-87.

Nikoloski, A. N. & Nicol, M. J., 2008. Effect of cobalt ions on the performance of lead anodes used for the electrowinning of copper—a literature review. *Mineral Processing and Extractive Metallurgy Review*, *29*(2), pp.143-172.

Ntengwe, F. W., Mazana, N. & Samadi, F., 2010. The Effect of Impurities and Other Factors on the Current Density in Electro-Chemical Reactors.

O'Keefe, T. J., 1984. Techniques for evaluating electrolytes for metal recovery. *J ournal of Electroanalytical Chemistry and Interfacial Electrochemistry*, *168*(1-2), pp.131-146.

Obaid, N., Sivakumaran, R., Lui, J. & Okunade, A., 2013. Modelling the Electroplating of Hexavalent Chromium. In *COMSOL Conference. Boston2013*.

Owais, A., 2009. Effect of electrolyte characteristics on electrowinning of copper powder. *Journal of Applied Electrochemistry*, 39(9), pp. 1587–1595.

Panda, B. & Das, S. C., 2001. Electrowinning of copper from sulfate electrolyte in presence of sulfurous acid. *Hydrometallurgy*, 59(1), pp. 55–67.

Pasa, A. A. & Munford, M. L., 2006. Electrodeposition. *Encyclopedia of Chemical Processing*, pp. 821–832.

Popov, K., Djokic, S. & Grgur, B., 2002. Fundamental Aspects of Electrometallurgy.

Popov, K. I., Pešić, S. M. & Živković, P. M. (2001) 'The current distribution in an electrochemical cell. Part VI.

The quantitative treatment for cells with three plane parallel electrode arrangements', *Journal of the Serbian Chemical Society*, 66(7), pp. 491–498.

Popov, K., Zivkovic, P. & Nikolic, N., 2011. A mathematical model of the current density distribution in electrochemical cells. *Journal of the Serbian Chemical Society*, 76(6), pp. 805–822.

Pradhan, N., Gopala Krishna, P. & Das, S. C., 1998. Synergistic Effects of LIX 64N and Fe^{3+} during copper electrowinning. *Transactions of the Institute of Metal Finishing*, 76(3), pp. 96–100.

Price, D. C. & Davenport, W. G., 1980. Densities, electrical conductivities and viscosities of $CuSO^4/H^2SO^4$ solutions in the range of modern electrorefining and electrowinning electrolytes. *Metallurgical Transactions B*, 11(1), pp. 159–163.

Price, D. C. & Davenport, W. G., 1981. Physico-chemical properties of copper electrorefining and electrowinning electrolytes. *Metallurgical Transactions B*, 12(4), pp. 639–643.

Quickenden, T. I. & Jiang, X. (1984) 'The diffusion coefficient of copper sulphate in aqueous solution', *Electrochimica Acta*, 29(6), pp. 693–700. doi: 10.1016/0013-4686(84)80002-X.

Quickenden, T. I. & Xu, Q., 1996. Toward a reliable value for the diffusion coefficient of cupric ion in aqueous solution. *Journal of the Electrochemical Society*, 143(4), pp. 1248–1253.

Radetzki, M., 2009. Seven thousand years in the service of humanity-the history of copper, the red metal. *Resources Policy*. Elsevier, 34(4), pp. 176–184.

Robinson, T. G., Sole, K., Sandoval, S. Moats, M.,2013. Copper Electrowinning: 2013 World Tankhouse Operating Data. *Copper 2013 International Conference*.

Robison, M. R., 2014. Modeling and experimental validation of electroplating deposit distributions in copper sulfate solutions. *Masters Thesis.* The University of Utah.

Rusli, E., Li, X., Drews, T.O., Xue, F., He, Y., Braatz, R. & Alkire, R., 2007. Effect of additives on shape evolution during electrodeposition I. Multiscale simulation with dynamically coupled kinetic Monte Carlo and moving-boundry finite-volume codes. *Journal of The Electrochemical Society*, *154*(4), pp.D230-D240.

Samson, E., Lemaire, G., Marchand, J. & Beaudoin, J.J., 1999. Modeling chemical activity effects in strong ionic solutions. *Computational Materials Science*, *15*(3), pp.285-294.

Schlesinger, M. E., King, M. J., Sole, K. C., Davenport, W. G., & William G., 2011. Extractive metallurgy of copper. *Elsevier*.

Shukla, A., 2013. Modeling and measuring electrodeposition parameters near electrode surfaces to facilitate cell performance optimization. *Masters Thesis*. University of Utah.

Subbaiah, T. & Das, S. C., 1989. Physico-chemical properties of copper electrolytes Physico-Chemical Properties of Copper Electrolytes. *Metallurgical Transactions B*, 20B.

Subbaiah, T. & Das, S. C., 1994. Effect of some common impurities on mass transfer coefficient and deposit quality during copper electrowinning. *Hydrometallurgy*, 36(3), pp. 271–283.

Suggu, S. K., 2014. Modeling the Electrodeposition Process of Copper on Cobalt Chrome. *Masters Thesis.* Wichita State University .

Tobias, C. W., 1959. Effect of Gas Evolution on Current Distribution and Ohmic Resistance in Electrolyzers. *Journal of the Electrochemical Society*, 106(9), pp. 833–838.

Vereecken, J. & Winand, R., 1976. Influence of polyacrylamides on the quality of copper deposits from acidic copper sulfate solutions. *Surface Technology*, 4(3), pp. 227–235.

Werner, J. M., 2017. Modeling and Validation for Optimization of Electrowinning Performance. *PhD Thesis.* University of Utah .

Werner, J. M., Zeng, W., Free, M. L., Zhang, Z. & Cho, J., 2018. Modeling and Validation of Local Electrowinning Electrode Current Density Using Two Phase Flow and Nernst–Planck Equations. *Journal of The Electrochemical Society*, *165*(5), pp. E190-E207.

Wilke, C. R., Eisenberg, M., & Tobias, C. W., 1953. Diffusion and Convection in Electrolysis—A Theoretical Review. *Journal of The Electrochemical Society*, *99*(12), 359C.

Willmott, C. J., 1981. On the validation of models. *Physical Geography*, *2*(2), 184–194

Zhang, Z., Werner, J. and Free, M., 2018, March. A current efficiency prediction model based on electrode kinetics for iron and copper during copper electrowinning. In *TMS Annual Meeting & Exhibition* (pp. 111-131).

Ziegler, D. & Evans, J. W., 1986. Mathematical Modeling of Electrolyte Circulation in Cells with Planar Vertical Electrodes. *Journal of The Electrochemical Society*, 133(3), p. 567-576.

APPENDICES

Appendix A : Experimental Methodology

A.1 Polyacrylamide Additive Preparation

The following is the procedure was followed during polyacrylamide (PAM) additive preparation.

1. Select 250 ml beaker and clean it thoroughly, and dry it.
2. Add exactly 100 ml of distilled water to the beaker.
3. Heat the water in the beaker to 40°C using the heater stirrer. Wait until the working temperature is reached. Note that the temperature reading on the stirrer may not heat the water the water to the required temperature. Hence, the temperature must be confirmed by the thermometer.
4. Weigh 200 mg of PAM additive. Confirm the water temperature.
5. When temperature is 40°C, add the PAM additive to the beaker containing distilled water. The 200 mg/l of additive translate to 1.9961 mg/ml concentration in beaker. Note that the final volume is the sum of volume of 100ml of water and volume of additive.
6. Heat and stir for 2 hours to ensure that the additives dissolves and is uniformly distributed.

A.2 Electrolyte Preparation

During the preparation of the electrolyte, the volume and composition of the electrolyte varied from experiment to experiment. The procedure is the same, with difference only being the volume of the volumetric flask being used as well as the calculated amounts copper sulphate, sulphuric acid, ferrous sulphate and PAM additive. As such, a procedure for preparing 500 ml electrolyte with known concentrations will be used as an example.

1. Add a known volume of water (approximately 200 ml of distilled water) to the 500 ml volumetric flask.
2. Weigh the required amount of copper (II) sulphate and iron (II) sulphate (calculated before the preparation procedure)
3. Add a known volume of sulphuric acid (also calculated beforehand based on the required electrolyte concentration) to the beaker containing water.
4. Add weighed amounts of copper sulphate and ferrous sulphate to the mixture of water and acid in the beaker. Also, add the calculated volume of PAM additive using the pipette.
5. Fill the volumetric flask to the 500 ml with distilled. Stir until all the compounds are completely dissolved.

A.3 Calibration procedure for pycnometer

Calibration of the pycnometer is necessary to determine the accurate volume of the pycnometer before using it for density measurements. The calibration is as follows:

1. Select a pycnometer and the respective stopper (lid). Make sure that it fits properly on the pycnometer.
2. Clean the pycnometer with distilled and dry it naturally. You may use compress air to eliminate any trace of moisture.
3. Weigh the empty pycnometer together with its lid, record the weight as M1.
4. Pour distilled in the beaker and take note of its temperature as T1. Then, carefully pour distilled water into the pycnometer to just above the neck (only leave space for the lid to fit).
5. Close the pycnometer by placing its lid on the pycnometer. A small amount of water must flow out of the capillary hole on the lid. Ensure that there is no entrapped air in the pycnometer as this will introduce errors in measurements.
6. Wipe excess water from the pycnometer with a non-sticking wiper until its completely dry.
7. Weigh the full pycnometer and lid and record weight as M2
8. Determine the weight of distilled water in the pycnometer by subtracting the weight of the empty pycnometer (M1) from the weight of the full pycnometer(M2)
9. Using the temperature/density chart below, determine the density of the distilled water at the measured temperature.

Table A.1: Density – temperature chart for distilled water

°C	Density (g/cm^3)	°C	Density (g/cm^3)	°C	Density (g/cm^3)	°C	Density (g/cm^3)
15	0.991	18	0.9986	21	0.99799	24	0.9973
16	0.99894	19	0.99841	22	0.99777	25	0.99705
17	0.99878	20	0.99821	23	0.99754	26	0.99679

10. Determine the volume of the pycnometer by dividing the weight of the distilled water by the density of the distilled water at the measured temperature

$$V_1 = \frac{(M2 - M1)}{\rho_{water}} \qquad 0.1$$

11. Repeat steps at least 3 times and average the results and record the volume for each pycnometer/lid set

A.4 Working Electrode Cleaning Procedure

The working electrode was cleaned before each measurement to ensure accurate results. The following is the working electrode cleaning procedure:

1. Attach appropriate micro-cloth on smooth, flat and hard surface using its adhesive back
2. Apply few drops of 3 µm diamond suspension solution on the micro-cloth
3. Rinse the working electrode surface with distilled water
4. Place the electrode on the micro-cloth. Note that the electrode should be face down when placing it.
5. Polish the electrode using a smooth figure-eight motion for 5 minutes until the mirror finish is reached. The pressure applied during the movement should be uniform and sufficient to have effective cleaning.
6. Thoroughly rinse the electrode using acetone and distilled water.
7. Dry the electrode in natural and mount it on the rotating shaft.

Appendix B : Experimental Results

B.1 : Electrolyte physicochemical property results

Table B.1 : Experimental design and corresponding results for electrolyte density, conductivity and diffusion coefficients.

Cu (g/l)	H_2SO_4 (g/l)	Fe (g/l)	PAM (mg/l)	Temp (ºC)	Density (g/cm^3)	Conductivity (mS/cm)	Diffusion Coefficient ($\times 10^{-5} cm^2/s$)	
							Levich	Koutecky-Levich
35	160	1	2	45	1.16598	553.00	8.79	9.58
35	160	1	5	45	1.16521	548.97	8.65	9.66
35	160	1	10	45	1.16673	562.03	8.88	9.67
35	160	3	2	45	1.17098	526.23	8.73	9.59
35	160	3	5	45	1.17068	545.90	8.60	9.51
35	160	3	10	45	1.17129	539.03	8.69	9.54
35	160	6	2	45	1.17793	525.40	8.25	9.19
35	160	6	5	45	1.17714	527.93	8.23	9.28
35	160	6	10	45	1.17718	525.90	8.29	9.28
35	180	1	2	45	1.17748	599.97	8.29	9.58
35	180	1	5	45	1.17706	597.00	8.29	9.44
35	180	1	10	45	1.17796	599.13	8.56	9.44
35	180	3	2	45	1.18220	583.83	8.01	9.16
35	180	3	5	45	1.18182	576.60	8.48	9.43
35	180	3	10	45	1.18283	585.80	8.18	9.20
35	180	6	2	45	1.18871	568.70	7.75	8.88

Cu (g/l)	H_2SO_4 (g/l)	Fe (g/l)	PAM (mg/l)	Temp (ºC)	Density (g/cm^3)	Conductivity (mS/cm)	Diffusion Coefficient ($\times 10^{-5} cm^2/s$)	
							Levich	Koutecky-Levich
35	180	6	5	45	1.18948	575.90	7.94	8.93
35	180	6	10	45	1.18951	577.97	7.87	8.94
45	160	1	2	45	1.18701	513.73	8.36	9.45
45	160	1	5	45	1.18695	516.30	8.55	9.43
45	160	1	10	45	1.18821	519.10	8.42	9.51
45	160	3	2	45	1.19431	508.10	8.40	9.57
45	160	3	5	45	1.19152	501.60	8.35	9.44
45	160	3	10	45	1.19318	511.63	8.36	9.53
45	160	6	2	45	1.19872	503.13	7.96	9.16
45	160	6	5	45	1.19970	494.67	8.05	9.13
45	160	6	10	45	1.19973	498.13	8.05	9.21
45	180	1	2	45	1.19996	563.70	8.36	9.15
45	180	1	5	45	1.20130	540.67	8.24	9.15
45	180	1	10	45	1.19980	551.60	8.21	9.40
45	180	3	2	45	1.19359	554.50	7.92	8.90
45	180	3	5	45	1.20531	551.07	7.70	8.90
45	180	3	10	45	1.20308	565.17	7.96	9.09
45	180	6	2	45	1.21104	525.90	7.58	8.72
45	180	6	5	45	1.20989	541.17	7.55	8.84
45	180	6	10	45	1.20770	550.80	7.63	8.86
35	160	1	2	55	1.16018	591.03	11.55	11.57
35	160	1	5	55	1.15973	583.07	11.30	11.32
35	160	1	10	55	1.16131	605.20	11.15	11.17
35	160	3	2	55	1.17148	567.53	11.07	11.26
35	160	3	5	55	1.16577	580.10	11.07	11.16
35	160	3	10	55	1.16598	574.73	11.17	11.62
35	160	6	2	55	1.17216	566.37	10.92	11.11
35	160	6	5	55	1.17214	563.07	10.70	10.88
35	160	6	10	55	1.17209	565.43	10.80	11.24
35	180	1	2	55	1.17275	643.90	11.00	11.13
35	180	1	5	55	1.17139	634.13	10.61	11.21
35	180	1	10	55	1.17229	642.17	10.87	11.00
35	180	3	2	55	1.17663	630.30	10.67	10.65
35	180	3	5	55	1.17220	617.40	10.82	11.01
35	180	3	10	55	1.18079	624.73	10.41	10.78
35	180	6	2	55	1.18332	608.83	10.24	10.70
35	180	6	5	55	1.18398	604.00	10.53	10.82
35	180	6	10	55	1.18441	615.13	10.50	10.79
45	160	1	2	55	1.18174	549.63	11.15	11.50
45	160	1	5	55	1.18115	549.15	10.95	11.16

Cu (g/l)	H_2SO_4 (g/l)	Fe (g/l)	PAM (mg/l)	Temp (ºC)	Density (g/cm^3)	Conductivity (mS/cm)	Diffusion Coefficient ($\times 10^{-5} cm^2/s$) Levich	Koutecky-Levich
45	160	1	10	55	1.18328	552.57	10.81	11.15
45	160	3	2	55	1.19005	544.37	10.85	11.16
45	160	3	5	55	1.18606	538.20	10.99	11.40
45	160	3	10	55	1.18776	546.20	11.19	11.26
45	160	6	2	55	1.19298	540.40	10.46	10.97
45	160	6	5	55	1.19454	533.57	10.19	10.68
45	160	6	10	55	1.19535	533.97	10.73	10.98
45	180	1	2	55	1.19317	601.27	10.22	10.65
45	180	1	5	55	1.19640	579.60	10.75	10.73
45	180	1	10	55	1.19385	595.23	10.62	11.07
45	180	3	2	55	1.19988	595.10	10.15	10.86
45	180	3	5	55	1.20057	596.23	10.33	10.84
45	180	3	10	55	1.19783	600.90	10.27	10.59
45	180	6	2	55	1.20522	586.40	10.09	10.52
45	180	6	5	55	1.20459	587.93	9.87	10.47
45	180	6	10	55	1.20753	583.40	9.95	10.55

B.2 : PAM Additive Results

Table B.2 : Results of electrolyte properties (density, conductivity and diffusion coefficient) measured at various concentrations of PAM additive at 35 g/l Cu, 160 g/l H2SO4 and 6 g/l Fe on

PAM (mg/l)	Temp (°C)	Density (g/cm^3)	Conductivity (mS/cm)	Diffusion Coefficient ($\times 10^{-5} cm^2/s$) Levich	Koutecky
5	45	1.17690	527.70	7.63	9.98
10	45	1.17784	528.80	8.45	8.48
15	45	1.17784	529.87	7.81	9.37
20	45	1.17775	528.77	8.60	8.25
25	45	1.17723	498.93	8.38	8.84
30	45	1.17745	527.53	8.04	9.57
5	55	1.17126	565.40	12.07	12.64
10	55	1.17209	568.07	11.12	10.50
15	55	1.17204	564.93	11.49	11.28
20	55	1.17213	570.87	9.18	10.26
25	55	1.17166	528.77	10.86	12.09
30	55	1.17191	564.87	10.12	10.61

B.3 : Confirmation Run Results

Table B.3: Results of the confirmation runs for the physicochemical properties carried out at 3 g/l Fe and 10 mg/l PAM additive

Run	Cu (g/l)	H_2SO_4 (g/l)	Temp (°C)	Density (g/cm^3)	Conductivity (mS/cm)	Diffusion Coefficient (X10-5 cm^2/s)
1	35	180	45	1.18128	592.50	10.95
2	40	180	45	1.18838	584.60	12.06
3	45	180	45	1.20248	561.00	9.32
4	35	180	55	1.17552	639.20	14.85
5	40	180	55	1.18584	628.50	13.60
6	45	180	55	1.19628	607.30	13.88
1	35	160	45	1.16871	541.47	10.79
2	35	170	45	1.17437	568.77	11.40
3	35	180	45	1.17989	592.80	9.26
4	35	160	55	1.14285	588.57	14.00
5	35	170	55	1.16844	612.33	11.85
6	35	180	55	1.17439	632.90	10.15

B.4 : Deposit thickness

The deposit thickness on three heights along the cathode are given in These points were 5 mm from the bottom of the cathode, center of the cathode, and 5 mm from top of the cathode. In the table, these points are referred to as FB, CP, and FT respectively. The thickness values reported were the average results.

Table B 4: Deposit thickness (in mm) electrowon at specific locations from the cathode bottom used in determination of current density distribution

Run	Cu (g/l)	H_2SO_4 (g/l)	Fe (g/l)	5 mm FB	Centre Point	5 mm FT
1	35	180	6	0.2733	0.1850	0.2600
2	35	160	1	0.2350	0.1850	0.2517
3	45	180	1	0.2450	0.2133	0.3017
4	45	160	1	0.2317	0.2183	0.3100
5	45	160	6	0.2300	0.2033	0.2400
6	45	180	6	0.2650	0.2183	0.2767
7	35	180	1	0.2317	0.2100	0.3067
8	35	160	6	0.2767	0.2050	0.3133

B.5 : Current Efficiency and Energy Consumption

The current efficiency was calculated as the ratio of the actual deposited weight to the theoretical weight expressed as a percentage:

$$Current\ Efficiency\ (C.E.) = \frac{M_{actual}}{M_{theoretical}} \qquad \text{B.1}$$

The theoretical weight was determined using equation *2.18*

The energy consumption is the energy consumed per deposit produced.

$$Energy\ Consumption\ (E.C.) = \frac{E_{cell} \times I \times t}{M_{actual}} \quad \text{or} \quad \frac{100nFE_{cell}}{3.6Aw_{Cu} \times C.E.} \qquad \text{B.2}$$

The results of the applied voltage (V), actual mass, current efficiency and energy consumption are given in table

Table B.5 : Results of electrowinning experiments indicating applied potential, deposit weight, current efficiency and energy consumption.

Cu (g/l)	H_2SO_4 (g/l)	Fe (g/l)	Cell Potential (V)	M_{actual} (g)	C.E. (%)	E.C. (kWh/t)
35	160	1	1.97	2.23	97.98	1693.21
35	160	6	2.05	2.23	97.83	1755.21
35	180	6	2.02	2.24	98.35	1738.84
35	180	1	1.94	2.25	98.61	1656.64
45	160	1	1.95	2.25	98.53	1666.55
45	160	6	1.95	2.24	98.21	1672.08
45	180	1	1.87	2.25	98.75	1594.75
45	180	6	1.93	2.24	98.43	1651.24

B.6 : Effect of Meshing on Current Density Profiles

The plots below show the effect of mesh size on current density distribution profile. Note that COMSOL Multiphysics range mesh size from extremely coarse to extremely fine

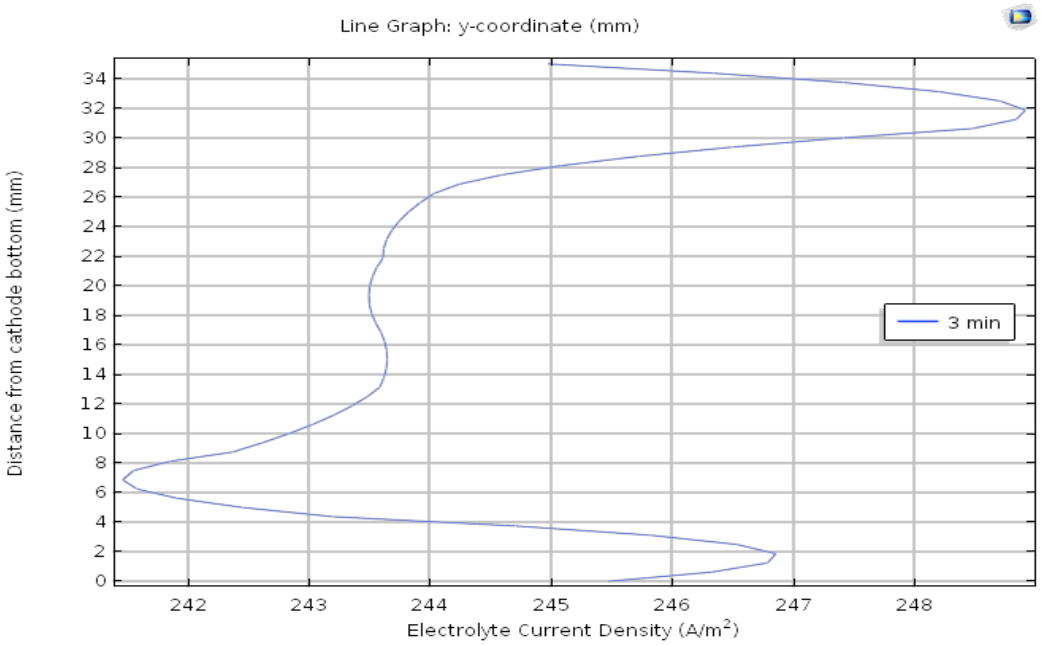

Figure B.1: Model current distribution profile of coarser mesh at 35 Cu g/l and 160 g/l H2SO4 at 45°C temperature

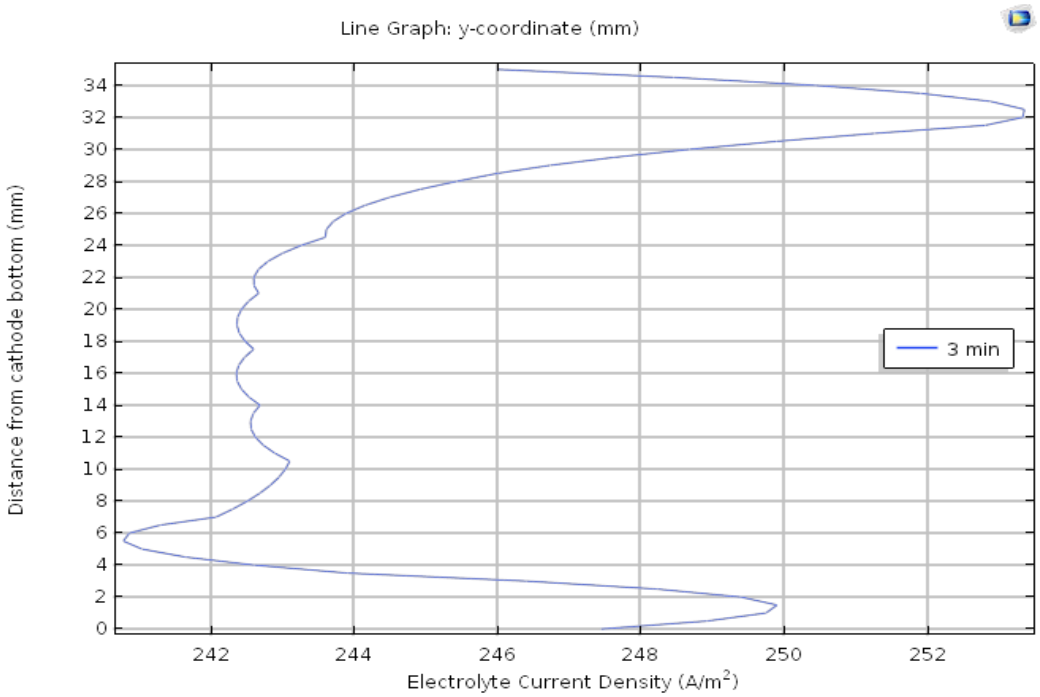

Figure B.2: Model current distribution profile of normal mesh at 35 Cu g/l and 160 g/l H2SO4 at 45°C temperature

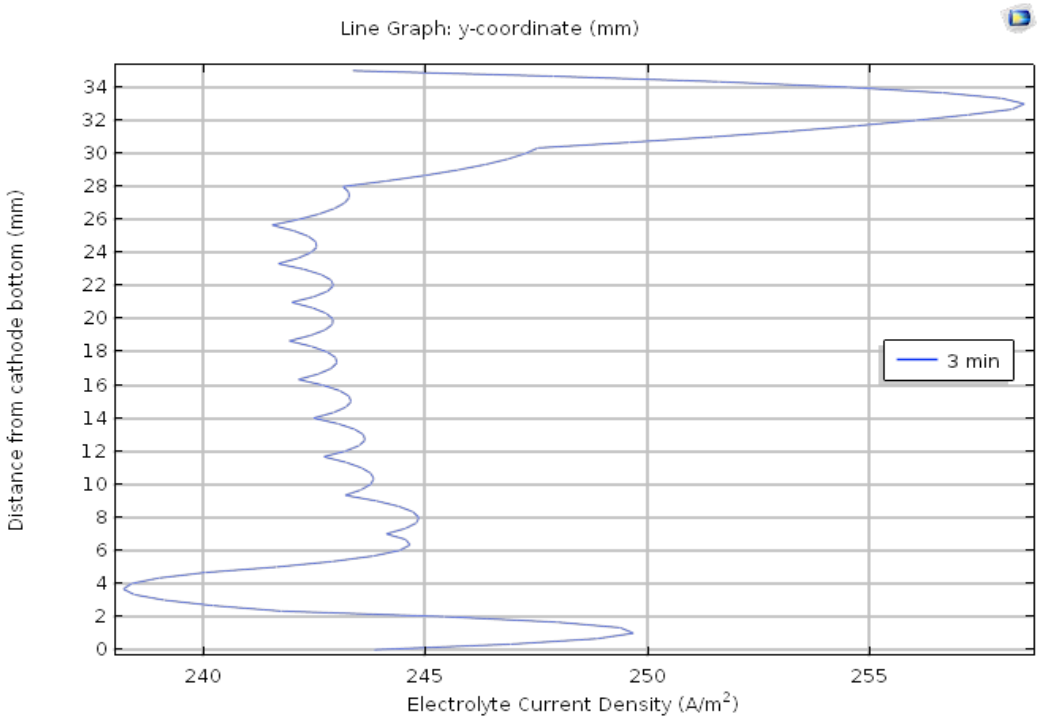

Figure B.3: Model current distribution profile of normal mesh at 35 Cu g/l and 160 g/l H2SO4 at 45°C temperature